Modelling of mitochondrial metabolism in breast cancer

MASTER'S DEGREE IN AUTOMATION ENGINEERING

CANDIDATE: *Alberto Zenere*

SUPERVISOR: *Professor Morten Gram Pedersen*

21 February 2017 A.Y. 2016-2017

Contents

Abstract

Recently two different metabolic phenotypes have been discovered in breast cancer cells. As increasing evidence shows how metabolism is directly connected to cancer invasiveness, it is of interest to identify which enzymes lead to the expression of each phenotype. As first contribution of this work, we present a novel kinetic model that approximates mitochondrial metabolism. Thereafter, we investigate the behaviour of the system through multiple numeric simulations. Ultimately, we show that it is possible to replicate each phenotype through the over-expression of a limited set of enzymes.

Abstract (versione italiana)

Recentemente sono stati identificati due distinti fenotipi metabolici nelle cellule di cancro al seno. Data la crescente evidenza di come il metabolismo cellulare sia fondamentale nel determinare l'invasivitá del cancro, é di interesse mettere in rilievo quali siano gli enzimi che portano all'espressione di ciascun fenotipo. Nella prima parte di questo lavoro viene presentato un modello originale per approssimare il metabolismo mitocondriale. Successivamente, il comportamento di questo sistema é analizzato tramite una serie di simulazioni numeriche. In tal modo si vuol dare evidenza come sia sufficiente modificare l'espressione di un ristretto gruppo di enzimi per manifestare ognuno dei due fenotipi.

Introduction

Mitochondria are cellular organelles that perform many fundamental tasks for the cell. Besides ATP production, they also provide important intermediates for the biosynthesis of macromolecules such as proteins, lipids and nucleotides. Accordingly, they qualify as primary determinants of the metabolism of the entire cell.

Since the studies of Otto Warburg in 1924, it is well-known that the behaviour of these organelles in cancer is consistently altered. The initial belief was that mitochondria were impaired in cancer cells, thus leading to their malfunctioning. Only in recent years this notion was refuted and mitochondrial metabolism has instead emerged as a crucial component of several signalling pathways involved in tumorigenesis. Thus a better understanding of the key steps involved in mitochondrial metabolism could reveal novel therapies to block these pathways, consequently hampering the proliferation of cancer cells. In particular in this work, starting from some new experimental data, we focus our attention on the metabolism of breast cancer cells. However it is important to remark that these metabolic pathways comprise numerous enzymes which, in turn, are characterized by multiple feedback mechanisms. Therefore the analysis of these networks is often not intuitive and requires an analytical approach to obtain trustworthy results. We addressed this problem through kinetic modelling.

Here is the organization of the present work. In Chapter 1 are summarized the main pathways that branch off from mitochondrial metabolism as well as their different regulation between healthy and cancer cells. In Chapter 2 is described the mathematical model we built in order to replicate mitochondrial metabolism in breast cancer cells. Thereafter, in Chapter 3, this model is utilised to analyse two distinguishable metabolic phenotypes that have been recently identified in breast cancer cells. In particular we aim to highlight a small set of enzymes that is responsible for the manifestation of each phenotype. Finally, in Chapter

4, we draw some conclusions and we give a brief review regarding alternative approaches that could be deployed in the future to further analyse this subject.

Chapter 1

Metabolism in Cancer

The aim of this chapter is to outline the primary reactions involved in energy production and biosynthesis. Thereafter we want to analyse the main differences between metabolism in normal and tumour cells. In particular we will see how mitochondria play a central role in these processes, hence the importance of modelling mitochondrial metabolism.

Glycolysis constitutes the first phase of most carbohydrate catabolism as it breaks down glucose to form pyruvate with the net production of two molecules of ATP. This pyruvate can be used in either anaerobic glycolysis (via lactate dehydrogenase) or in aerobic respiration (via the tricarboxylic acid cycle). Notice that the latter results in a production of ATP significantly higher (38 versus 2 molecules of ATP produced per molecule of glucose). Consequently, the first pathway is usually used by the cell only if there is no oxygen available. However we will see that this does not hold true in the case of tumour cells.

It is important to note that from this route, that starts from glucose and arrives to pyruvate, branch off other major pathways such as the pentose phosphate pathway (PPP) and the synthesis of serine, see Fig.1.1. In particular PPP leads to the production of reducing equivalents (namely NADPH) that are in turn used for lipid synthesis, and also ribose-5-phosphate (R5P) that is instead essential for nucleotides production, see Fig.1.3. On the other hand serine is implicated in the production of numerous metabolites such as glycine, cysteine, sphingolipids and folate.

If pyruvate enters the mitochondria, it is then oxidized in order to generate energy and other species that are in turn used for the synthesis of lipids and

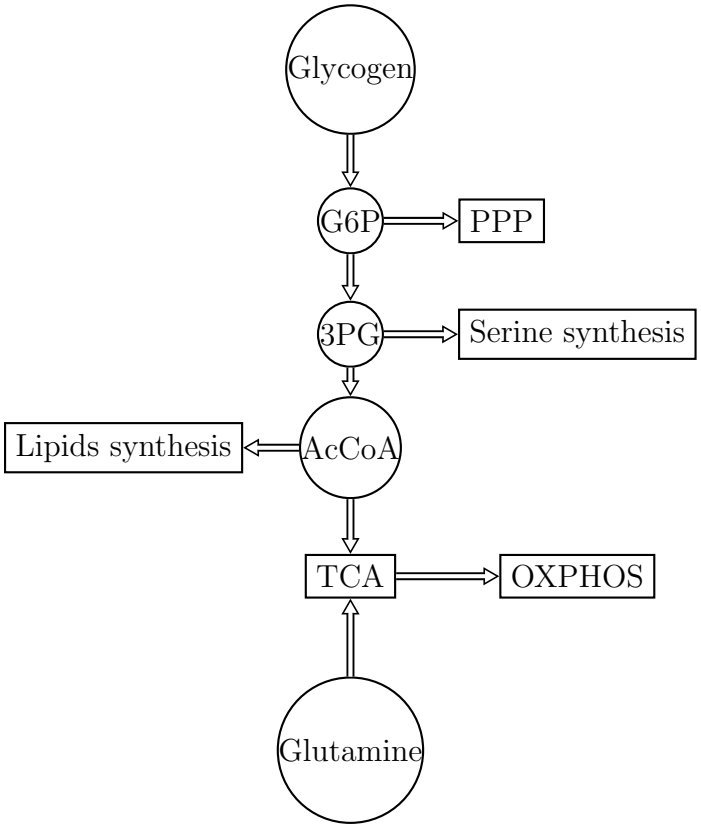

Figure 1.1: Main branches of metabolism departing from glycolysis. G6P: glucose-6-phosphate; PPP: pentose phosphate pathway; 3PG: 3-phosphoglycerate; TCA: tricarboxylic acid cycle; OXPHOS: oxidative phosphorylation.

proteins (citrate and oxalacetate respectively).

More precisely, the mitochondrial ATP production relies on the electron transport chain (ETC), composed of respiratory chain complexes I-IV, which transfer electrons taken from NADH and $FADH_2$ to reduce oxygen to water. Simultaneously, H^+ are pumped in the intermembrane space, thus forming a strong electrochemical gradient across the inner membrane. Consequently this gradient is used to produce energy by the ATP synthase complex, as H^+ protons tend to return inside the inner membrane. Thereafter the adenine nucleotide translocase (ANT) catalyses the exchange of mitochondrial ATP with cytosolic ADP. It is important to note that ATP has a strong inhibitor effect on glycolysis creating thus a feedback mechanism.

1.1 Warburg effect

Now we will describe the overall characteristics that distinguish the metabolism observed in tumour cells versus that of normal cells.

The fundamental observations, that constitute the basis of our current knowledge, arise from the studies of Otto Warburg dating back to 1924. Precisely, what Otto Warburg discovered is that most cancer cells produce energy by a high rate of glycolysis followed by lactic acid fermentation in the cytosol, rather than by the oxidation of pyruvate in mitochondria, even in the presence of O_2. For this reason this kind of metabolism is also denominated 'aerobic glycolysis'. This seems counter-intuitive as we already explained how this pathway is quite inefficient in terms of ATP production with respect to aerobic respiration. Otto Warburg proposed that this atypical behaviour was due to defects in the mitochondria.

However, this explanation appears nowadays not founded since it was observed in many cancers an upregulated aerobic glycolysis without any mitochondrial dysfunction or oxidative phosphorylation (OXPHOS) disruption [5, 6]. In these cancers, OXPHOS continues as normal and produces as much ATP as OXPHOS in normal tissues under the same oxygen pressures. In general, tumour cells display a wide variety of levels of aerobic glycolysis, in fact the contribution of glycolysis to ATP production ranges from over 50% to less than 5% in some cells [13].

Furthermore it is important to note that this type of metabolism is not solely found in cancer cells but constitutes a common feature of rapid cell proliferation [10, 11].

In recent years, extensive research has been devoted to the study of the peculiarities of tumour cells metabolism. Consequently, a copious literature has been developed regarding the various metabolic mutations that have been identified in cancer. In the following paragraphs we will try to give a comprehensive summary about the central results. In particular, we will describe the overall regulation of the main pathways (PPP, ROS production, serine synthesis, etc) whereas in Chapter 2 we will focus on the individual enzymes involved in mitochondrial metabolism.

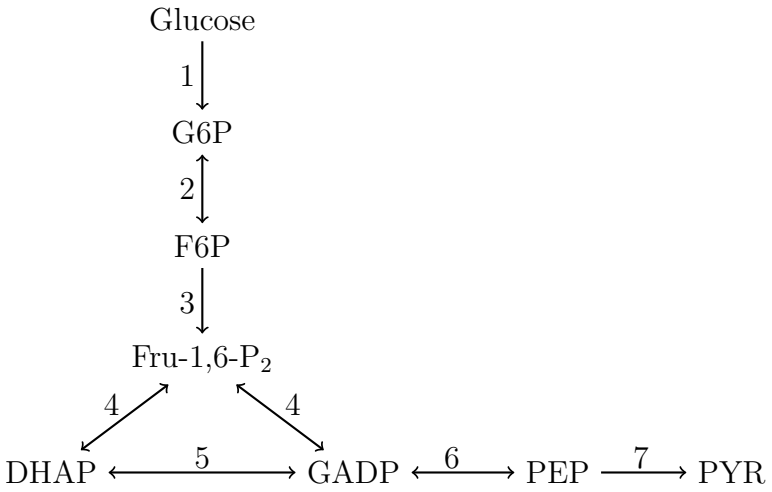

Figure 1.2: Main steps of glycolysis. DHAP: dihydroxyacetone phosphate; GADP: glyceraldehyde-3-phosphate. 1: hexokinase; 2: phosphoglucose isomerase; 3: 6-phosphofructo-kinase; 4: fructose-biphosphate aldolase; 5: trisephosphate isomerase; 6: glyceraldehyde phosphate dehydrogenase + phosphoglycerate kinase + phosphoglycerate mutase + enolase; 7: pyruvate kinase.

1.1.1 Glycolysis and OXPHOS

Glucose enters cells via a family of twelve functional glucose transporters (GLUTs), denominated GLUT-1 to GLUT-12. The majority of them are tissue-specific, for example, GLTU-1 (all tissues but abundance in brain and erythrocyte), GLUT-2 (liver), GLUT-3 (brain), GLUT-4 (muscle/fat), and GLUT-5 (small intestine). Among the GLUTs, GLUT-1 is a rate-limiting transporter for glucose uptake, and its expression correlates with anaerobic glycolysis. GLUT-1 has an influence not only on glucose uptake/utilization but also on tumorigenic features [7, 8, 9].

The first, and arguably major, point of regulation of the glycolysis pathway is constituted by the enzyme 6-phosphofructo-kinase (PFK) which catalyzes the phosphorylation of fructose-6-phosphate (F6P) to fructose-1,6-bisphosphate (Fru-1,6-P_2), see Fig. 1.2. Four different genes coding different isozymes (PFKFB14) have been identified to date [51, 52, 53, 54, 55]. They differ not only in their tissue distribution but also in their kinetic and regulatory properties. These isoforms were found to be over expressed in various types of cancer [56, 57, 58, 59].

Another important step of glycolysis reprogramming, that leads to the Warburg effect, is the switch in isoform of pyruvate kinase (PK). Many types of

cancer cells use the M2 isoform of pyruvate kinase (PKM2) instead of the M1 isoform of the enzyme (PKM1) as normal tissues do [107, 154, 158, 155]. This is a significant difference since PKM2 exhibits an activity considerably lower than PKM1. More specifically PKM2 can exist in two forms: tetrameric (active) or dimeric (inactive). PKM2 is also is tightly regulated, its allosteric effectors include Fru-1,6-P_2 and numerous amino acids. It is believed that this enzyme acts as a switch channelling the carbon flux to ATP production (active form) or into biosynthetic pathways (inactive form) according to the state of the cell. More precisely, when the levels of amino acids are low, the slower PKM2 leads to accumulation of earlier glycolytic intermediates, diverting them to pathways such as hexosamine synthesis, PPP, amino acids production. Moreover this results in the accumulation of phosphoenolpyruvate (PEP), which functions as a feedback inhibitor of the glycolytic enzyme triosephosphate isomerase. This in turn activates PPP [14, 15].

Another characteristic of cancer metabolism resides in the increased ROS production [17, 107], in particular superoxide (O_2^-) and hydrogen peroxide (H_2O_2) appear to be increasingly produced by mitochondria in cancer cells. ROS are involved in tumour angiogenesis [18] as well as in promoting invasion and metastasis of cancer cells [19]. However, it is important to note that ROS act as a double-edged sword for cancer cells since they are also a major contributor to oxidative damage [16]. Thus the cellular level of ROS must be maintained within a certain range so that they promote cancer cell growth without causing severe oxidative damage. Up to a certain extent of glycolysis, the malate-aspartate shuttle through the mitochondria is able to restore the NADH imbalance [5]. Also de novo serine metabolism, which feeds into the one-carbon metabolism, produces NADPH and glutathione, which modulate ROS levels [20, 21]. In this regard it has been validated that the increased glucose metabolism in cancer cells compensates partially for increased fluxes of H_2O_2 produced in mitochondria by producing higher amounts of both NADPH as a cofactor for H_2O_2 metabolism and pyruvate for directly scavenging H_2O_2 in a deacetylation reaction to form acetic acid and H_2O [22, 23, 24]. In addition, ROS and PKM2 form a negative feedback loop to maintain ROS in a tolerable range. PKM2 can be oxidized by H_2O_2, which leads to a reduction of its activity and augmentation of flux of glycolytic intermediates into PPP [14, 15]. In [111] was proposed the idea that the

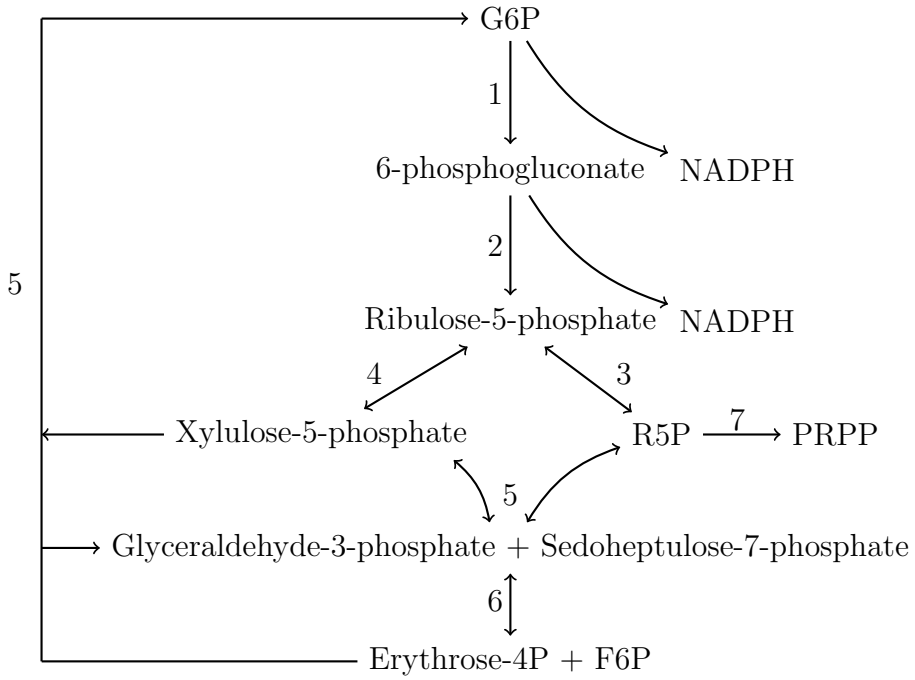

Figure 1.3: Main steps of the pentose phosphate pathway. R5P: ribose-5-phosphate; F6P: fructose-6-phosphate; PRPP: phosphoribosyl pyrophosphate. 1: glucose-6-phosphate dehydrogenase+glucolactonase; 2: 6-phosphogluconate dehydrogenase; 3: phosphopentose isomerase; 4: phosphopentose epimerase, 5: transketolase; 6: transaldolase; 7: phosphoribosyl pyrophosphate synthetase.

feedback mechanism between glycolysis and ATP could be compromised in cancer cells, thus promoting the high levels of glycolysis observed in tumour cells. More specifically, it is known that the level of free tubulin varies over the course of the cell cycle and thus undergoes a periodic pattern during cell proliferation. What they found out is that this protein affects the activity of the voltage dependent anion channel (VDAC), which allows the passage of small hydrophilic molecules, including ATP, across the outer membrane of mitochondria. Consequently free tubulin, through inhibition of VDAC, could potentially avoid the inhibition of glycolysis that usually happens when ATP is produced.

1.1.2 Genes involved in cancer metabolism

So far, different transcriptional factors have been identified as possible promoters of the Warburg effect.

Perhaps the most famous transcriptional factor is hypoxia-inducible factor

(HIF). There are three isoforms in the HIF family: HIF-1, HIF-2 and HIF-3 with HIF-1 and HIF-2 better studied and HIF3 functions poorly understood. Among the three, HIF-1 is the only one that is ubiquitously expressed and it is the most relevant to cancer. HIF-1, like all HIFs, consists of an oxygen-dependent α-subunit and a constitutively expressed β-subunit. Under normoxia, HIF-1α is modified by prolyl hydroxylases (PHDs). Consequently HIF-1α is recognized by the von Hippel-Lindau protein and its associated ubiquitinase, resulting in the degradation of the protein. Under hypoxia, on the other hand, the reduced oxygen supply diminishes the activity of PHDs, which are further inhibited by ROS released from stressed mitochondria. Consequently, HIF-1α binds to HIF-1β to form a stabilized HIF-1. HIF-1 complex then promotes the transcription of numerous genes involved in glucose transport, glycolysis, pH regulation and vasculogenesis, allowing cancer cells to rapidly adapt to hypoxia [36, 38, 37, 112]. Notably, HIF-1 was found to regulate the activity of both PFK [60] and to be a PHD-induced coactivator for HIF [39]. Furthermore, the activity of HIF-1α is regulated by the sirtuin gene (SIRT) family. SIRT is a mitochondrial NAD-dependent deacetylase that has the capacity of destabilizing HIF-1α. In particular it has been shown that the loss of SIRT3 leads to HIF-1α stabilization through an increase of ROS production. Accordingly, the loss of SIRT3 has been shown to result in aberrant mitochondrial metabolism while its over-expression represses glycolysis and proliferation in breast cancer cells [33, 34, 35]

Another important transcription factor is c-Myc, which has been implicated in regulating glycolysis in tumour cells through transactivation of lactate dehydrogenase A [29], up-regulation of GLUT-1 genes [28] and coordinate induction of all glycolytic enzymes [26].

Notably, there exists cross talk between Myc and HIF. More precisely, the former can stimulate HIF-1α, HIF-1α can inhibit the activity of c-Myc and HIF-2α can instead enhance it [25, 27]. Moreover, both HIF and Myc activate hexokinase 2 (HK2) and pyruvate dehydrogenase kinase1 (PDK1), leading to augmented glycolytic rates and conversion of glucose to lactate [31].

The phosphoinositide 3-kinase (PI3K) signalling pathway is linked to both growth control and glucose metabolism. PI3K signalling, through Akt, can regulate glucose transporter expression, enhance glucose capture by hexokinase and stimulate phosphofructokinase activity [50]. The PI3K pathway also renders cells

dependent on high levels of glucose flux [49].

In [113] they observed that the Warburg effect shows significant correlation with the levels of c-Myc and HIF-1α in breast cancer cell lines. Notably, in the same study, Akt did not appear to play a significant role. However in [30] it was reported that human glioblastoma cells metabolize glucose in correlation with Akt activity in vitro.

Finally it is necessary to mention the transcriptional factor p53, which is a well known tumour suppressor [40]. In particular, this transcriptional factor can induce the arrest of the cell cycle in case of DNA damage and it is also able to trigger apoptosis if this damage proves to be irreparable. Recent studies have revealed a number of functions of p53 in the regulation of glucose metabolism and energy production pathways, including glucose transport [44], glycolysis [43], TCA cycle [45] and glutaminolysis [41, 42], ETC/OXPHOS [46] and PPP [47, 48].

1.2 Glutamine

The main substrates to mitochondrial metabolism are by far glucose and glutamine. For example, in rapidly proliferating cultured glioblastoma cells most of acetyl-CoA comes from glucose whereas essentially all of oxacelate comes from glutamine [64]. The simplest mechanism to explain the enhanced use of both glutamine and glucose by tumour cells is that metabolism of the two nutrients is co-regulated. However, recent findings suggest that they can be regulated by independent signalling pathways within the same cells. In a glioblastoma cell line with genomic c-Myc amplification, the inhibition of Akt signalling led to a decrease in glycolysis but had no effect on glutamine metabolism, which was only inhibited when c-Myc was suppressed to normal levels [65].

In the following paragraphs we will describe the transporters that allow the entry of glutamine inside the cell, then we will discuss in more detail glutamine metabolism and we will finally give an overview of the major transcriptional factors involved in its regulation.

1.2.1 Glutamine transporters

The SLC (solute carrier) transporters ($\approx$ 400 in number) in mammalian cells comprise of 52 distinct gene families [62]. Among them, fourteen are capable

of transporting glutamine across the plasma membrane. They are found in four families: SLC1, SLC6, SLC7, and SLC38. More precisely we have one transporter in SLC1, two transporters in SLC6, five transporters in SLC7 and six transporters in SLC38. However, it is generally thought that the members of the SLC38 family are the principal transporters for glutamine. It is important to note that none of these transporters is exclusively selective for glutamine and that not all of these transporters function in the influx of glutamine into cells. Some of the glutamine transporters are obligatory exchangers (i.e. capable of mediating either the influx or efflux of glutamine depending on the concentration gradients) whereas some function as active transporters in one direction. While most glutamine transporters mediate the influx of the amino acid into cells, some mediate the efflux of the amino acid out of the cells. We now describe in more detail these glutamine transporters.

SLC1 family

The SLC1 gene family consists of transporters for anionic amino acids (aspartate and glutamate) or neutral amino acids [71]. SLC1A4 (also known as ASCT1) and SLC1A5 (also known as ASCT2) are the transporters for neutral amino acids, the former being selective for alanine, serine, and cysteine and the latter for alanine, serine, cysteine, threonine and glutamine. The term ASCT stands for Alanine-Serine-Cysteine Transporter. Both transporters are Na^+-coupled and function as obligatory exchangers.

SLC1A5 is expressed in the intestine, kidney, lung, testis, skeletal muscle, and adipose tissue. It mediates the Na^+-coupled influx of glutamine in exchange for the efflux of any of the other four amino acid substrates. Recently, SLC1A5 is was found to be up-regulated in many cancer types, including triple-negative breast cancer [68, 69] and melanoma [70].

The activity of SLC1A5 seems to be coupled with two other amino acid transporters, namely SLC7A5 and SLC7A11. SLC7A5 mediates the efflux of glutamine from the cells in exchange for the influx of leucine. On the other hand, SLC7A11 is a cystine-glutamate exchanger, which functions always in the import of cystine into cells under physiologic conditions, and the imported cystine is then used in the synthesis of the antioxidant molecule glutathione. The expression of SLC7A11 is also increased in several cancers [72].

SLC6 family

The SLC6 gene family is known as the Na^+/Cl^-- coupled neurotransmitter transporter family because of the inclusion of transporters for a variety of neurotransmitters in this family (e.g. GABA, serotonin, dopamine, norepinephrine, and glycine) [73]. However, the SLC6 gene family does also contain transporters for amino acids that do not function as neurotransmitters; among these transporters are the glutamine transporters SLC6A14 and SLC6A19.

SLC6A14 is characterized by a broad substrate selectivity and it is obligatorily coupled to a Na^+ gradient as well as a Cl^- gradient [74]. It recognizes 18 of the 20 amino acids as substrates, with glutamate and aspartate being the only two amino acids excluded by the transporter. SLC6A14 appears to be up-regulated in certain cancer types that comprise estrogen receptor-positive breast cancer [75].

SLC6A19 transports all neutral amino acids including glutamine and it is coupled only to Na^+.

SLC7 family

Among the five glutamine transporters in the SLC7 gene family, four (SLC7A5, SLC7A6, SLC7A7, and SLC7A8) specifically interact with SLC3A2 whereas SLC7A9 interacts specifically with SLC3A1. Each of these transporters functions as an obligatory exchanger. SLC7A5 and SLC7A8 are known as LAT1 and LAT2 respectively; 'LAT' refers to 'system L amino acid transporter' where 'L' indicates their preference for leucine. Both transporters do interact with all neutral amino acids but prefer large amino acids such as leucine, isoleucine, valine, tyrosine, phenylalanine, tryptophan, glutamine, andmethionine. Both are expressed in a wide variety of tissues and cells. SLC7A5 is the primary transporter for neutral amino acids in the endothelial cells lining the bloodbrain barrier [76]. On the other hand, SLC7A8 is highly expressed in the absorptive cells of the intestine and kidney where it is present in the basolateral membrane, thus participating in the efflux of amino acids from the cells into the circulation. SLC7A5 expression is increased in many cancers, particularly in melanoma, lung cancer and colon cancer [77]. On the other hand, there is very little information on whether SLC7A8 plays any role in cancer.

SLC7A6 and SLC7A7 are Na^+-dependent, they mediate the influx into cells

of neutral amino acids coupled to the efflux of cationic amino acids. These transporters are expressed in the basolateral membrane of absorptive epithelial cells of the intestine and kidney.

SLC7A9 involves an obligatory exchange of cationic amino acids with neutral amino acids. It is expressed predominantly in the absorptive tissues such as the intestine, kidney, and placenta, and is located on the apical membrane of the absorptive epithelial cells in these tissues. Under physiologic conditions, the transporter facilitates the influx of cationic amino acids in the cells coupled to the efflux of neutral amino acids from the cells.

SLC38 family

The SLC38 transporters are functionally identified as amino acid transport systems A and N; system A (A stands for alanine-preferring) refers to a Na^+-dependent transport process selective for neutral amino acids including alanine while system N (N stands for amino acids with nitrogen in the side chain) refers to a Na^+-dependent transport process selective for glutamine, asparagine, and histidine, which all contain nitrogen atom in the side chain. SLC38A1 and SLC38A2 belong to the group of system A transporters whereas SLC38A3 and SLC38A5 belong to the group of system N transporters. Unfortunately detailed functional studies are not available for SLC38A7 and SLC38A8 for definitive classification into either system A group or system N group.

SLC38A1 and SLC38A2 are Na^+-coupled transporters and belong to group A, they also transport including glutamine. Both are expressed ubiquitously in many mammalian tissues. They represent one of the major routes of glutamine entry into cells under physiologic conditions. In the central nervous system, SLC38A1 and SLC38A2 are expressed almost exclusively in neurons where they function in glutamate/GABA-glutamine cycle that takes place between neurons and astrocytes [78]. There is some evidence that SLC38A2 might be involved in promoting tumour growth. Moreover the gene encoding this transporter is a transcriptional target for the tumour suppressor p53; the expression of SLC38A2 is repressed by active p53 [79].

SLC38A3 and SLC38A5 are referred to as SN1 (system N1) and SN2 (system N2) transporters. These are Na^+-coupled and selective for glutamine, asparagine, and histidine. SLC38A5 recognizes alanine and serine as additional substrates. SLC38A3 is expressed abundantly in the liver, brain, retina, and pancreas [80]

whereas SLC38A5 is expressed primarily in the intestinal tract, kidney, retina, lung, and cervix [81]. In the brain, both transporters are expressed in astrocytes where they function in the release of glutamine from the cells as a part of the glutamate/GABA-glutamine cycle. In the liver, the transporters function differentially in periportal hepatocytes versus perivenous hepatocytes. In the periportal hepatocytes, which express both SLC38A3 and SLC38A5, the transporters mediate the influx of Na^+/glutamine into cells from the portal blood, for subsequent conversion into urea in the liver. On the other hand, in the perivenous hepatocytes, which express mostly SLC38A3, the transporter functions to release Na^+/glutamine from the cells into the venous circulation.

SLC38A7 and SLC38A8 are Na^+-coupled glutamine transporters that are expressed in the central nervous system, almost exclusively in the neurons [82, 83]. Even though SLC38A7 has been classified as a system N transporter and SLC38A8 as a system A transporter, additional studies might be necessary to confirm this classification.

1.2.2 Glutamine metabolism

Glutamine is usually oxidized in the mitochondria and is used as a primary source of energy. This requires its conversion to α-ketoglutarate, typically through a glutaminase (GLS) activity, followed by conversion of glutamate to α-ketoglutarate by either transaminases or glutamate dehydrogenase. [32, 67]. GLS presents three isoforms, namely GLS1, GLS2 and GLSC [84]. In particular GLS1 is required for cell cycle progression through S phase to cell division [85].

We now present a summary of the main functions of glutamine in the cell, see Fig.1.4. First, glutamine is involved in the synthesis nonessential aminoacids. This happens more specifically through the activity of different transaminases, particularly alanine aminotransferase and aspartate aminotransferase. Alanine is then used in protein synthesis, but is also secreted by tumour cells. Aspartate, in contrast, remains inside the cell and contributes to the synthesis of proteins and nucleotides and to electron transfer reactions through the malate-aspartate shuttle.

Alternatively, some tissues can reductively carboxylate α-KG to generate citrate [86, 87] that can be used to synthesize acetyl-CoA for lipid synthesis. This IDH1-dependent pathway is active in most cell lines under normal culture con-

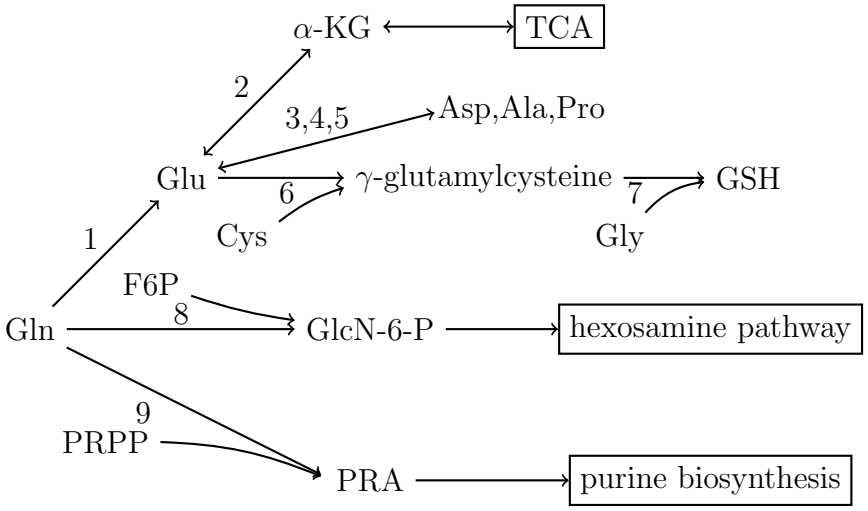

Figure 1.4: Different uses of glutamine in the cell. Gln: glutamine; Glu: glutamate; α-KG: α-ketoglutarate; Asp: aspartate; Ala: alanine; Pro: proline; Cys: cysteine; Gly: glycine; GSH: glutathione; GlcN-6-P: glucosamine-6-phosphate; PRPP: 5-phosphoribosyl-1-pyrophosphate; PRA: 5-phosphoribosyl-1-amine. 1: glutaminase; 2: glutamate dehydrogenase; 3: aspartate aminotransferase; 4: alanine aminotransferase; 5: glutamate-5-kinase + glutamate-5-semialdehyde dehydrogenase + proline dehydrogenase, pyrroline-5-carboxylase reductase; 6: glutamate cysteine ligase; 7: glutathione synthase; 8: glutamine-fructose-6-phosphate amidotransferase; 9: glutamine phosphoribosylpyrophosphate amidotransferase.

ditions, but cells grown under hypoxia rely almost exclusively on it for de novo lipogenesis.

Furthermore, the cyclization of glutamate produces proline, an amino acid important for synthesis of collagen and connective tissue.

Glutamine can also be converted directly to glutathione (GSH) by glutamate cysteine ligase (GCL, EC 6.3.2.2). The reduced GSH, one of the most abundant anti-oxidants present in mammalian cells, is vital to controlling the redox state of the subcellular compartments, thus protecting cells from oxidative stress-induced apoptosis [88]. In particular GLS2 activity was found to be associated to an increase of GSH levels. In this regard, GLS2 over-expression reduces tumour cell colony formation abilities in human liver tumours. Furthermore, GLS2 expression is reduced in liver tumours compared with normal tissues.

Also, there is evidence indicating that a fraction glutamine-derived carbon can exit the TCA cycle as malate and serve as substrate of malic enzymes 1,

which produces NADPH [64].

Glutamine is also important for the production of nucleotides during cell proliferation since it is required a nitrogen donor for the de novo synthesis of both purines and pyrimidines [32]. Other nitrogens are supplied by glycine and aspartate, but many of these are actually derived from glutamine. Moreover, pyrimidine rings contain one nitrogen from glutamine amido group and one from aspartate. However, the glutamine utilization rate exceeds nucleic acid synthesis by more than an order of magnitude in proliferating cells, and accounts for only a small fraction of total glutamine consumption.

Glutamine plays also an important role in hexosamine biosynthesis and glycolsylation reactions [32]. In fact the rate-limiting step in the formation of hexosamine is catalysed by glutamine-fructose-6-phosphate amidotransferase, which forms glucosamine-6-phosphate, which is also a precursor for glycolsylation reactions.

Finally, glutamine is an amino acid that plays a key role in many metabolic and signalling pathways [61, 12]. In fact it has a regulatory role in several cell processes that include metabolism, signal transduction, cell defence and repair. Of interest, cultured tumour cells require at least 10 times as much glutamine as any other amino acid [64].

It should be noted, however, that glutamine is not used to completion by cell lines in vitro. Rather, a significant fraction of glutamines nitrogens are secreted from cells as they proliferate.

1.2.3 Genes involved in glutamine metabolism

Regarding the expression of the glutaminases, we already saw that GLS1 expression is up-regulated by c-Myc [65, 66] and that GLS2 expression is up-regulated by p53 [41, 42]. However, it is noteworthy to add that GLS1 and GLS2 seem to have contrasting effects in tumorigenesis. In fact GLS1 downregulation inhibits oncogenic transformation and cancer cell proliferation [90, 91] while overexpression of GLS2 is tumour suppressive [41, 42]. Notably, both enzymes have been implicated in regulating glutathione production and redox homeostasis, which is important for mediating cell survival in Myc-driven cells, as well as for protecting against p53-dependent apoptosis [66, 41, 42].

Rho GTPases have also recently been reported to regulate glutamine metabolism

[89]. Cancer cells dependent on Rho GTPase signaling display higher glutaminase activity, regulated in an NF-κB-dependent manner, and glutaminase activity is required for the transforming capability of at least three different Rho GTPases (Cdc42, Rac1 and RhoC).

Glucose availability was recently shown in an IL-3-dependent hematopoietic cell line to modulate the uptake of glutamine through the hexosamine biosynthetic pathway [92].

Reciprocally, a mechanism has been described through which glutamine availability can modulate glucose uptake, it is based on the transcription factor MondoA. More precisely, upon glucose uptake, the MondoA complex detects elevations in glucose-6-phosphate levels and transits into the nucleus. There, it stimulates expression of thioredoxin interacting protein (TXNIP), which constrains glucose uptake [93]. A recent study showed that glutamine availability inhibited transcriptional activation of TXNIP expression [94]. Reduced TXNIP expression led consequently to enhanced glucose uptake, as well as cell growth and proliferation. Interestingly, supplementation of cells with α-ketoglutarate can also promote transcriptional repression of TXNIP [94].

1.3 Serine

Serine is a small, neutral amino acid and, as such, can be transported by one of three systems [98]. Two of the systems are sodium dependent: the alanine/serine/cysteine/threonine transporters ASCT1 and ASCT2 (encoded by SLC1A4 and SLC1A5, respectively) and the system A transporters SAT1 and SAT2 (encoded by SLC38A1 and SLC38A2, respectively). The third is a family of neutral amino acid antiporters, the alanine/serine/cysteine transporter (ASC) system [95]. Serine metabolism is frequently dysregulated in cancers; however, the benefit that this confers to tumours remains controversial. In many cases, extracellular serine alone is sufficient to support cancer cell proliferation, whereas some cancer cells increase serine synthesis from glucose and require de novo serine synthesis even in the presence of abundant extracellular serine. There is increasing evidence that serine biosynthesis from glucose is important for many cancers [96, 97]. In human colon cancer and lung cancer cell lines, proliferation in medium that contains serine without glycine is indistinguishable from proliferation in medium

containing both amino acids, whereas withdrawal of serine alone affects proliferation to the same degree as depletion of both amino acids [99]. Moreover, providing increased concentrations of glycine in the absence of serine results in even more severe suppression of proliferation than withdrawal of both serine and glycine. In fact, the conversion of glycine to serine consumes a one-carbon unit, so a high-glycine environment might limit the availability of one-carbon units for nucleotide biosynthesis, potentially contributing to glycine toxicity. Conversely, the conversion of serine to glycine donates a one-carbon unit to the folate pool, so this might explain the preferential consumption of serine over glycine. Confirming this, the addition of one-carbon units by adding formate rescued nucleotide synthesis and growth of glycine-fed cells [99].

1.3.1 Serine metabolism

The biosynthesis of serine starts with the oxidation of 3-phosphoglycerate (i.e. an intermediate from glycolysis) to 3-phosphohydroxypyruvate and NADH by phosphoglycerate dehydrogenase (PHG DH). Then the reaction catalysed by phosphoserine transaminase (PSAT) yields 3-phosphoserine which is finally hydrolyzed to obtain serine by phosphoserine phosphatase (PSPH). Notably, PHG DH activity appears to be increased in various types of cancer [99, 100, 103, 104].

Serine can be converted to glycine by the enzyme serine hydroxymethyl transferase (cytoplasmic, SHMT1; mitochondrial, SHMT2), a reaction that yields one carbon units, which then enter the tetrahydrofolate (THF) cycle and are critical for nucleotide synthesis. Glycine can also be cleaved by the mitochondrial glycine cleavage system to yield one-carbon units that are transferred to the THF cycle [102]. Amplification of the glycine cleavage system in cancers [101] suggests that this pathway is an important source of one-carbon units. In addition, glycine can also be converted into serine by SHMT1 and SHMT2. The activity of SHMT, seems to be selectively retained in tumours [98].

In purine biosynthesis, conversion of the precursor glycineamide ribonucleotide (GAR) to AMP or GMP requires the addition of two one-carbon units from the folate pool. Cells supplied with glycine, but not serine, show an accumulation of GAR and the depletion of both AMP and GMP, implying that they have insufficient one-carbon units [99].

One-carbon units derived from serine can also be used to support s-adenosyl

methionine (SAM) synthesis. The reactions by which folate metabolism donates one-carbon units to the SAM pool appear to have a low level of activity in many cancer cells, but recent work has found that serine availability is still needed to maintain SAM levels [105].

1.4 Leptin

Obesity greatly influences risk, prognosis and progression of certain types of cancer [115, 121, 125]. In particular, various studies have shown that leptin promotes breast cancer proliferation, metastasis and invasiveness [122, 124]. Leptin is a peptide hormone principally secreted by adipocytes [117, 124] and a hyper active leptin-signalling network leads to the activation of multiple pathways involved in proliferation, resistance to apoptosis, cell adhesion, invasion and migration in breast cancer cells [124, 118, 123].

More specifically leptin appears to reprogram the metabolic flux in breast cancer enhancing fatty acid oxidation and thus enabling the use of glucose for biosynthetic purposes. Accordingly, leptin was shown to increase the activity of glucose-6-phosphate dehydrogenase (G6PDH), that is the rate limiting enzyme of the pentose phosphate pathway. Moreover, the intake of glucose does not appear to be depressed by leptin and the levels of the glycolytic enzyme glyceraldehyde 3-phosphate dehydrogenase were quite similar to control cells. On the other hand, the lactate dehydrogenase levels were decreased and the pyruvate carboxylase activity was increased.

It is worth noting that the stromal cells in a breast tumour microenvironment are mainly adipocytes and this can have two important implications. First, they could potentially supply cancer cells with fatty acids and second they could secrete leptin.

Regarding the upstream mechanism that triggers this metabolic shift, the AMPK signalling pathway is a strong candidate. In fact previous studies in muscle have demonstrated that leptin activates AMPK signalling pathway [116, 119, 120], which is known to control the transcriptional factor PPAR [116]. This transcriptional factor regulates the expression of key proteins involved in fatty acid metabolism, like FAT/CD36 and CPT1, which were found increased by leptin.

1.5 Causes and advantages of the Warburg effect

In this chapter we have given an overview on the main characteristics of cancer metabolism. Surprisingly, despite the intense interest that this topic has received in the past years, the function of the Warburg effect still remains unclear. Therefore, it is worth to conclude this chapter analysing the main explanations that have been proposed so far about the causes and advantages that the Warburg effect yields.

1.5.1 Causes

It has been proposed that tumour metabolism is the results of an adaptation to intermittent hypoxia in pre-malignant lesions [110]. Blood vessels are confined to the stromal compartment and, therefore, early development of the malignant phenotype occurs in an avascular environment. As a result, substrates, such as oxygen and glucose, must diffuse from the vessels across the basement membrane and through layers of tumour cells, where they are metabolized. Some experimental studies have demonstrated that near-zero partial pressures of oxygen (pO_2) are observed at distances of only 100 μm from a vessel [142, 143]. Therefore, pre-malignant lesions, provided their basement membranes remain intact, will inevitably develop hypoxic regions near the oxygen diffusion limit. Moreover, oxic-hypoxic cycles in tumours have been measured to occur with different periodicities [144, 145]. In summary, this theory suggests that the glycolytic phenotype initially arises as an adaptation to local hypoxia. Subsequently, persistent or cyclical hypoxia would exert selection pressures that lead to constitutive upregulation of glycolysis, even in the presence of oxygen.

However, there are major objections to this theory [109]. Cancer cells appear to use glycolytic metabolism before exposure to hypoxic conditions. For example, leukemic cells are highly glycolytic [30, 146], yet these cells reside within the bloodstream at higher oxygen tensions than cells in most normal tissues. Similarly, lung tumours arising in the airways exhibit aerobic glycolysis even though these tumour cells are exposed to oxygen during tumorigenesis [147, 148].

Recently an innovative idea, termed "The Reverse Warburg effect", has been proposed [149]. It is based on the idea that cancer-associated cells (e.g. fi-

broblasts) can actually help the adjacent cancer cells. More precisely, they undergo aerobic glycolysis resulting in the production of high-energy metabolites (such as lactate and pyruvate), which can then be transferred to adjacent epithelial cancer cells that are instead undergoing oxidative mitochondrial metabolism [149, 150, 151].

1.5.2 Advantages

Numerous theories have been developed to explain the advantages that the Warburg effect gives to cancer cells. Notably, there still is not a complete consensus, therefore in this paragraph we will summarise the most noteworthy theories developed so far [108].

Rapid ATP synthesis

Per unit of glucose, aerobic glycolysis is an inefficient means of generating ATP compared with mitochondrial respiration. In fact the metabolism of glucose to lactate generates only 2 ATPs per molecule of glucose, whereas oxidative phosphorylation generates up to 36 ATPs upon complete oxidation of one glucose molecule. However, the rate of glucose metabolism through aerobic glycolysis is higher since the production of lactate from glucose occurs 10-100 times faster than the complete oxidation of glucose in the mitochondria. Overall, the amount of ATP synthesized over any given period of time is comparable between the two types of glucose metabolism [127].

Moreover, theoretical calculations using evolutionary game theory support the hypothesis that cells that use aerobic glycolysis may gain a selective advantage when competing for shared and limited energy resources [126, 129]

Despite this attractive proposal, simple empirical calculations indicate that the amount of ATP required for cell growth and division may be less than that required for normal cellular maintenance [128, 130]. Thus, ATP demand may never reach limiting values during tumour cell growth.

Warburg Effect and Biosynthesis

To produce two daughter cells, a proliferating cell must replicate all of its cellular contents. This imposes a large requirement for nucleotides, amino acids, and lipids. For instance the synthesis of palmitate, a major constituent of cellular

membranes, requires 7 molecules of ATP, 16 carbons from 8 molecules of acetyl-CoA, and 28 electrons from 14 molecules of NADPH. Likewise, synthesis of amino acids and nucleotides also consumes more equivalents of carbon and NADPH than of ATP. A glucose molecule can generate up to 36 ATPs, or 30 ATPs and 2 NADPHs (if diverted into the pentose phosphate shunt), or provide 6 carbons for macromolecular synthesis. Thus, to make a 16-carbon fatty acyl chain, a single glucose molecule can provide five times the ATP required, whereas 7 glucose molecules are needed to generate the NADPH required. This 35-fold asymmetry is only partially compensated by the consumption of 3 glucose molecules in acetyl-CoA production to satisfy the carbon requirement of the acyl chain itself.

Consequently, it is hypothesised that the metabolic reprogramming promotes the biosynthesis of cellular biomass. In accordance, under conditions of high ratios of ATP/ADP and NADH/NAD^+ (exhibited by most proliferating cells), citrate is excreted back into the cytosol. In the cytosol, acetyl-CoA is reformed from citrate through the enzyme ATP citrate lyase (ACL) and is used as the carbon source for the growing acyl chains. It was reported that disruption of ACL impairs tumour growth [131]. Also, glutamine uptake appears to facilitate lipid synthesis in that it supplies carbon (in the form of mitochondrial oxaloacetate) to maintain citrate production [64]. In other words, the increased glucose consumption is used as a carbon source for anabolic processes needed to support cell proliferation [109, 50, 132]. This excess carbon is diverted into the multiple branching pathways that emanate from glycolysis and is used for the generation of nucleotides, lipids, and proteins. One example is the diversion of glycolytic flux into de novo serine biosynthesis through the enzyme phosphoglycerate dehydrogenase (PHGDH) [128].

However, there are major limitations for this proposed function of the Warburg Effect. First, during aerobic glycolysis, most of the carbon is not retained and is instead excreted as lactate [130]. Moreover, recent estimates from quantitative proteomics show that the cost of protein production for conducting aerobic glycolysis is enormous. In fact, cells devote as much as 10% of their entire proteome and half of all of their metabolic genes to produce proteins involved in glycolysis [133]. Thus, the cost of producing proteins for aerobic glycolysis is as large, if not larger, than the cost of producing proteins for biosynthesis.

Multicellular environment

Separate from the cell-intrinsic functions, the Warburg Effect may present an advantage for cell growth in a multicellular context. In this regard, elevated glucose metabolism decreases the pH in the microenvironment due to lactate secretion [137]. This in turn leads to an alteration of the tumour-stroma interface, allowing for enhanced invasiveness [135, 137]. Also, the high rates of glycolysis from cancer cells could limit the availability of glucose to tumour-infiltrating lymphocytes (TILs), which require sufficient glucose for their effector functions [134, 136].

Cell signalling

The status of chromatin structure is responsible for regulating different cellular functions, including DNA repair and gene transcription. It has been established that acetyl-CoA, the substrate for histone acetylation, can be regulated by glucose flux [139]. The activity of ATP-citrate lyase, which converts citrate into acetyl-coA, can influence histone acetylation levels as well [138]. Elevated levels of acetyl-CoA may be enough to drive cells into the growth phase via histone acetylation [141]. Removal of glucose or reduction of ATP-citrate lyase results in loss of acetylation on several histones and causes decreased transcription of genes involved in glucose metabolism. This indicates that there is some interplay between glucose metabolism and histone acetylation. In addition to histone acetylation responding to glucose availability in cells, deacetylation can also be influenced by nutrient availability [140]. However, difficulties also limit this proposal from being the general mechanism that benefits cancer cells by undergoing aerobic glycolysis. One such limitation is that it is hard to imagine how molecular specificity arises through such a gross global signalling mechanism.

Chapter 2

Mathematical Model

In the current chapter we describe the mathematical model that we constructed in order to study mitochondrial metabolism observed in breast cancer cells. This work starts from the model of β pancreatic cells already presented in [212]. From this basis, we added some reactions and we modified the parameters of the model to adjust it to breast cancer cells. Our model consists of 25 differential equations, that correspond to as many fluxes in the cell, and 12 different chemical species. The overall system is represented in Fig.2.1.

The fluxes are modelled in accordance to the methods described in [213, 214]. More precisely, each metabolite concentration is normalized according to Tab.2.1 and we denote with x_i the normalized value of the i-th metabolite. The metabolites are produced and consumed by reactions with rates denoted V_E, where E represents the catalyzing enzyme. The ODE system becomes:

$$\dot{x}_1 = f_1\ (V_{CS} - V_{IDH_3} - V_{IDH_2} - c\ V_{ACS} - c\ V_{IDH_1})/S_1^{IDH_3}$$
$$\dot{x}_2 = f_2\ (V_{IDH_3} + V_{IDH_2} - c\ V_{AAT_2} - V_{AAT_1} - V_{OGDH} - V_{GDH_1} - V_{GDH_2} + c\ V_{IDH_1})/S_2^{OGDH}$$
$$\dot{x}_3 = f_3\ (-c\ V_{ME_1} - V_{ME_2} - V_{ME_3} - V_{MDH_2} + V_{OGDH} - c\ V_{MDH_1})/S_3^{MDH_2}$$
$$\dot{x}_4 = (V_{PC} + V_{MDH_2} + V_{AAT_1} - V_{CS} - V_{PEPCK_2})/S_4^{CS}$$
$$\dot{x}_5 = (c\ V_{AAT_2} + c\ V_{MDH_1} - c\ V_{PEPCK_1} + c\ V_{ACS})/P_5^{MDH_1}$$
$$\dot{x}_6 = f_6\ (c\ V_{PK} + c\ V_{ME_1} + V_{ME_2} + V_{ME_3} - c\ V_{LDH} - V_{PDH} - V_{PC})/S_6^{PDH}$$
$$\dot{x}_7 = (V_{CS} - V_{PDH})/[CoA]_{tot}$$
$$\dot{x}_8 = (-V_{RESP} - V_{GDH_1} + V_{ME_2} + V_{PDH} + V_{IDH_3} + V_{OGDH} + V_{MDH_1})/[NAD_m]_{tot}$$
$$\dot{x}_9 = c\ (V_{MDH_1} + V_{GPDH} - V_{G3DH} - V_{LDH})/[NAD_c]_{tot}$$

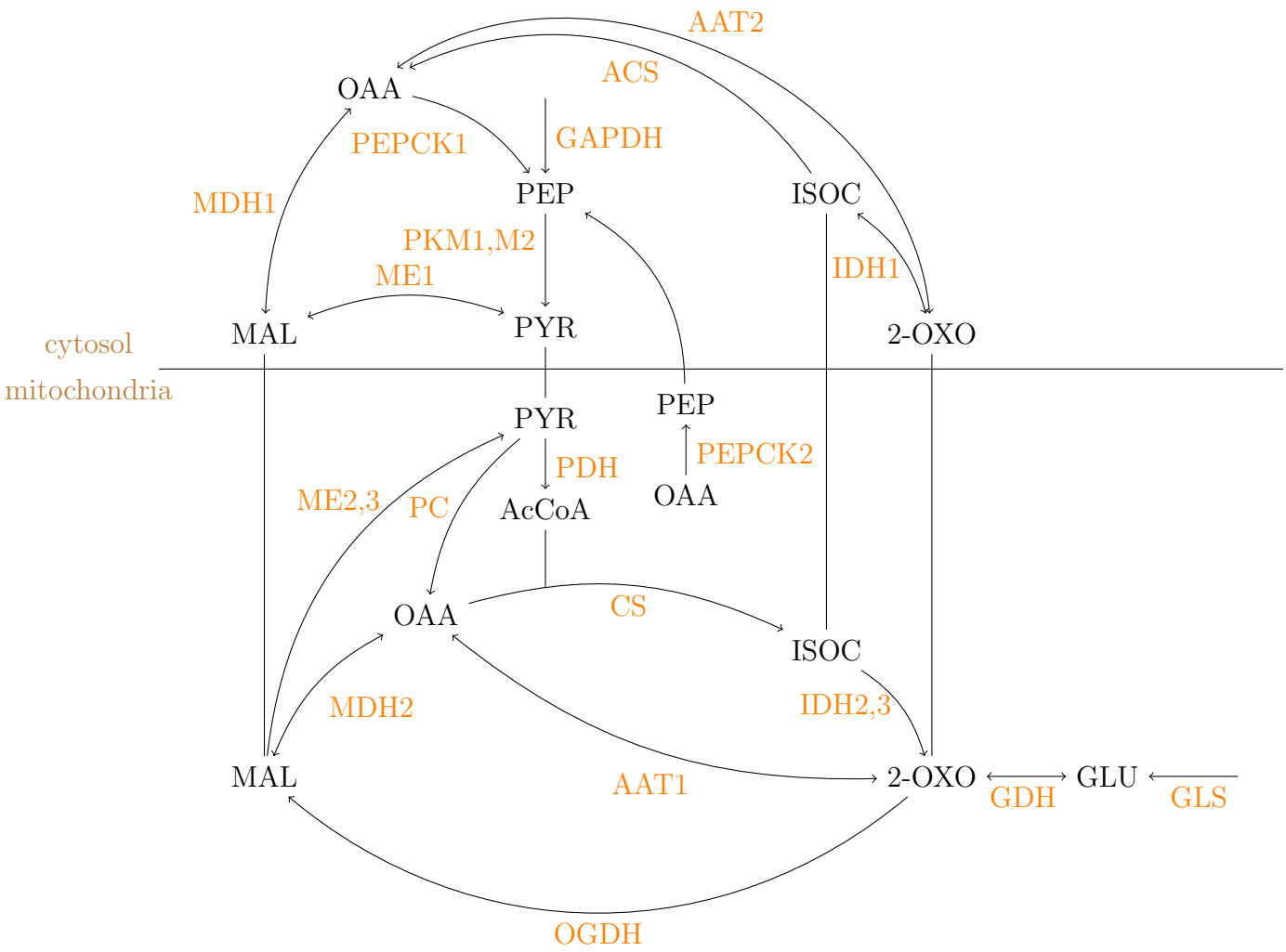

Figure 2.1: Reactions considered in our model of mitochondrial metabolism.

$$\dot{x}_{10} = (-V_{ME_3} + V_{GDH_2} - V_{IDH_2})/[NADP]_{tot}$$
$$\dot{x}_{11} = (V_{GLS} + V_{AAT_1} + cV_{AAT_2} + V_{GDH_1} + V_{GDH_2})/P_{11}^{GLS}$$
$$\dot{x}_{12} = (c\ V_{GPDH} + V_{PEPCK_2} + c\ V_{PEPCK_1} - c\ V_{PK})/S_{12}^{PK}$$

where the coefficients f_i are computed in eq.2.1 and c is the ratio between cytosolic and mitochondrial volume. Each flux is described in detail in Sec.2.1. Notice that we have two inputs, namely the influx of PEP by GAPDH and the flux of glutamate that enters through GLS.

In accordance to [212], to which we refer for a more in-depth explanation, we

Variable	*Species*	*Normalization constant*	*Value* [mM]
x_1	Isocitrate (mitochondrial)	$S_1^{IDH_3}$	0.6
x_2	2-oxoglutarate (mitochondrial)	S_2^{OGDH}	3
x_3	Malate (mitochondrial)	$S_3^{MDH_2}$	3
x_4	Oxalacetate (mitochondrial)	S_4^{CS}	0.009
x_5	Oxalacetate (cytosolic)	$P_5^{MDH_1}$	0.06
x_6	Pyruvate (mitochondrial)	S_6^{PDH}	0.1
x_7	CoA (mitochondrial)	$[CoA]_{tot}$ (mitochondrial)	0.1
x_8	NADH (mitochondrial)	$[NAD_m]_{tot}$ (mitochondrial)	0.3
x_9	NADH (cytosolic)	$[NAD_c]_{tot}$ (cytosolic)	0.05
x_{10}	NADP (mitochondrial)	$[NADP]_{tot}$ (mitochondrial)	0.2
x_{11}	Glutamate (mitochondrial)	P_{11}^{GLS}	5
x_{12}	Phosphoenolpyruvate (cytosolic)	S_{12}^{PK}	0.07

Table 2.1: Normalization constant corresponding to each variable of the model.

approximate the mitochondrial carriers as being in quasi equilibrium. In this way we can compute the cytosolic concentrations of those metabolites for which we consider only the mitochondrial fraction, see Tab.2.1.

First, pyruvate is transported across the mitochondrial inner membrane in exchange for a hydroxide ion through an antiport. This process can be described by the equation:

$$\frac{[\text{pyruvate}]_{mit}}{[\text{pyruvate}]_{cyt}} = \frac{[H^+]_{cyt}}{[H^+]_{mit}} = K_{anti}^{pyr} \approx 2.$$

Malate is exchanged electroneutrally with divalent phosphate by means of the dicarboxylate carrier:

$$\frac{[\text{malate}]_{mit}}{[\text{malate}]_{cyt}} = \frac{[P_i^{2-}]_{mit}}{[P_i^{2-}]_{cyt}} = K_{anti}^{mal} \approx 4.$$

Malate and 2-oxoglutarate are carried across the mitochondrial membrane by means of an electroneutral antiport, therefore we can also write:

$$\frac{[\text{2-oxoglutarate}]_{mit}}{[\text{2-oxoglutarate}]_{cyt}} = K_{anti}^{mal}.$$

Furthermore, malate is electroneutrally exchanged for a trivalent (iso)citrate molecule and a proton through the tricarboxylate carrier:

$$\frac{[\text{citrate}]_{mit}}{[\text{citrate}]_{cyt}} = \frac{[\text{isocitrate}]_{mit}}{[\text{isocitrate}]_{cyt}} = K_{anti}^{mal}\frac{[H^+]_{cyt}}{[H^+]_{mit}} = K_{anti}^{cit} \approx 8.$$

Glutamate is transported with a proton or in exchange with a hydroxide ion. Here, we assume that glutamate attains equilibrium according to the pH difference:

$$\frac{[\text{glutamate}]_{mit}}{[\text{glutamate}]_{cyt}} = \frac{[H^+]_{cyt}}{[H^+]_{mit}} = K^{glu}_{port} \approx 2.$$

Aspartate is transported through an electrogenic antiport in exchange for glutamate and a proton. We use the Nernst equation and write:

$$\frac{[\text{aspartate}]_{mit}}{[\text{aspartate}]_{cyt}} = K^{glu}_{port}\ e^{\frac{-\Delta\mu F}{RT}} = K^{asp}_{anti}$$

where $\Delta\mu$ is the proton motive force which is about 200 mV, F represents the Faraday constant, R is the gas constant and T is the absolute temperature.

We assume that the aconitase reaction is in quasi-equilibrium:

$$\frac{[\text{isocitrate}]_{mit}}{[\text{citrate}]_{mit}} = K^{aco}_{eq}.$$

Lastly, the coefficients f_i can be computed as:

$$\begin{aligned} &f_1 = K^{aco}_{eq}K^{cit}_{anti}/(c\ (1 + K^{aco}_{eq}) + K^{cit}_{anti}(1 + K^{aco}_{eq})),\\ &f_2 = K^{mal}_{anti}/(c + K^{mal}_{anti}), \quad f_3 = K^{mal}_{anti}/(c + K^{mal}_{anti}), \quad f_6 = K^{pyr}_{anti}/(c + K^{pyr}_{anti}). \end{aligned} \tag{2.1}$$

The entire mathematical model was implemented in MATLAB through the package SimBiology.

2.1 Rate equations

To compact the rate equations we use the following notation. The terms s_i denote the ratio between the i-th normalization parameter and the half-saturation point of the corresponding metabolite. We use them when the i-th species plays the role of a substrate in the reaction. Analogously, p_i and m_i are computed in the same way but they indicate that the metabolite is, respectively, a product or an effector in the reaction. The majority of the reactions in our model derive from the following archetypes relative to irreversible Michaelis-Menten (MM) equations

$$V = V_f\ \frac{\prod_k^k s_k x_k}{\prod_k (1 + s_k x_k)}$$

and reversible MM rates

$$V = \frac{V_f \prod^{k} s_k x_k - V_r \prod^{k} p_k x_k}{\prod^{k} (1 + s_k x_k + p_k x_k)}$$

where V_f and V_r denote respectively the maximal flux rate in the forward and reverse direction. In case there is a modifier x_i that affects the maximal rate or the half saturation point, it is sufficient to modify the rates in the following way:

$$V = \frac{(1 + m_{if} x_i) V_f \prod^{k} s_k x_k - (1 + m_{if} x_r) V_r \prod^{k} p_k x_k}{\prod^{k} ((1 + m_{ik} x_i) + s_k x_k + p_k x_k)}.$$

For the rest of the chapter, we are going to consider each enzyme taken individually and we are going to indicate its different isoenzymes as well as their expression in cancer. Then we are going to evaluate the rate equation that we deemed more appropriate according to its kinetics.

Glyceraldehyde-3-phosphate dehydrogenase

In our model the GAPDH reaction represents the net flux of phosphoenolpyruvate into the system. The glycolytic flux is affected by NAD and is also subject to product inhibition by NADH [209]. We do not consider the possible dynamics of other glycolytic intermediates.

$$V = V_f \ \frac{s_9(1 - x_9)}{1 + s_9(1 - x_9) + m_9 x_9}$$

Glycerol-3-phosphate dehydrogenase

Reaction

$$\text{G3P} + \text{NAD}^+ \longleftrightarrow \text{DHAP} + \text{NADH} + \text{H}^+$$

The dependence of cytosolic G3PDH on NADH is modelled as an irreversible MM equation reaction where the irreversibility assumption stems from the coupling of the reaction to that of the mitochondrial G3PDH isozyme, which is coupled to the respiratory chain.

$$V = V_f \ \frac{s_9 x_9}{1 + s_9 x_9}$$

Pyruvate Kinase

Reaction

PEP+ADP $\longrightarrow$ PYR+ATP

Isoenzymes

- PKM1: expressed in tissues with high catabolic demands (e.g. muscle, heart, brain).
- PKM2: embryonic isoform also expressed in cancer and normal proliferating cells (e.g. lymphocytes and intestinal epithelium). It can be found in some non proliferating tissues such as quiescent T cells, lung and white adipose tissue.
- PKR: found exclusively in red blood cells.
- PKL: the major isoform in liver, also expressed to a lesser extent in kidney.

Expression in cancer

The presence of PKM2 activity is usually indicative of malignant tumours [154]. Furthermore, many human breast cancers express little to none pyruvate kinase activity suggesting the prevalence of the dimeric form [158],[155].

On the other hand in [152] is reported that in different cell lines tumorigenic cells have higher PK activity than non tumorigenic ones.

Kinetics of PKM1

Every isoform has a similar regulation with respect to ADP. The M1-type shows hyperbolic kinetics and is not activated by fructose-1,6-bisphosphate (FB6).

Kinetics of PKM2

This isoform is very tightly regulated, the major allosteric effectors are FB6, serine (activators) and alanine (inhibitor).

The list of inhibitors also includes amino acids like cysteine, methionine, phenylalanine, valine, leucine and saturated or mono-unsaturated fatty acids.

The enzyme exists in two states: an activated form (tetrameric) and an inactived one (dimeric). It seems to act as a metabolic sensor and determines whether the glucose carbons are degraded to pyruvate and lactate with production of energy (highly active tetrameric form) or are channeled into synthetic processes (nearly inactive dimeric form).

FB6-activated PKM2 exhibits almost the same kinetics of PKM1 but shows sigmoidal activation by PEP.

In our model we supposed PKM2 was in its activated form since we are interested in modelling mitochondrial metabolism when it has a significant effect. In particular PKM2 exhibits sigmoidal kinetics with respect to FB6.

$$V = V_f \frac{s_{ADP}\ (s_{12}x_{12})}{(1 + (s_{12}\ x_{12}))\ (1 + s_{ADP})}$$

where $s_{ADP} = [\mathrm{ADP}_c]/\mathrm{K}_{ADP}$.

Phosphoenolpyruvate Carboxykinase

Rection

GTP+OAA $\longleftrightarrow$ GDP+PEP

Isoenzymes

- PEPCK1: cytosolic form, it is expressed in liver, kidney and adipose tissue.
- PEPCK2: mitochondrial form, it is expressed in a variety of non-gluconeogenic tissues such as pancreas, brain, leukocytes, heart and neurons.

Transport out of mitochondria

After PEP is produced in the mitochondria by PEPCK2 it has been reported an efflux of the same metabolite to the cytosol [163] suggesting the existence of a specific transporter. At the moment ANT (adenine nucleotide transporter) and CIC (citrate-isocitrate carrier), modelled in [167], have been identified as possible candidates but it has been postulated that there are still unknown mechanisms involved [164], [165], [166].

Given the absence of definitive information, we suppose that the totality of PEP produced in the mitochondria goes directly in the cytosol leaving $[\mathrm{PEP}_m]$ constant.

Expression in cancer

Whereas in mice and rat PCK1 accounts for over 90% of total PEPCK activity, in both pigs and humans each isoenzyme is responsible for about 50% of total PCK activity[162]. In a wide variety of tumours, that includes breast cancer, PEPCK2 is highly expressed whereas PEPCK1 is below the detection level [160], [161].

Kinetics of PEPCK2

Its kinetics are very similar to the cytosolic form, the only notable difference is that the MM constant for GDP is an order of magnitude lower than PCK1. The enzyme follows MM kinetics regarding every substrate, furthermore it requires Mn^{2+} ions to be active. Its specificity constant is 100 fold larger for oxaloacetate than for phosphoenolpyruvate suggesting that oxaloacetate phosphorylation is the favoured reaction in vivo [162].

Mitochondrial PEP is not considered as a dynamic variable. We modelled both the cytosolic and mitochondrial isoform as reversible MM reactions, respectively:

$$V = \frac{V_f \ s_5 x_5 - V_r \ p_{12} x_{12}}{1 + s_5 x_5 + p_{12} x_{12}}$$

$$V = \frac{V_f \ s_4 x_4 - V_r \ s_{PEP}}{1 + s_4 x_4 + s_{PEP}}$$

where $s_{PEP} = [\mathrm{PEP}_m]/\mathrm{K}_{PEP}$.

Lactate Dehydrogenase

Reaction

$$\mathrm{PYR+NADH} \longleftrightarrow \mathrm{LAC+NAD^+}$$

Isoenzymes

- LDH1: expressed in the heart, the red blood cells as well as in the brain.
- LDH2: located in the reticuloendothelial system.
- LDH3: found in the lungs.
- LDH4: expressed in the kidney, placenta and pancreas.
- LDH5: located in the liver and striated muscle.

Expression in cancer

The isoenzyme LDH5 was found in the majority of cancer cell lines and its expression seems to be directly correlated to the malignancy of the tumour. The greater part of LDH activity appears to be from LDH1, LDH2, LDH3 [154]. Moreover LDH5 is usually overexpressed in breast cancer cells [153].

Kinetics

In the forward reaction (i.e. formation of lactate) it shows sigmoidal kinetics with respect to both NADH and pyruvate, on the other hand the reverse reaction follows MM kinetics with both substrates [168].

For simplicity we modelled it as an irreversible reaction since in vivo it follows the direction of lactate production.

$$V = V_f \ \frac{(s_6 \ x_6)^{h_6} \ (s_9(1-x_9))^{h_9}}{(1+(s_6 \ x_6)^{h_6})(1+(s_9(1-x_9))^{h_9})}$$

Pyruvate Dehydrogenase Complex

Reaction

$$\text{PYR+CoA}^{-}\text{+SH+NAD}^{+} \longleftrightarrow \text{AcCoA+NADH+CO}_2\text{+H}^{+}$$

Expression in cancer

In normal tissues SIRT3 (NAD-dependent deacetylase sirtuin-3) increases PDH activity through deacetylation, from the study of *Ozden et al* [169] it was shown that at least one copy of SIRT3 was deleted in 40% of breast and ovarian cancers. Cells lacking SIRT3 exhibit also abnormally high concentrations of ROS and glucose consumption.

Moreover it was detected an overexpression of pyruvate dehydrogenase kinases (PDK) that leads also to reduced PDH activity [170].

In [171] were detected two different types of metabolism in breast cancer cells: the first was characterized by high glycolysis, low glutamine intake and high PDK1; the second by higher oxphos and glutamine intake.

Kinetics

The PDH complex exhibits complex regulatory patterns involving activation by Ca^2+ as well as regulation through phosphorylation and dephosphorylation. The enzyme is subject to competitive product inhibition by Ac-CoA with respect to CoA and by NADH with respect to NAD.

$$V = V_f \ \frac{s_6 x_6 \ s_7 x_7 \ s_8(1-x_8)}{(1+s_6 x_6)(1+s_7 x_7+m_7(1-x_7))(1+s_8(1-x_8)+m_8 x_8)}$$

Glutaminase

In our model GLS activity represents the net influx of glutamate in the system. As described in Sec.1.2.2 it accounts for the algebraic sum of different fluxes.

Reaction

$$GLN+H_2O \longleftrightarrow GLU+NH_3$$

Isoenzymes

Two genes, GLS1 and GLS2, encode for different phosphate-activated glutaminases (PAGs) [203]. More precisely:

- GLS1: kidney-type PAG (K-PAG) and glutaminase C (GAC). Expressed mainly in kidney, brain, heart, placenta, lung and pancreas.
- GLS2: liver-type PAG (L-PGA) and glutaminase B (GAB), expressed mainly in the liver.

Expression in cancer

Co-expression of both transcripts and higher amounts of L-type mRNA were always found in various cancer cells [204].

Kinetics

The main kinetic differences consist in the dependence of the activator inorganic phosphate (P_i), low for L-type and high for K-type, and the relative affinity for glutamine, higher in K- than in L-types. Moreover glutamine has an inhibitory effect only for the K-type isozymes [205, 206]. In our model we consider the K-type isoenzyme, consequently the reaction is:

$$V = V_f \frac{p_{11}x_{11}}{1 + p_{11}x_{11}}$$

Pyruvate Carboxylase

Reaction

$$PYR+ATP+HCO_3^- \longrightarrow OAA+ADPH+P_i$$

Expression in cancer

The involvement of PC in breast cancer cell lines was tested in [173], in particular they found abundance of both PC mRNA and protein in more invasive cell

lines with respect to the others. They also observed a 50% reduction of cell proliferation, migration, under both glutamine-dependent and glutamine-depleted conditions, following siRNA-mediated knockdown. On the other hand an overexpression of PC in MCF-7 cells resulted in a 2-fold increase in their proliferation rate, migration and invasion abilities.

Furthermore another study highlighted an increase in PC activity in lung metastatic cells compared to the primary breast tumour, [174].

Kinetics

The reaction catalyzed by PC uses, in addition to pyruvate, both MgATP and HCO_3^- substrates, the two latter species not being included in the present model and thus assumed to be constant. Ac-CoA acts as a strong activator of the enzyme, both lowering the K_m value of pyruvate and increasing V_f, [176], [175].

$$V = V_f \frac{s_6 x_6 (1 + a_7 m_7 g_7 s_7 (1 - x_7))}{(1 + a_7 m_7 s_7 (1 - x_7)) \left(s_6 x_6 + (1 + m_4 x_4) \dfrac{1 + m_7 s_7 (1 - x_7)}{1 + a_7 m_7 s_7 (1 - x_7)} \right)}$$

Citrate synthase

Reaction

$$\text{AcCoA+OAA+H}_2\text{O} \longrightarrow \text{CIT+CoA-SH}$$

Expression in cancer

Human cancer cell lines exhibit a wide spectrum of CS expression levels. Very low CS expression was found in MCF7 cell line and it coincided with an overexpression of glycolytic enzymes expression and a deficit in the respiratory activity; moreover the inhibition of CS lead to an augmented malignancy [177]. On the other hand in ovarian tumours, higher CS activity was found to be linked to higher malignancy [178].

Kinetics

CS is regulated by many metabolites, including inhibition by ATP and succinyl-CoA which are not included in the present model. In addition, it is subject to product inhibition by CoA, which is a competitive inhibitor for aC-CoA

$$V = V_f \frac{s_4 x_4 s_7 (1 - x_7)}{(1 + s_7 (1 - x_7) + m_7 x_7)(1 + s_4 x_4 + m_1 x_1)}$$

Isocitrate Dehydrogenase

Reaction

$$\text{ISOC}+\text{NAD}^+ \longrightarrow \text{2-OXO}+\text{CO}_2+\text{NADH}+\text{H}^+$$

$$\text{ISOC}+\text{NADP}^+ \longleftrightarrow \text{2-OXO}+\text{CO}_2+\text{NADPH}+\text{H}^+$$

$$\text{ISOC}+\text{NADP}^+ + \text{Mg}^{2+} \longleftrightarrow \alpha\text{-KG}+\text{NADPH}+\text{CO}_2+\text{H}^+$$

Isoenzymes

- IDH1: cytosolic, $NADP^+$-dependent. It is highly expressed in mammalian liver and moderately in other tissues.
- IDH2: mitochondrial, $NADP^+$-dependent. It is highly expressed in mammalian heart, muscle, and activated lymphocytes and moderately elsewhere.
- IDH3: mitochondrial, NAD^+-dependent.

Expression in cancer

Mutations in one of the IDH1 and IDH2 are associated with different subtypes of cancer, in particular gliomas and leukemias. The IDH forward reaction, isocitrate decarboxylation, is inactivated by the common mutations associated with cancers. These mutations are particularly notable since they cause neomorphic activity, that is these mutant IDHs produce 2HG (2-hydroxyglutarate) from NADPH and KG. This leads to the accumulation of 2HG that acts as an inhibitor of αKG-dependent enzymes. Furthermore mutations of IDH1 appear to increase its affinity for NADPH, which may promote reduction of αKG to 2HG under low concentrations of NADPH [182], [183], [181].

Kinetics

NAD-dependent IDH is activated by Ca^{2+} and ADP, whereas it is inhibited by ATP and NADH. Among these species, only NADH is included in our model. More specifically, the inhibition exerted by NADH is competitive with respect to NAD. Moreover, IDH_m exhibits cooperativity with a Hill coefficient of almost 3.

$$V = V_f \, \frac{s_8(1-x_8)(s_1x_1)^h}{(1+(s_1x_1)^h)(1+s_8(1-x_8)+m_8x_8)}$$

NADP-dependent IDH (here abbreviated IDHP_m) is not generally considered to be allosterically regulated, but it exhibits competitive product inhibition of NADPH with respect to NADP.

$$V = V_f \ \frac{s_1 x_1 s_{10} x_{10}}{(1 + s_1 x_1)(1 + s_{10} x_{10} + m_{10}(1 - x_{10}))}$$

Regarding cytosolic NADP-dependent IDH (IDHP_c), we have neglected the kinetic regulation by NADPc and therefore we modelled it with Michaelis-Menten kinetics:

$$V = V_f \ \frac{s_1 x_1}{1 + s_1 x_1}$$

2-Oxoglutarate Dehydrogenase

Reaction

α-KG+NAD^++CoA $\longrightarrow$ Suc-CoA+CO_2+NADH

Here, for simplicity, we have summed up the three reactions catalyzed by OGDH (succinate-CoA ligase, succinate dehydrogenase and fumarate hydratase) into a single, and physiologically irreversible, reaction controlled by the enzyme OGDH.

Expression in cancer

OGDH is often considered to be switched off in tumours due to mutations of isocitrate dehidrogenase, succinate dehydrogenase and fumarate hydratase [182, 189, 190]. However the flux through the mitochondrial TCA cycle in cancer remains under debate [188].

Kinetics

The OGDH complex is allosterically regulated by Ca^2+, however this property that is not considered in our model. It is also subject to product inhibition by succinyl-CoA and NADH, the former of which is not included here. Inhibition by NADH is close to noncompetitive [185].

$$V = V_f \ \frac{(1 + m_8 g_8 x_8) s_2 x_2 \ s_8(1 - x_8) \ s_7 x_7}{(1 + m_8 x_8)(1 + s_2 x_2)(1 + s_8(1 - x_8))(1 + s_7 x_7)}$$

Malate Dehydrogenase

Reaction

$$\text{MAL}+\text{NAD}^+ \longleftrightarrow \text{OAA}+\text{NADH}+\text{H}^+$$

Isoenzymes

- MHD1: cytoplasmic
- MDH2: mitochondrial

Expression in cancer

There is some indication that MDH activity is increased in breast cancer cells [153].

Kinetics of MDH1

MDH1 is not allosterically regulated, consequently it is here modelled with a reversible Michaelis-Menten equation. We have ignored inhibition by oxaloacetate since it occurs only at unphysiological concentrations [193].

$$V = \frac{V_f\ s_3x_3s_9(1-x_9) - V_r\ p_5x_5p_9x_9}{(1+s_3x_3+p_5x_5)(1+s_9(1-x_9)+p_9x_9)}$$

Kinetics of MDH2

On the other hand, MDH2 is allosterically regulated in a peculiar manner [191], in fact citrate may act as an inhibitor or an activator for the malate oxidation reaction, depending on the NAD concentration. More precisely, citrate increases the effective limiting rate of MDH2 while at the same time also increases the half-activation points for malate and NAD. In the reverse direction, citrate increases the half-activation point for NADH while leaving the half-activation point for oxaloacetate and the limiting rate unchanged.

$$V = \frac{(1+m_1a_{13}a_{18}g_1x_1)(V_f\ s_3x_3s_8(1-x_8) - V_r\ p_4x_4p_8x_8)}{\begin{array}{l}(1+m_1a_{18}x_1)s_8(1-x_8) + (1+m_1a_{13}x_1)s_3x_3 \\ \quad +(1+m_1b_{18}x_1)p_8x_8 + (1+m_1b_{14}x_1)p_4x_4 + m_1x_1(a_{13}s_3x_3 + b_{14}p_4x_4) \\ \quad\quad (s_8(1-x_8)a_{18} + b_{18}p_8x_8) + 1 + m_1x_1 + (s_3x_3+p_4x_4)(s_8(1-x_8)+p_8x_8)\end{array}}$$

Malic Enzyme

Reaction

$$\text{MAL}+\text{NAD}^+ \longleftrightarrow \text{PYR}+\text{NADH}+\text{H}^+ + \text{CO}_2$$

$$\text{MAL}+\text{NAD(P)}^+ \longleftrightarrow \text{PYR}+\text{NAD(P)H}+\text{H}^+ + \text{CO}_2$$

$$\text{MAL}+\text{NADP}^+ \longleftrightarrow \text{PYR}+\text{NADPH}+\text{H}^+ + \text{CO}_2$$

Isoenzymes

We have three distinct isoenzymes:

- ME1: cytosolic and uses NADP^+. Found in liver and adipose tissue.
- ME2: mitochondrial and uses NAD^+ or NADP^+. Found in proliferating cells, particularly in cancer cells.
- ME3: mitochondrial and uses NADP^+. Found in tissues with low proliferating rates (e.g. heart, muscle and brain).

Expression in cancer

ME2 was found to be highly expressed in many solid tumours [195]. Moreover, In the A549 non-small cell lung cancer cell line, ME2 depletion inhibited cell proliferation and induced cell death.

In [194] was reported that cancer cells do not exhibit a noticeable ME3 activity. Furthermore, different studies have observed an overexpression of ME3 in cancer cells [158], [195].

Kinetics of ME1

ME1 is described using the reversible Michaelis-Menten equation. The enzyme is inhibited by oxaloacetate, but only at very high concentrations [199], leading us to ignore this property. Also, NADP_c and NADPH_c are not included as dynamic variables in our model.

$$V = \frac{V_f \ s_3 x_3 - V_r \ p_6 x_6}{(1 + s_3 x_3)(1 + p_6 x_6)}$$

Kinetics of ME2

This enzyme can use both NAD^+ and NADP^+ as cofactor for the oxidative decarboxylation of malate. ME2 is strongly activated by fumarate, ATP is instead

a competitive inhibitor of NAD(P)$^+$ [198, 196]. However we do not consider fumarate and ATP as dynamic variables, we consider irreversible MM with NADP$^+$ and MAL as substrates.

$$V = V_f \frac{s_3 x_3 s_8 (1 - x_8)}{(1 + s_3 x_3)(1 + s_8(1 - x_8))}$$

Kinetics of ME3

The ME3 isoenzyme presents the same allosteric effectors of ME2. However it only accepts NAD$^+$ as cofactor [200, 198].

$$V = V_f \frac{s_3 x_3 s_{10} (1 - x_{10})}{(1 + s_3 x_3)(1 + s_{10}(1 - x_{10}))}$$

Glutamate Dehydrogenase

Reaction

$$\text{GLU}+\text{H}_2\text{O}+\text{NAD}^+ \longleftrightarrow \text{2-OXO}+\text{NH}_3+\text{NADH}+\text{H}^+$$

$$\text{GLU}+\text{H}_2\text{O}+\text{NADP}^+ \longleftrightarrow \text{2-OXO}+\text{NH}_3+\text{NADPH}+\text{H}^+$$

Expression in cancer

In [201] has been observed that breast cancer cells couple glutamine and nitrogen metabolism by suppressing glutamate dehydrogenase and synthesizing amino acids via transaminases. In other words, highly proliferative breast tumours have high transaminase and low GDH expression.

Kinetics

GDH can use either NAD or NADP as an electron acceptor, therefore we model its activity as the sum of two separate fluxes. Moreover, with regard to glutamate, NAD and NADP, the reciprocal plots of reaction velocity versus substrate concentration are nonlinear, denoting a negative cooperativity behaviour.

The model is very insensitive to variations in the ammonia concentration [212]. We could not use the reversible Hill equation in this case, since negative cooperativity applies only to the oxidized pyridine species.

The form that uses NAD is modelled by:

$$V = \frac{(V_f s_2 x_2 s_8 x_8 - V_r p_{11} x_{11} p_8 (1 - x_8))(1 + a_8 m_8 (1 - x_8) + a_{10} m_{10} x_{10})}{(1 + s_2 x_2 + p_{11} x_{11})(s_8 x_8 + p_8 (1 - x_8) + (1 + m_8 (1 - x_8) + m_{10} x_{10} + 1 + a_8 m_8 (1 - x_8) + m_{10} a_{10} x_{10})(p_{10} x_{10} + s_{10} (1 - x_{10})))}$$

Whereas the part corresponding to NADP is:

$$V = \frac{(V_f s_2 x_2 s_{10}(1-x_{10}) - V_r p_{11} x_{11} p_{10} x_{10})(1 + a_{10} m_{10} x_{10} + a_8 m_8 (1-x_8))}{(s_{10}(1-x_{10}) + p_{10} x_{10} + (1 + m_{10} x_{10} + m_8(1-x_8) + (1 + a_{10} m_{10} x_{10} + a_8 m_8 (1-x_8))(p_8(1-x_8) + s_8 x_8)))(1 + s_2 x_2 + p_{11} x_{11})}$$

Aspartate aminotransferase

Reaction

2-OXO+GLU $\leftrightarrow$ OAA+ASP

Isoenzymes

- AAT1: mitochondrial isoenzyme.
- AAT2: cytosolic isoenzyme.

Kinetics

AAT catalyzes the reversible reaction between glutamate and 2-oxoglutarate versus oxalacetate and aspartate. Neither of the two isoenzymes is considered allosterically regulated. The reactions are modelled as a Ping Pong Bi Bi mechanism [211].

More precisely, the reaction corresponding to the cytosolic form is:

$$V = \frac{V_f s_2 x_2 s_{ASP} - V_r p_5 x_5 p_{11} x_{11}}{s_{ASP} + s_2 x_2 + s_{ASP} s_2 x_2 + p_5 x_5 + p_{11} x_{11} + p_5 x_5 p_{11} x_{11} K_{p2} + s_{ASP} p_5 x_5 K_{ip2} + s_2 x_2 p_{11} x_{11} K_{iq2}}$$

where s_{ASP}=[ASP_c]/K_{ASP_c}

Whereas, the reaction of the mitochondrial isoenzyme is:

$$V = \frac{V_f s_2 x_2 s_{ASP} - V_r p_4 x_4 p_{11} x_{11}}{s_{asp} + s_2 x_2 + s_{ASP} s_2 x_2 + p_4 x_4 + p_{11} x_{11} + p_4 x_4 p_{11} x_{11} K_p + s_{ASP} p_4 x_4 K_{ip} + s_2 x_2 p_{11} x_{11} K_{iq}}$$

where s_{ASP}=[ASP_m]/K_{ASP_m}

ATP Citrate Synthase

Reaction

CIT+ATP+CoA $\longleftrightarrow$ OAA+ADP+P_i + AcCoA

Kinetics

The ratio between ac-CoA and CoA, ATP and ADP are not considered as dynamic variables. Studies of the kinetics of the reaction [207, 208] motivate the use of a reversible Michaelis-Menten equation for ACS.

$$V = \frac{V_f \ s_1 x_1 - V_r \ p_5 x_5}{(1 + s_1 x_1)(1 + p_5 x_5)}$$

Respiration

Through aerobic respiration cells use the electrons taken from NADH and $FADH_2$ to reduce oxygen to water and simultaneously produce ATP. Detailed descriptions of all these processes are beyond the scope here, consequently we model the dependence of the respiratory rate on NADH in the simplest possible way [210].

$$V = V_f \sqrt{\frac{x_8}{1 - x_8}}$$

Enzyme	*Parameter*	*References*
GAPDH	V_f=180 s_9=0.25 m_9=166	[209]
GLNase	V_f=1800 p_{11}=0.4	[203]
G3DH	V_f=1800 s_9=12.5	[212]
PK	V_f=72000 s_{12}=0.07 K_{ADP}=0.26 [ADP_c] = 0.4	[157], [156], [159], [152], [154]
PEPCK1	V_f=360 V_r=14400 s_5=6 p_{12}=1.4	[162]
PEPCK2	V_f=360 V_r=0.16 s_4=1 K_{PEP}=0.6 [PEP_m]= 0	[162]
LDH	V_f=144000 s_6=0.17 s_9=0.17 h_6=1.36 h_9=2.8	[153] [168]
PDH	V_f=2160 s_6=1 s_7=1 s_8=6 m_7=3.3 m_8=7.5	[212]
PC	V_f=7200 m_4=0.09 s_6=0.025 s_7=1 m_7=10 a_7=8 g_7=15	[174], [176], [175], [153]
CS	V_f=14400 m_1=0.37 s_4=1 s_7=25 m_7=5	[179], [180], [153]
IDH3	V_f=1080 s_1=1 s_8=5 h=2 m_8=15	[184], [185], [186], [153]
IDH2	V_f=1800 s_1=30 s_{10}=667 m_{10}=667	[184], [185], [186], [153]
IDH1	V_f=1800 s_1=7.5	[184], [185], [186], [153]
OGDH	V_f=1440 s_2=1 s_7=50 s_8=7.5 m_8=60 g_8=0.3	[187], [185]
MDH1	V_f=18000 V_r= 7 s_3=0.8 p_5=1 s_9=0.12 10^7 p_9=2.5	[192], [193], [191]
MDH2	V_f=180000 V_r = 4 10^7 m_1=8.3 g_1=3 a_{13}=0.3 a_{18}=0.1 b_{14}=1 b_{18}=0.1 s_3=1 p_4=0.45 s_8=5 p_8=10	[192], [193], [191]
ME1	V_f=360 V_r=6.7 s_3=10 p_6=0.01	[194] [194], [198]
ME2	V_f=360 s_3=6 s_8=3	[196], [197], [194]
ME3	V_f=360 s_3=4.3 s_{10}=2	[196], [197], [194]
GDH_{NAD}	V_f=1800 V_r= 5.7 s_2=7.5 s_8=10 p_8=0.75 a_8=0.3 m_8=0.75 s_{10}=6.7 p_{10}=4 m_{10}=6.7 a_{10}=0.3	[212]
GDH_{NADP}	V_f=1800 V_r=5.7 s_2=3/0.4 s_{10}=6.7 p_{10}=4 p_8=0.75 s_8=10 a_8=0.3 m_8=0.75 a_{10}=0.3 m_{10}=6.7	[212]
AAT2	V_f=720 V_r=788 s_2=1.97 p_5=1.1 K_{ASP_c}=4.4 [ASP_c]= 3 p_{11}=0.18 K_{p2}=0.057 K_{ip2}=1.1 K_{iq2}=0.52	[211]
AAT1	V_f=18000 V_r=1.8 10^4 s_2=7 p_4=0.16 K_{ASP_m}=3.9 [ASP_m] = 0.001 p_{11}=0.39 K_p=0.63 K_{ip}=1.1 K_{iq}=42.75	[211]
ACS	V_f=360 V_r=0.02 s_1=0.94 p_5=0.3	[212]

Table 2.2: The flux values (namely V_f and V_r) are measured in mM/h per kg of tissue. The concentrations of the metabolites not considered as dynamic variables (ADP_c,PEP_m,ASP_c,ASP_m) are expressed in mM.

Chapter 3

Simulations

In this chapter we describe new experimental data regarding mitochondrial metabolism in breast cancer cells, consequently we use the mathematical model we developed in the previous chapter to analyse these data and to provide further insights. More specifically it was found that breast cancer cells can be divided into two distinguishable groups, namely upper fork (UF) and lower fork (LF), based on their genes expression (G. Szabadkai et al 2017, Unpublished Data),[215]. Every cell appears to belong to one group or the other, in other words it seems that it does not exist an in-between group. The aim of the present work is to characterize these two phenotypes, more specifically we are interested in knowing which enzymes are ultimately fundamental for the manifestation of each phenotype. Although we already have information about which enzymes are over-expressed at mRNA-level, it is important to recall that the activity of an enzyme is regulated across multiple checkpoints and therefore an increase in mRNA does not automatically determine an increase in the activity of the protein. Thus, the need to clarify which enzymes activity is ultimately responsible for the manifestation of UF and LF phenotypes through a mathematical model.

3.1 Upper fork and lower fork phenotypes

First of all it is appropriate to illustrate more accurately the differences between these two phenotypes in order extract which characteristics can be used to identify them in our model. Experimentally, the most striking difference on the overall behaviour is that LF cells depend heavily on external pyruvate. In fact, when the

cultured cells are deprived of an external source of pyruvate, only the UF type is able to survive. It is hypothesized that this is due to the fact that the glycolytic flux in UF cells is higher than LF cells and this enables them to compensate for the absence of external pyruvate.

However, it is important to notice that it is very problematic to express this phenomenon mathematically since cell proliferation is a complex mechanism that comprises multiple steps and involves numerous genes not considered in our model [1, 2, 3]. Therefore it is not feasible to utilize the dependence of LF cells on external pyruvate for proliferation to distinguish between the UF and LF mathematically. However it is reasonable to assume that

1. UF cells denote higher levels of pyruvate that LF.

Furthermore, additional observations that we utilised were derived from isotopic labelling. More precisely in each experiment the carbon atoms of glucose, glutamine or pyruvate were substituted with ^{13}C. In this way, after the concentration of the metabolites of the cell reached steady state, it was possible to visualize how the ^{13}C were distributed in the various metabolites. We observed the following:

2. When glucose was labelled, the total concentration of labelled metabolites was higher in UF.

3. When glutamine was labelled, the total concentration of labelled metabolites was instead higher in LF.

4. The concentrations of citrate and malate appeared to be higher in UF, on the other hand the opposite could be said about glutamate.

Regarding the first observation we also tested the quantity of extracellular glucose that each cell line absorbed, the results indicated that this amount was roughly the same both in UF and LF. Furthermore other experiments indicate:

5. UF cells show an increase in respiration with respect to LF, Fig.3.2.

To summarize, the benchmarks we considered in our model to distinguish between the UF and LF phenotype are [CITm],[MALm],[PYRm], V_{resp} (higher in UF) and V_{glut} (higher in LF).

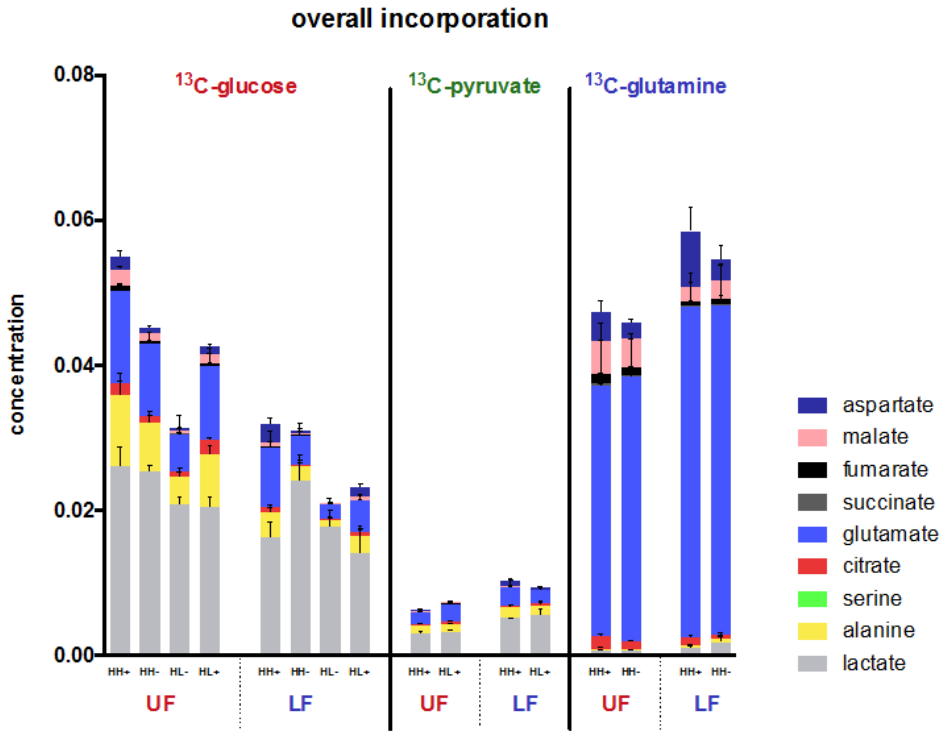

Figure 3.1: Isotopic labelling.

Now, it is fundamental to verify if it is possible to reproduce the UF and LF phenotype with our model of mitochondrial metabolism by modifying appropriately the expression of the various enzymes. In its general form this problem is a computationally prohibitive given that we have 25 enzymes (or equivalently 25 variables) in our model, therefore an exploration of the parameter space cannot be, due to its dimensionality, exhaustive. Hence, we start from some experimental data that reveal which enzymes are more expressed, at mRNA level, in each phenotype. These data are summarised in Fig.3.3: the colour red (blue) denotes the enzymes that are over-expressed in UF (LF) cells.

3.2 Ranges of over-expression

As a first simulation, we tried to replicate UF and LF phenotypes changing the expression of the enzymes randomly, accordingly to Fig.3.3. It is important to add that the genes linked to Complex I and Complex II of the electron transport chain appear to be over-expressed in UF. We represent them under the fictitious

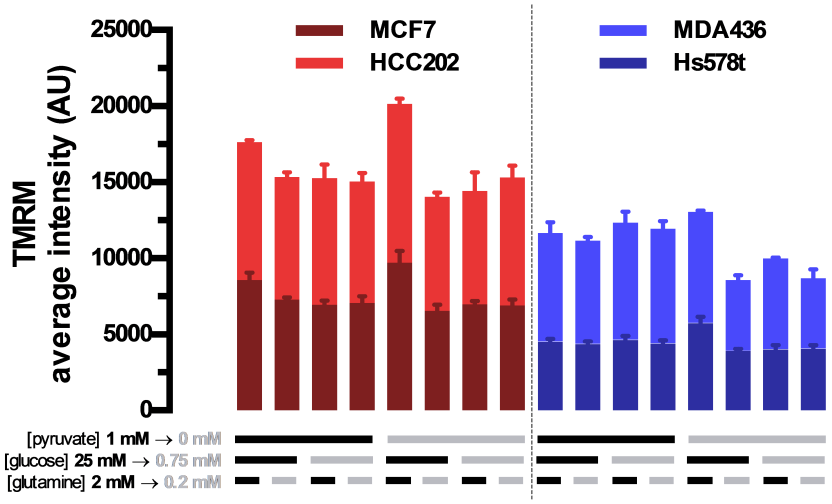

Figure 3.2: The membrane potential of mitochondria was measured using tetramethylrhodamine methyl ester (TMRM) as fluorescent probes. Different combinations of pyruvate,glucose and glutamine concentrations were tested. Notice that in our model we do not treat the mitochondrial membrane potential as a variable but we do consider the value of the respiration flux, which is strictly linked to it.

enzyme RESP.

Before commencing the simulations, notice that we already have information regarding the activity of some enzymes. In fact we observe from Fig.3.1 that UF phenotype is characterized by a value of GAPDH about 100% higher than LF; on the other hand the activity of GLS1 appears to be approximatively 50 % higher in LF. Although this does appear as a rough approximation it is important to clarify that our aim is not to find the exact values of expression but rather to give a qualitative analysis about the most relevant enzymes and possibly the equilibria that have to exist between them to manifest UF or LF phenotype. This is motivated by the fact that both the experimental data we are furnished with and the parameters of our model are characterized by significant error variance. Thus, currently a thorough quantitative analysis is out of reach. However this kind of examination can still give valuable insights as a preliminary study of the phenomena.

Regarding the other enzymes, we emulated UF by enhancing the maximum activity of the red enzymes in Fig.3.3 randomly between 0 and 3 fold; similarly we replicated LF by increasing the activity of the blue enzymes. Follow-

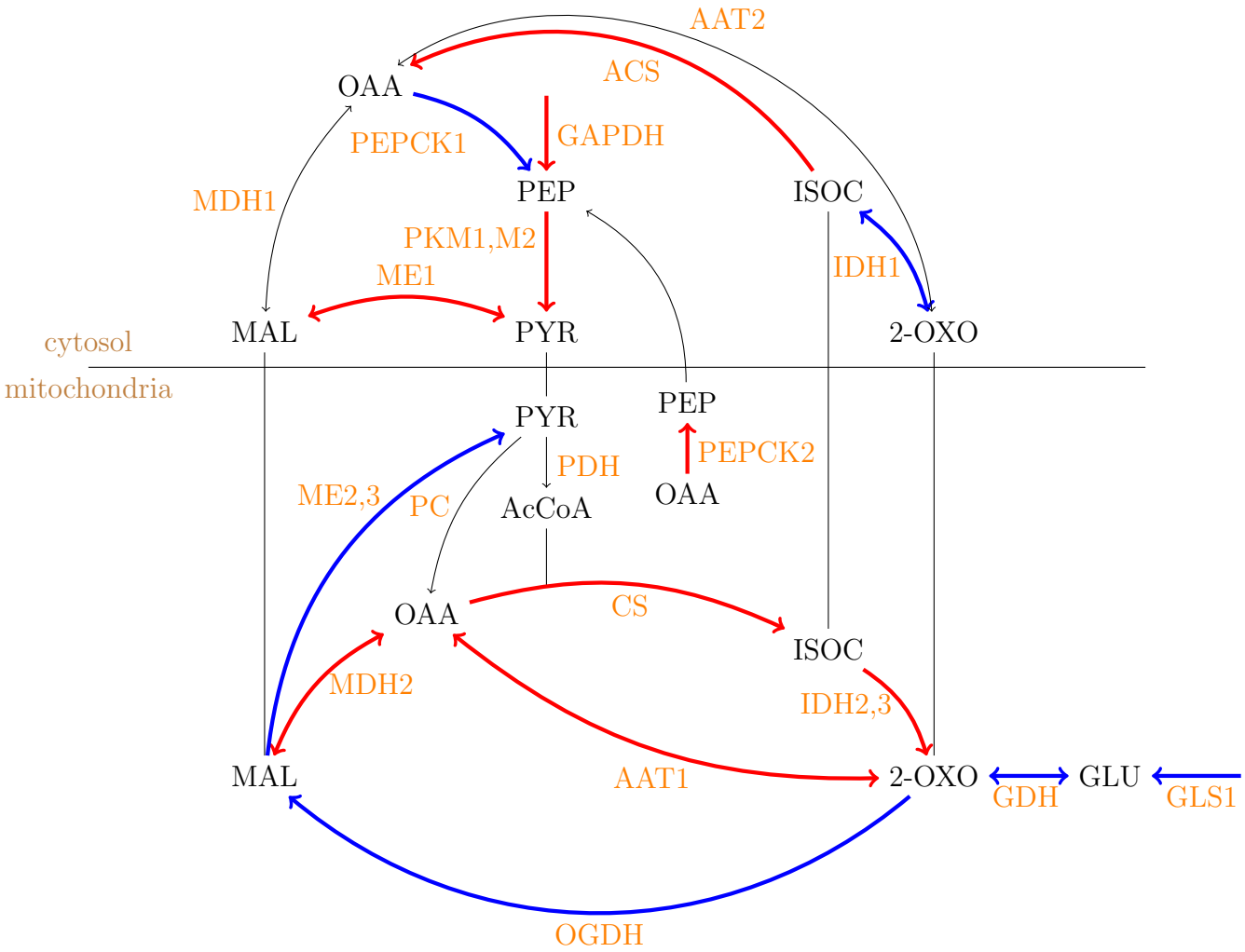

Figure 3.3: Red arrows denote enzymes more expressed in UF cells and blue arrows more expressed in LF cells.

ing this procedure, we collected 2000 samples for both UF and LF type. We recall that from our experimental data we expect UF cells to exhibit higher [PYR_m],[CIT_m],[MAL_m],V_{resp} and LF cells to show higher V_{glut}. In Fig.3.4 are reported the values of these benchmarks by the use of box plots. We immediately observe that V_{glut} is always higher when the LF enzymes are over-expressed. On the other hand, the situation is quite different regarding [CITm], [MALm], [PYRm], V_{resp}. Although we expected values significantly higher in UF, we notice that this is not always the case, especially if we observe the box plots depicting [MAL] and [PYR].

The natural follow-up question is: *"What are the levels of enzymes expression that determine UF and LF phenotype ?.* More precisely, how can we maximize the benchmarks in the UF case and how can we minimize them in the LF case?

To conduct this type of analysis we split the samples of each parameter into two clusters through a K-means algorithm, as can be seen in Fig.3.5. Moreover we notice that some of the samples are in accordance with the experimental data, see Fig.3.6.

For each enzyme E, we then introduced a coefficient μ_E denoting its activation (i.e. we multiplied the corresponding V_M by μ_E). Notice that $0 < \mu_E < 1$ can be seen as a repression of the activity of the enzyme E whereas $\mu_E > 1$ as an increase of it. Thus, in the following paragraphs, we will analyse the relations between μ_E and the benchmarks values.

This is a complex problem since we have numerous variables (10 enzymes in UF and 8 in LF) therefore a thorough exploration of the parameter space is infeasible. However it may not even be necessary to attempt such an exploration since, maybe, only a couple of enzymes play an important role in determining the values of the benchmarks at steady state.

3.2.1 Gains of the enzymes involved

As a preliminary examination, it is quite intuitive to study the effect of each enzyme taken singularly. Consequently we varied each μ_E from 1 to 5 and we gathered the corresponding gains of the values of [CIT_m], [MAL_m], [PYR_m], V_{glut} (glutamate net production), V_{resp} at steady state, Tab.3.1.

Already from a superficial inspection of Tab.3.1 we can notice that inside the

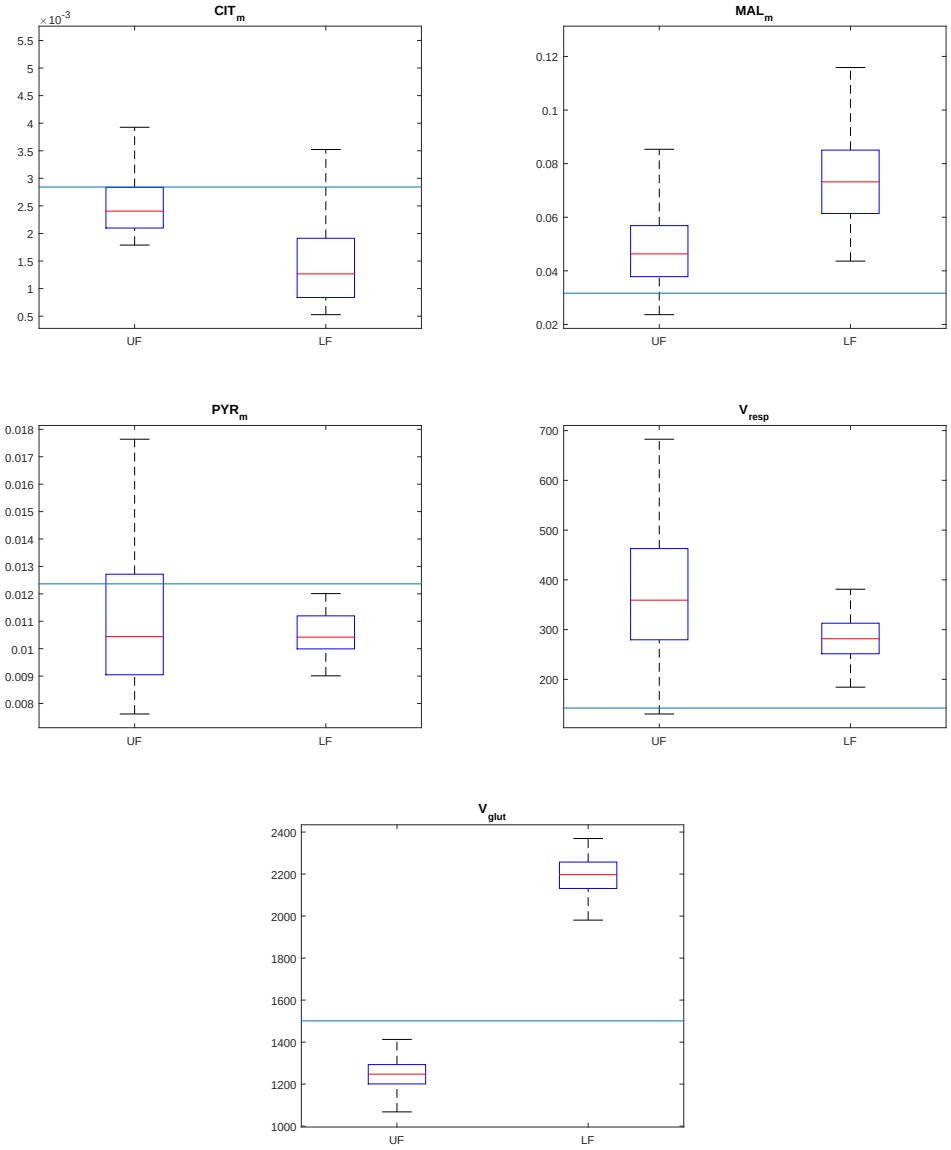

Figure 3.4: Boxplots of the parameters in UF and LF. The horizontal line in light blue represent the value when no enzyme is over-expressed (i.e. $\mu_E = 1$, for each enzyme). The metabolites concentrations are measured in mM and the fluxes in $\frac{\text{mM}}{\text{h}}$ per Kg of tissue.

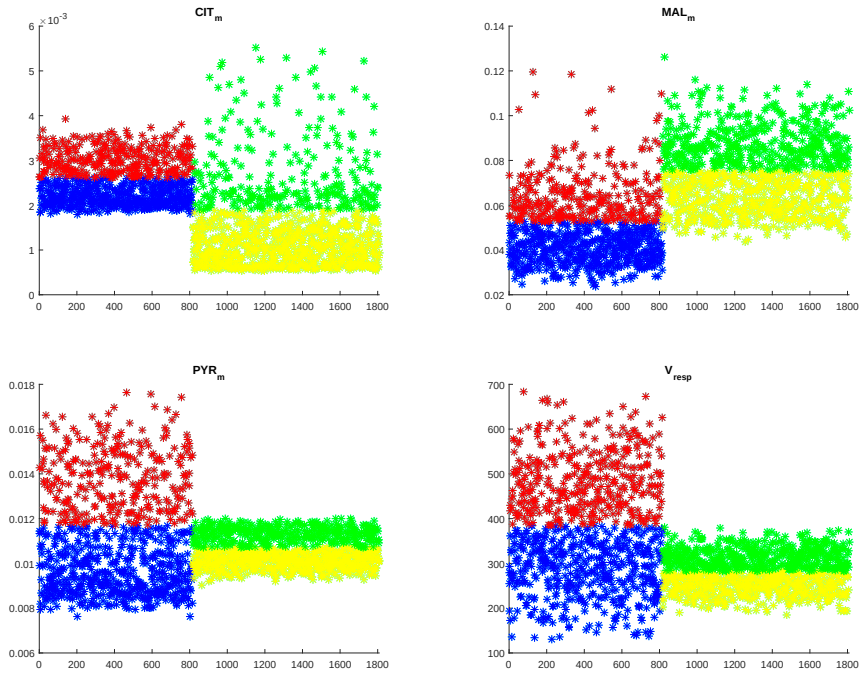

Figure 3.5: The samples of each parameter are split into two clusters through a K-means algorithm. The left part of each figure depicts the values of each parameter obtained in UF, the other half represents those corresponding regarding LF. The points of UF that belong to the lower cluster are coloured in blue whereas those who belong to the higher cluster are in red. Similarly the points of LF are coloured in yellow or green depending on which cluster they belong.

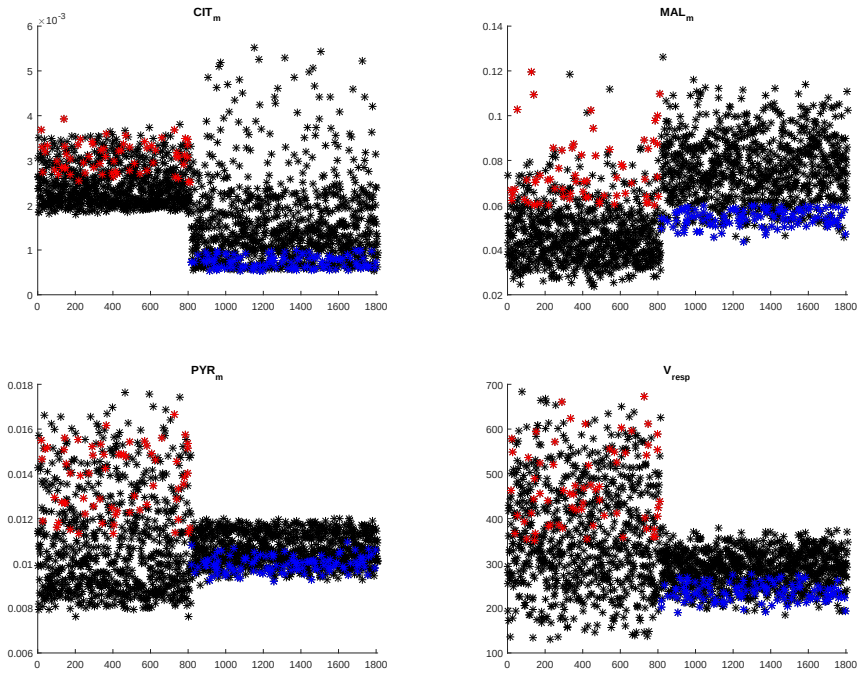

Figure 3.6: A subset of the samples that is in accordance with the experimental data.

same group coexist enzymes with contrasting impacts. For example OGDH and ME3, both over-expressed in LF cells, cause opposite effects regarding [MAL_m]. Therefore we expect that there has to be a balance between the expression of different enzymes in order to obtain UF or LF phenotype.

In the next section we will analyse the UF and LF phenotype, taken singularly, to identify the enzymes that are most significant to manifest each phenotype.

The procedure will be the following in both cases. First, we are going to highlight the sets of μ for which every benchmark belongs to the upper (and lower) cluster. In particular we will denote these sets *upper UF/LF* (*lower UF/LF*). Thereafter we are going to draw some observations from the distribution of each μ_E in upper UF/LF and lower UF/LF and we are going to verify them graphically.

3.2.2 Lower fork analysis

The first noticeable difference in the distributions of μ is related to OGDH, in fact out of the 132 sets in upper LF only 7 exhibit $\mu_{OGDH} < 2$. On the other hand, in lower LF about half of the sets denote values of μ_{OGDH} in the same

	$\frac{\Delta[CIT_m]}{[CIT_m]}$	$\frac{\Delta[MAL_m]}{[MAL_m]}$	$\frac{\Delta[PYR_m]}{[PYR_m]}$	$\frac{\Delta V_{resp}}{V_{resp}}$	$\frac{\Delta V_{glut}}{V_{glut}}$
GAPDH	0.6	1.8	0.9	0.21	-0.08
ME1	0.08	-0.61	0.12	-0.37	0.09
CS	0.68	-0.37	0.075	0.06	0.07
RESP	0.08	-0.37	0.088	0.95	<0.01
LDH	-0.33	-0.33	-0.3	-0.2	0.04
IDH2	<0.01	<0.01	<0.01	<0.01	<0.01
MDH2	<0.01	<0.01	<0.01	<0.01	<0.01
AAT1	<0.01	<0.01	<0.01	0.16	0.015
AAT2	-0.08	0.09	-0.02	0.26	-0.14
ACS	-0.09	-0.01	<0.01	<0.01	<0.01
PEPCK2	-0.19	0.48	<0.01	-0.13	<0.01
GLS1	<0.01	<0.01	<0.01	<0.01	4
OGDH	-0.05	0.3	-0.08	0.48	-0.19
ME3	-0.14	-0.5	-0.13	-0.26	0.1
IDH1	-0.6	0.09	0.05	<0.01	<0.01
ME2	0.03	-0.16	0.026	0.15	0.03
PEPCK1	<0.01	-0.09	<0.01	-0.03	<0.01
GDH	-0.01	<0.01	<0.01	<0.01	<0.01
PDH	0.3	-0.2	-0.5	0.27	0.07
MDH1	-0.08	0.06	-0.1	0.3	-0.19
PC	0.3	0.5	-0.13	-0.14	-0.1
PK	0.04	-0.44	0.05	-0.27	0.07

Table 3.1: This table reports the fraction changes of the outputs in response to a variation of each activation coefficient μ_i from 1 to 5. Red enzymes are over-expressed in UF phenotype whereas blue ones in the LF cells. Red gains denote effects in accordance to UF phenotype and blue to LF phenotype.

interval, Fig.3.7.

Moreover from Fig.3.8, we notice that μ_{ME3} in lower LF has a minimum value of 1.62 suggesting that high activity of ME3 is a necessary condition to have low benchmarks, in particular regarding [MAL].

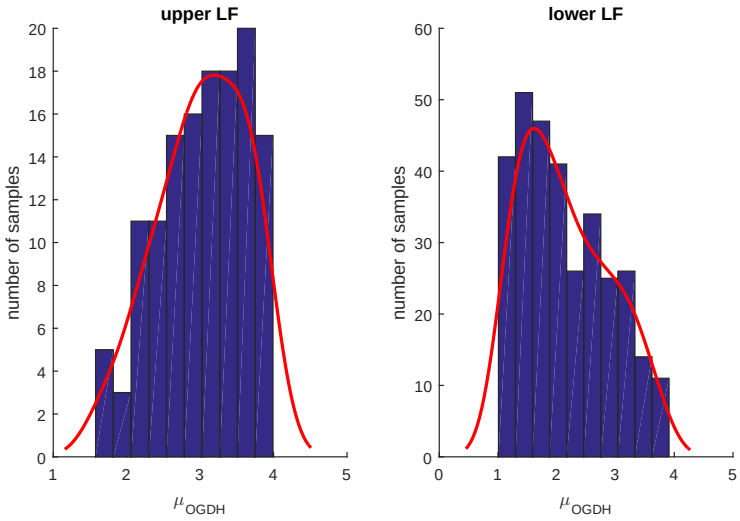

Figure 3.7: Number of samples of upper/lower LF as function of μ_{OGDH}. The red line denotes a kernel distribution fit. Upper (lower) LF indicates the set of μ_E such that every parameter belongs to the upper (lower) cluster.

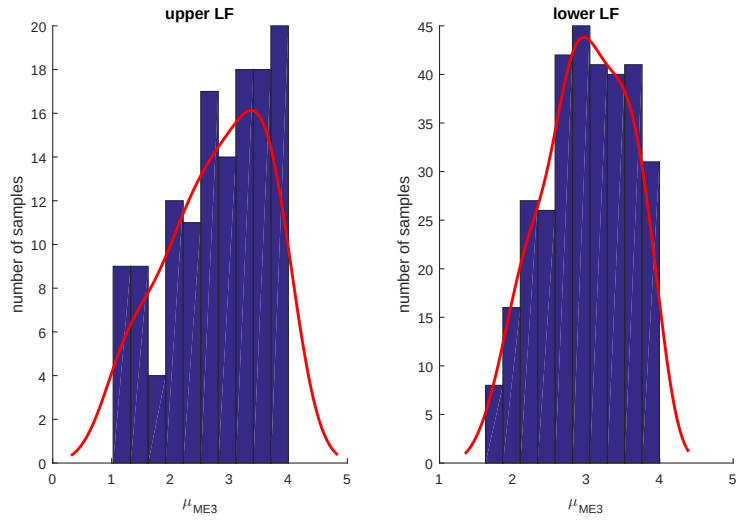

Figure 3.8: Number of samples of upper/lower LF as function of μ_{ME3}. The red line denotes a kernel distribution fit. Upper (lower) LF indicates the set of μ_E such that every parameter belongs to the upper (lower) cluster.

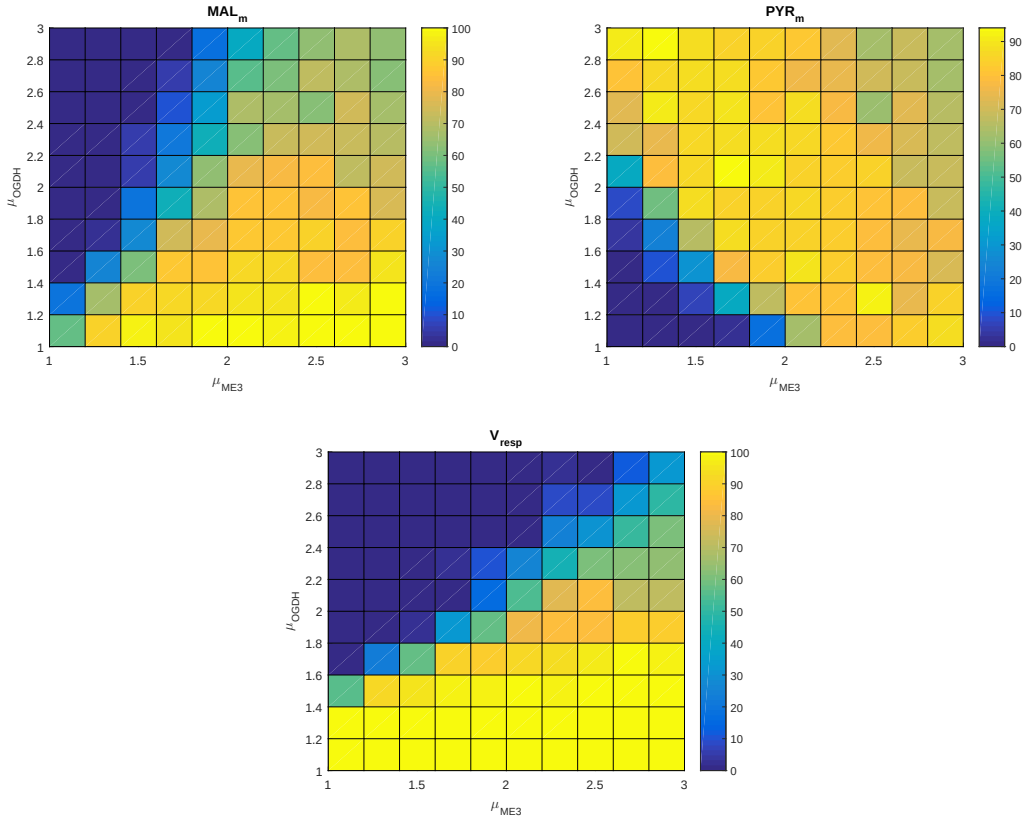

Figure 3.9: Percentage of LF samples with [MAL],[PYR],V_{resp} in the lower cluster as function of μ_{OGDH} and μ_{ME3}.

Thereafter, we conducted the following experiment to test these observations. We considered the enzymes OGDH,ME3 and IDH1 and we computed eleven values of μ_E ranging from 1 to 3. Then, for each couple of these enzymes, we ran our model 100 times for each combination of the two μ_E, assigning a random value to the remaining LF enzymes. Finally, we computed the percentage of sets for which each benchmark belonged to the lower cluster Fig.3.9,3.10,3.11.

We notice how IDH1 single-handedly determines the value of [CIT], in fact such benchmark belongs to the lower cluster if and only if $\mu_{IDH1} > 1.4$. In contrast, IDH does not appear to play a significant role in any other benchmark.

On the other hand, [MAL],[PYR] and V_{resp} heavily depend on the activation of ME3 and OGDH. More precisely, both these enzymes influence negatively [PYR] while they exhibit opposite effects on [MAL] and V_{resp}. As can be seen in Fig. 3.9, the percentage of samples with [PYR] in the lower cluster raises as the values of μ_{OGDH} and μ_{ME3} increase. Accordingly, the percentages regarding

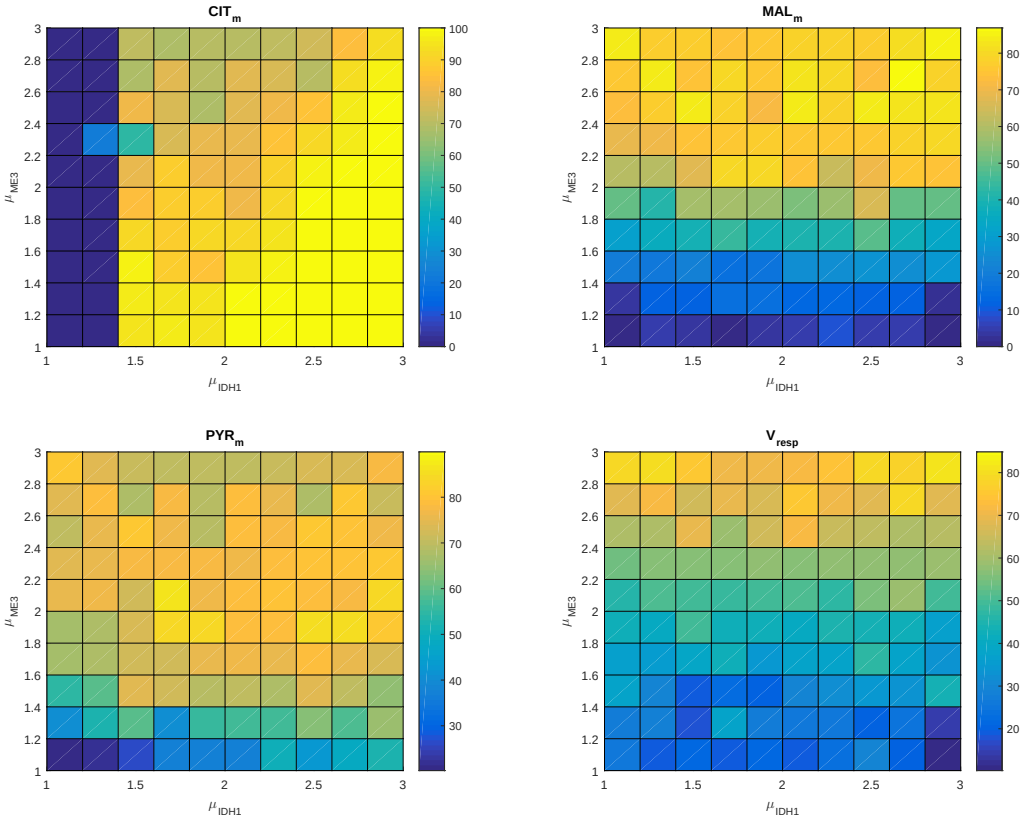

Figure 3.10: Percentage of LF samples with each benchmark in the lower cluster as function of μ_{ME3} and μ_{IDH1}.

[MAL] and V_{resp} increase along the μ_{ME3}-axis and diminish along the μ_{OGDH}-axis. This suggest that there exist a balance between the activation of OGDH (positive effect) and ME3 (negative effect) to appropriately regulate these benchmarks.

3.2.3 Upper fork analysis

Analogously to the LF case, we introduce a similar notation for the activation of the UF enzymes. As previously said, RESP takes into account the over-expression observed in Complex I and III of the electron transport chain.

Regarding the distribution of the different μ_E in the upper UF and lower UF set, the only noticeable difference relates to μ_{RESP} since lower UF presents diminished values, Fig.3.12.

The gains computed in Tab.3.1 point out the importance of LDH, ME1, RESP, CS and PEPCK2 in the UF phenotype. As one would expect, μ_{RESP} is the main

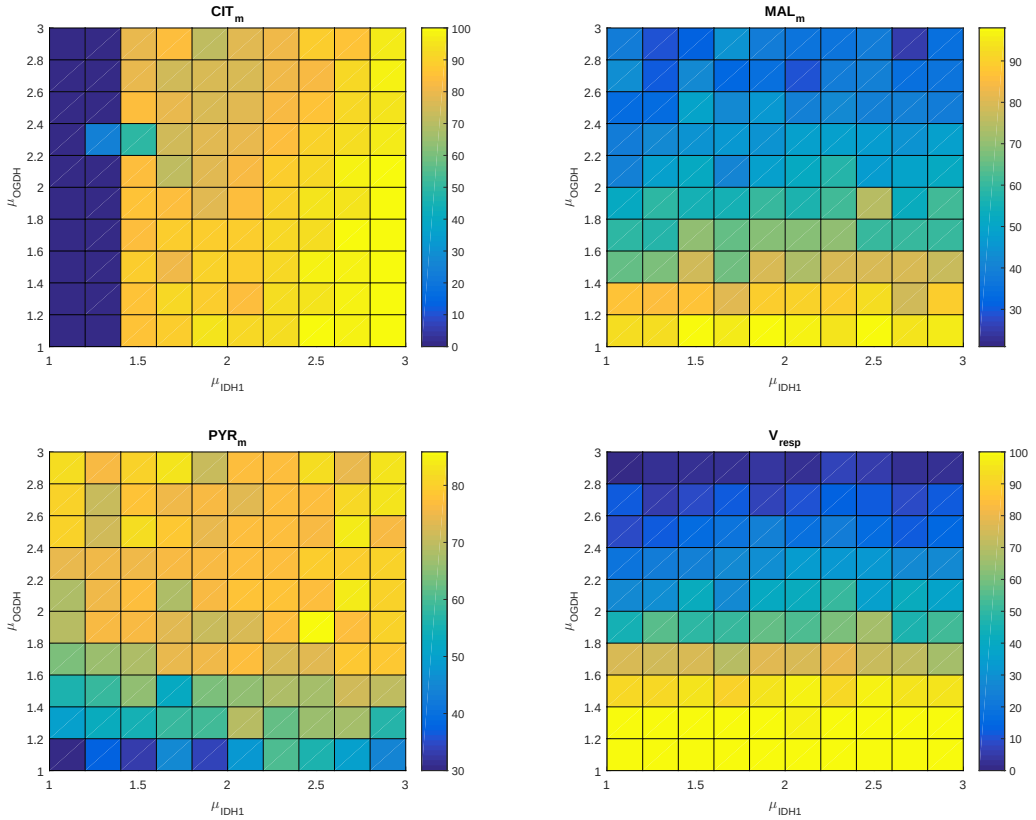

Figure 3.11: Percentage of LF samples with each benchmark in the lower cluster as function of μ_{OGDH} and μ_{IDH1}.

responsible for V_{resp}, as can be seen in Fig.3.15,3.13. Interestingly enough, the same can be said about LDH regarding [CIT] and [PYR], in fact high values of μ_{LDH} always are associated with increased percentages of samples with these benchmarks in the lower cluster, Fig.3.13, 3.14, 3.16. However the situation regarding [MAL] is more complex, in particular these simulations suggest that ME1, CS, RESP and LDH have a negative impact on it while PEPCK2 has a positive effect, see Fig.3.13, 3.14, 3.15, 3.16, 3.17. Furthermore, none of these enzymes seems to have a prevalent role.

3.2.4 Results

It is worthy to summarize what we accomplished in the present chapter. First of all, we introduced two different phenotypes that have been recently identified in breast cancer cells and we highlighted the variables that allow to distinguish

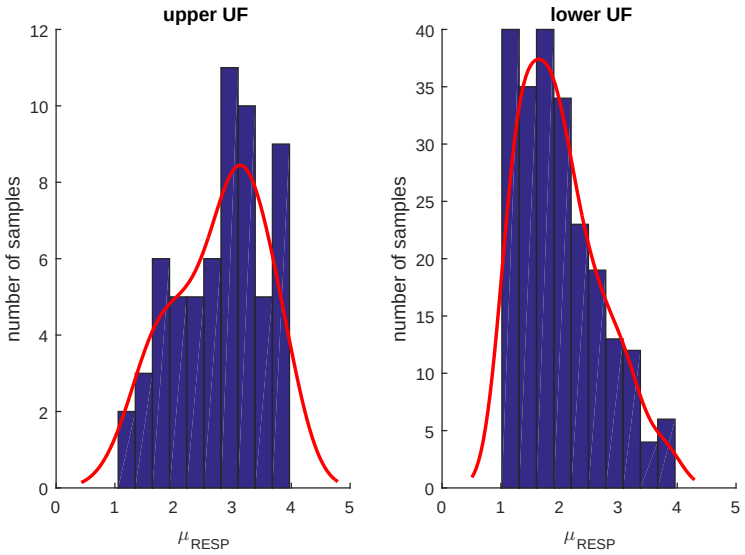

Figure 3.12: Number of samples of upper/lower UF as function of μ_{RESP}. The red line denotes a kernel distribution fit. Upper (lower) UF indicates the set of μ_E such that every parameter belongs to the upper (lower) cluster.

between them. Namely the values of [CIT], [MAL], [PYR], V_{resp} appear to be increased in the UF phenotype while V_{glut} seem to be enhanced in the LF case. Consequently, following experimental data on the mRNA expression of the enzymes involved, we tried to replicate these two behaviours assigning a random activation to each enzyme whose mRNA is over-expressed in UF or LF. Surprisingly, the values of the benchmarks we obtained in this way were in contrast with the experimental data. Thus, the need to explore in more detail the effect that each enzyme plays on the benchmarks.

To lead our investigation we first collected the corresponding gains in Tab.3.1. Then we split the values of each benchmark into two groups through a K-means algorithm and we focused on the samples in which [CIT], [MAL], [PYR], V_{resp} belonged to the upper cluster and those in which they all belonged to the lower set. Thereafter we analysed the main differences between these two set of activations. Following the observations we obtained up to this point, we narrowed our analysis to few enzymes. Namely IDH1, ME3, OGDH for the LF case and RESP, LDH, CS, ME1, PEPCK2 regarding the UF type.

Overall we can make a number of observations. In the LF phenotype the simulations above suggest that:

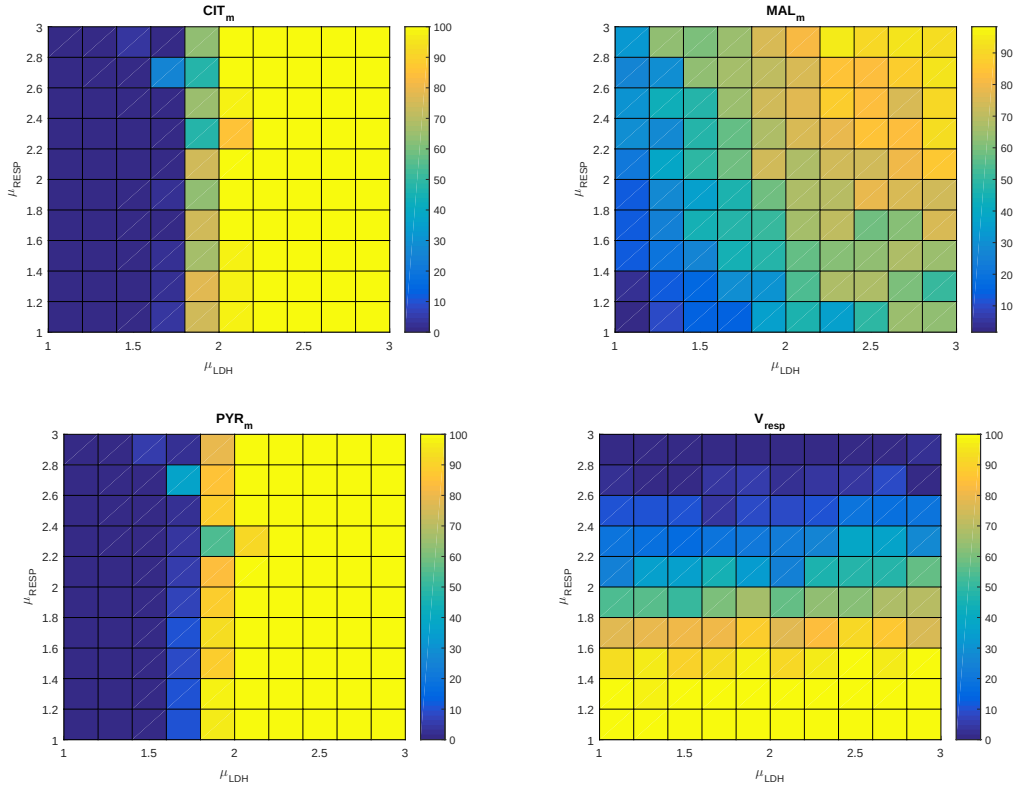

Figure 3.13: Percentage of UF samples with each benchmark in the lower cluster as function of μ_{RESP} and μ_{LDH}.

- the value of [CIT] is single handedly determined by the activation of IDH1; as can be seen in the upper-left plots of Fig.3.10 and 3.11 the percentage of samples in the lower cluster depends only on the value of μ_{IDH1};
- ME3 and OGDH have both a strong negative effect on [PYR], in the upper-right plot of Fig.3.9 we notice that elevated percentages correspond to high values of both μ_{OGDH} and μ_{ME3};
- ME3 and OGDH have opposite impacts on [MAL] and V_{resp}, in particular OGDH has a positive effect and ME3 a negative one; in fact in Fig.3.9 we observe that the percentage increases for high values of μ_{ME3} and low values of μ_{OGDH}.

Similarly in the UF case we notice that:

- the value of [CIT] and [PYR] are single handedly determined by the activation of LDH, Fig.3.13, 3.14, 3.16;

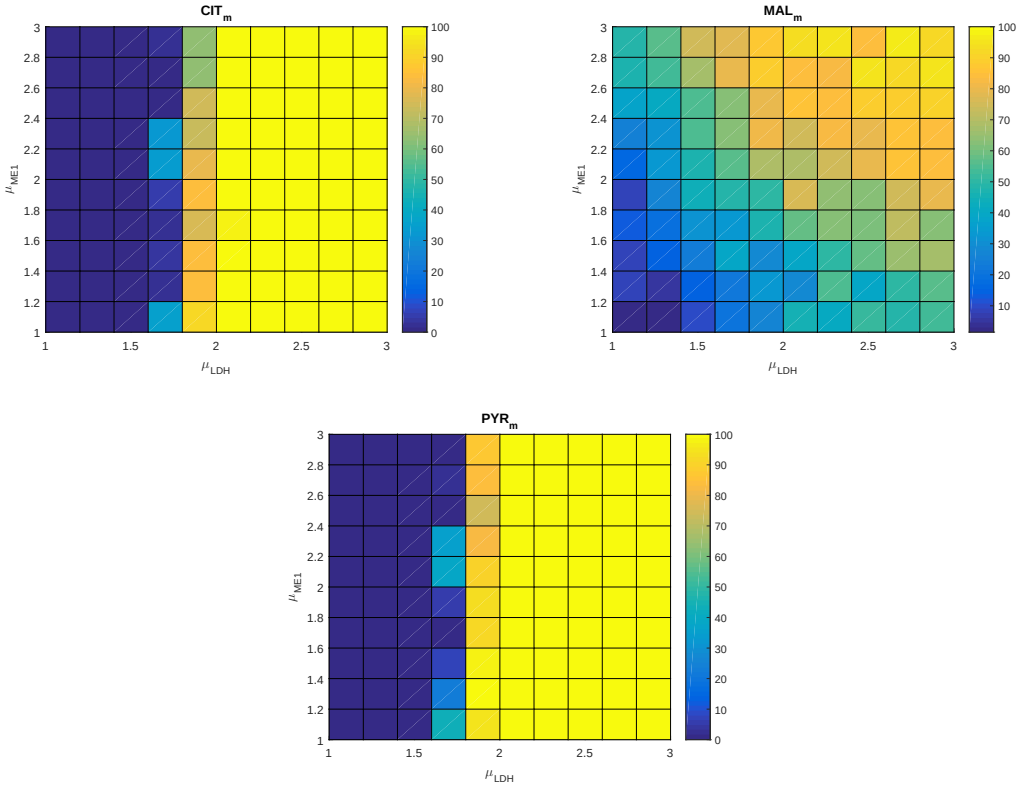

Figure 3.14: Percentage of UF samples with each benchmark in the lower cluster as function of μ_{ME1} and μ_{LDH}.

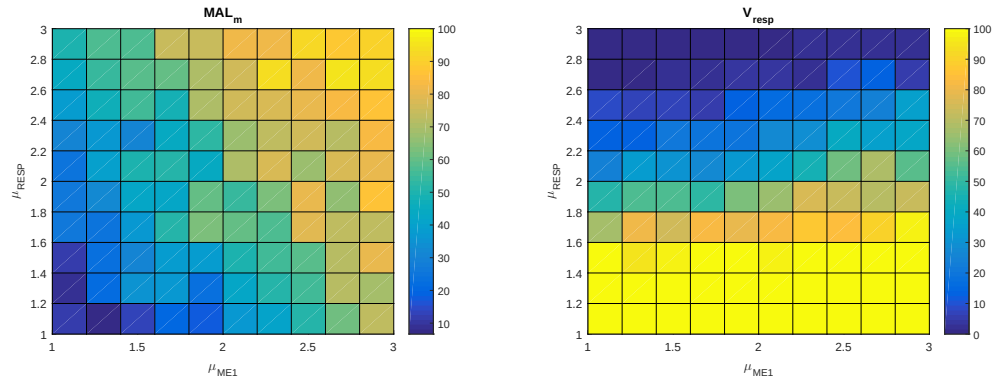

Figure 3.15: Percentage of UF samples with each benchmark in the lower cluster as function of μ_{RESP} and μ_{ME1}.

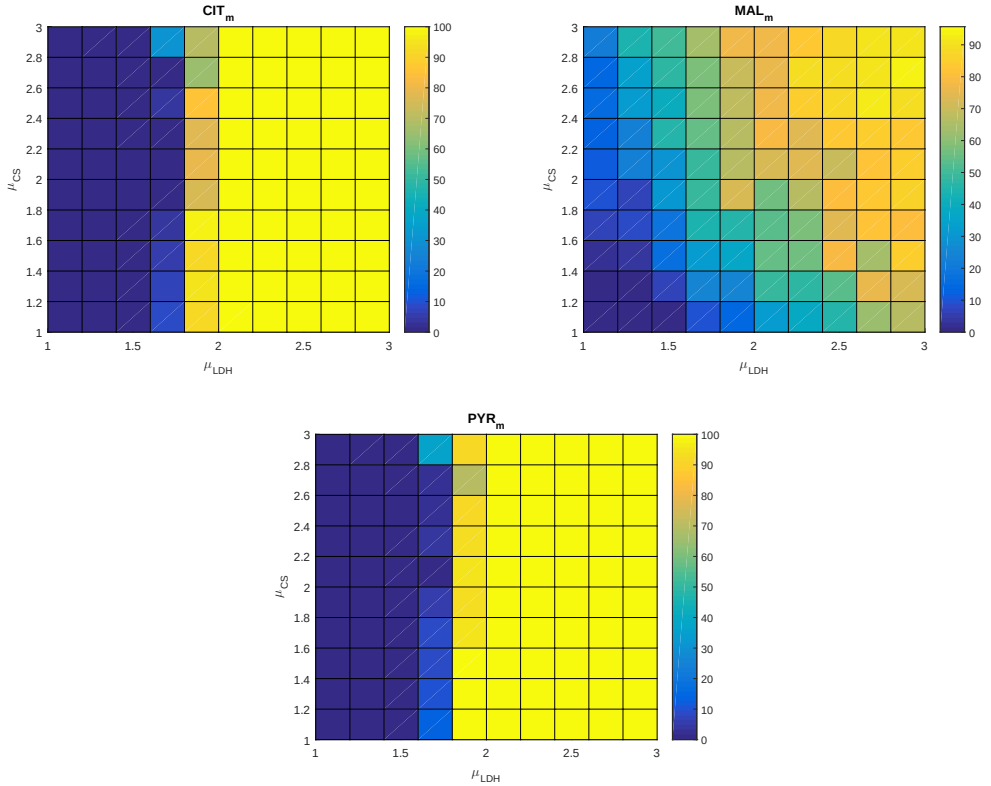

Figure 3.16: Percentage of UF samples with each benchmark in the lower cluster as function of μ_{CS} and μ_{LDH}.

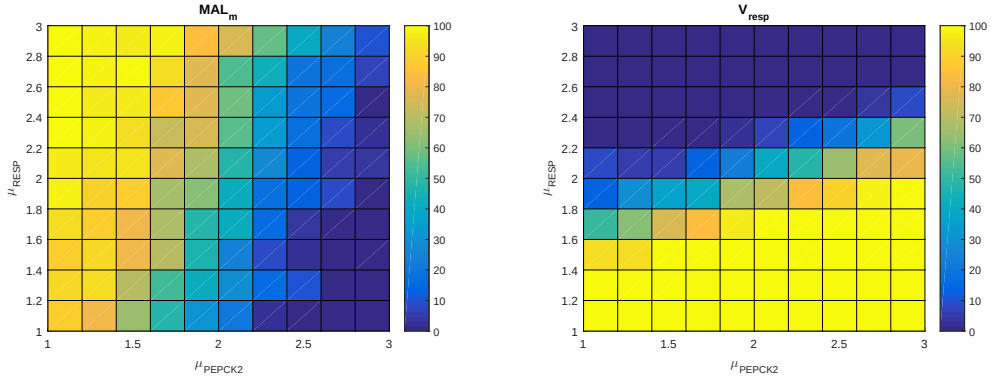

Figure 3.17: Percentage of UF samples with each benchmark in the lower cluster as function of μ_{RESP} and μ_{PEPCK2}.

- the value of V_{resp} is single handedly determined by the activation of RESP, Fig.3.15, 3.13, 3.17;
- regarding [MAL], PEPCK2 plays a positive effect while ME1, CS, RESP and LDH have a negative impact, see Fig.3.13, 3.14, 3.15, 3.16, 3.17.

To confirm these hypothesis, we set the ranges as indicated in Tab.3.2 for the activation-coefficients. In particular to obtain low levels of [PYR] in the LF type, we notice that the more μ_{OGDH} is increased the more we have to also enhance μ_{OGDH}. In our case we considered $\mu_{OGDH} = 1$ and $\mu_{ME3} \in (1.5, 3.5)$ but we can achieve the same results setting $\mu_{OGDH} \in (1, 2)$ and $\mu_{ME3} \in (1.5, 4.5)$.

Regarding UF, first the activity of LDH has to be limited to satisfy the conditions on [CIT] and [PYR]. Moreover it is important to adjust μ_{OGDH}, in fact the activation of RESP has a strong positive effect on V_{resp} but also a negative impact on [MAL].

UF	range	LF	range
μ_{GAPDH}	2	μ_{GLS1}	1.5
μ_{RESP}	$(1, 2)$	μ_{OGDH}	1
μ_{PEPCK2}	$(1, 2)$	μ_{ME3}	$(1.5, 3.5)$
μ_{ME1}	$(1, 2)$	μ_{GDH}	$(1.5, 3.5)$
μ_{AAT1}	$(1, 1.5)$	μ_{IDH1}	$(1.5, 3.5)$
μ_{LDH}	$(1, 2)$	μ_{ME2}	$(1, 5)$
μ_{ACS}	$(1, 5)$	μ_{PEPCK1}	$(1, 5)$
μ_{AAT2}	$(1, 5)$		
μ_{MDH2}	$(1, 2)$		
μ_{IDH2}	$(1, 5)$		
μ_{CS}	$(1, 5)$		

Table 3.2: Ranges of activation that satisfy the benchmarks.

Accordingly we obtained the values of benchmarks we hoped for, Fig.3.18.

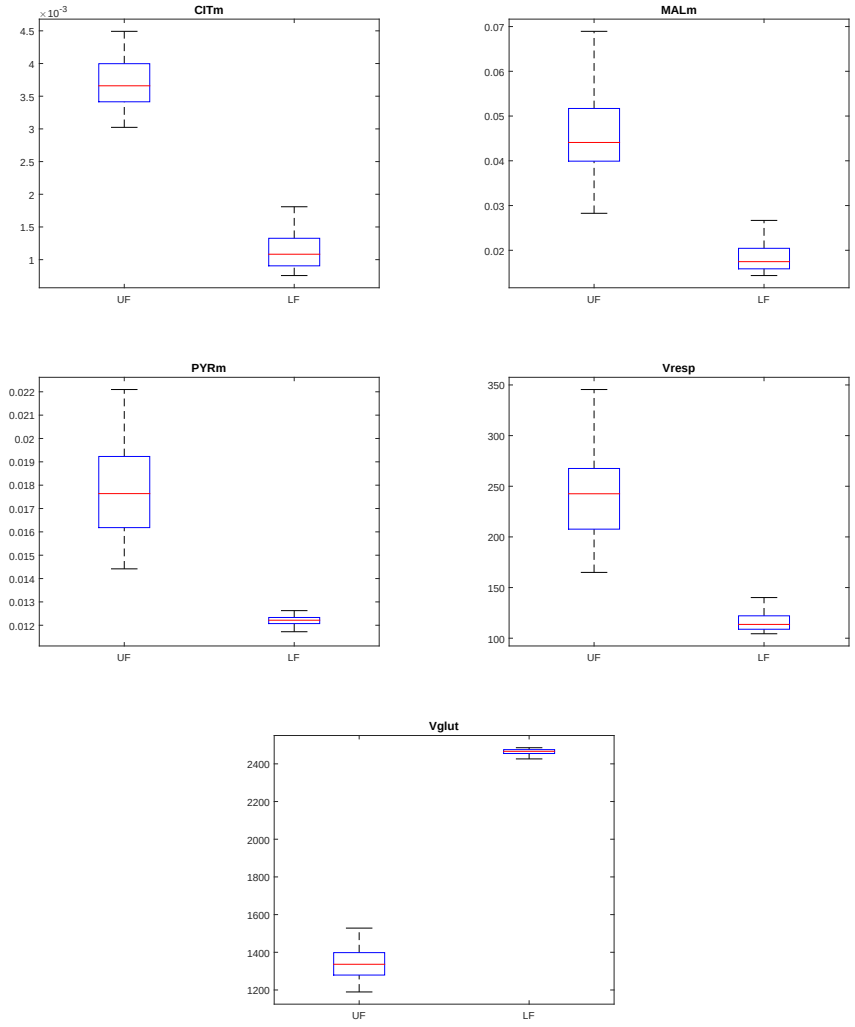

Figure 3.18: These box plots depict the values of the benchmarks obtained with the activation-coefficients listed in Tab.3.2. As can be seen, they are now in accordance to the experimental data discussed in Sec.3.1.

Chapter 4

Conclusions

In this chapter, we summarise what we have accomplished in the current work and we also give a brief review of the state of the art regarding metabolic networks analysis. First, in Chapter 1, we described the main components of metabolism as well as the most noticeable differences between healthy and breast cancer cells. In particular, mitochondrial metabolism emerged as a focal point that connects the principal pathways. Consequently, in Chapter 2, we built a mathematical model of mitochondrial metabolism describing individually each reaction, both in terms of kinetic characteristics and expression in cancer. In Section 3.1 we have introduced two different metabolic phenotypes that have been recently identified in breast cancer cells, denominated upper fork and lower fork phenotypes (G. Szabadkai et al 2017, Unpublished Data), [215]. Then we highlighted how they can be distinguished from one another in terms of metabolites concentrations and fluxes activities, both quantities that are easily measured in a mathematical model. Overall, starting from data about which enzymes are over-expressed in UF/LF cells at mRNA level, our goal was to investigate which enzymes are necessary to manifest each phenotype.

In this regard, we ran different simulations, presented in Sec.3.2. In the first simulation we supposed that the enzymes were over-expressed randomly, following an uniform distribution. Although some samples were in accordance with the experimental data (see Fig.3.6), the majority of them did not meet the experimental criteria, Fig.3.5. Thus, the need to highlight which enzymes influence each benchmark the most, in order to consistently replicate the samples in Fig.3.6. Tab.3.1 gives an overview of the gains of each enzyme taken singularly: we used

these information to select a smaller set of enzymes to focus our attention on. To conduct a general analysis, we split the samples of each parameter in two clusters through a K-means algorithm. Thereafter, we considered two enzymes at a time and the corresponding two-dimensional plane. We then computed, for numerous points of the plane, the percentage of samples that belonged to the lower cluster, see Fig.3.9-3.11 Fig.3.13-3.17. In this way we were able to identify, for each parameter, the enzymes that have the major effects. Following these graphs, we introduced a set of activation parameters (Tab.3.2) that should have satisfied our criteria. Indeed these ranges of activation determined benchmarks in accordance to the experimental data, Fig.3.18. In conclusion, Algorithm 1 summarises the whole procedure.

Algorithm 1 Analysis of upper/lower fork metabolic phenotype

1: *1st Simulation:* random over-expression → few samples satisfy the criteria
2: Computation of gains → highlights the effects of the enzymes taken singularly
3: *2nd Simulation:* two-dimensional analysis through K-means algorithm
4: Draw possible ranges of expression
5: Test if these ranges satisfy the criteria

To give a wider prospective about how the present work fits into the current knowledge about metabolism, it is worth to briefly describe the main methods that have been developed so far to analyse metabolic networks. As discussed in Chapter 1, several alterations in cancer cells metabolism are intricately linked to the principal hallmarks of cancer. Consequently, the particular metabolism displayed by cancer cells has been receiving increasing attention during the past decades with the aim of finding novel therapies able to target specifically cancer cells. However it is important to notice that the links between metabolism and cancer can established in distinct scenarios. As a matter of fact, metabolic reprogramming may be only a consequence of non-metabolic oncogenic events and not necessarily the cause of them. Overall, the preclinical and clinical evaluation of metabolic inhibitors for cancer therapy is in its infancy. This is in part due to the lack of enzymatic inhibitors acting at an acceptable degree of specificity [4]. Over the years, different mathematical approaches have been developed to analyse metabolic networks.

The most direct way to investigate the main properties of a certain metabolic

pathway is to build a mathematical model that replicates the real phenomenon. We refer to this as kinetic modelling and the present work constitutes one example of such methodology. In practice, every chemical reaction is approximated by its enzyme kinetics. Then, if the obtained system replicates with satisfying accuracy the real metabolic network, the advantages are huge. In fact it becomes possible to recreate virtually every experiment simply by running the corresponding simulations on the mathematical model. However, despite considerable advance in the topological analysis of metabolic networks, kinetic modelling is still often severely hampered by inadequate knowledge of the enzyme kinetic rate laws and their associated parameter values. Therefore, the knowledge of the modeller on the subject becomes crucial. First to decide which processes are actually important and need to be included in the model. Next to evaluate if it is possible to introduce some assumptions, in order to simplify the analysis phase. In any case, there can still be certain physiological processes that are still unclear and therefore very difficult to quantify.

Genome-scale metabolic models (GEMs) represent the collection of the existing knowledge regarding the metabolism of a specific organism and offer a valuable tool to study metabolic networks [106, 225]. More precisely, GEMs employ a stoichiometric matrix S to represent all the coefficients in the metabolic reactions. The ij-th element in S indicates the stoichiometric coefficient of the i-th metabolite in the j-th reaction in the GEM. If the coefficient is positive, the metabolite is produced; otherwise, it is consumed. Moreover, GEMs are stoichiometric-balanced networks, meaning that they consider mass, energy, as well as reduction and proton, balances. Gene-protein-reaction (GPR) are also annotated in GEMs, but the interactions are not quantitatively described. The GPR relationships in GEMs are simplified into a two-dimensional binary matrix showing the association between genes and reactions, in which the ij-th element is one if the i-th reaction is associated with the j-th gene, and it is zero if they are not associated. Even though GEMs describe the metabolism, concentrations of metabolites are not directly included and flux balance analysis (FBA) is usually employed for flux simulations [227]. FBA is often utilised to analyse how much each reaction in the network contributes to a particular objective function (e.g. biomass production). Furthermore, this method has found uses in gap-filling efforts and genome-scale synthetic biology [226]. However it is important to mention that FBA has some

limitations, in fact it is only suitable for determining fluxes at steady state and it is not able to predict metabolite concentrations. Moreover, except in some modified forms, FBA does not account for regulatory effects such as activation of enzymes by protein kinases or regulation of gene expression, so its predictions may not always be accurate.

Metabolic Control Analysis (MCA) has also received a lot of attention in recent years. This approach aims to highlight the few enzymes that exert the major effects inside a network through the study of the *control coefficients*. These describe how a variable the system V, typically a metabolic flux or the concentration of a metabolite, will respond to variation of a parameter P, typically an enzyme concentration. Mathematically, they are defined as the fractional change of V, in response to a fractional change in P tending to zero:

$$C_P^V = \lim_{\delta P \to 0} \frac{\delta V/V}{\delta P/P} = \frac{\delta V}{\delta P}\frac{P}{V} = \frac{\partial \ln|V|}{\partial \ln P}.$$

Moreover, coefficients denoted as *elasticities* also play an important role in this framework. They indicate the effect of metabolite S on the velocity v of enzyme E, with all other effectors of the enzyme held constant. Although they have the same form as the control coefficients, they are not a property of the metabolic system, but refer instead to an individual enzyme:

$$\varepsilon_S^E = \lim_{\delta E \to 0} \frac{\delta v_E/v_E}{\delta S/S} = \frac{\delta v_E}{\delta S}\frac{S}{v_E} = \frac{\partial \ln|v_E|}{\partial \ln S}.$$

Notice that this kind of analysis can be conducted both on real experimental data and on simulation-generated ones, obtained by a mathematical model of the metabolic network under study. How this approach can be utilised in practice, as well as some phenomena that have been analysed, are described in [217].

A valid critique about modelling of biological processes regards its limitation with respect to the uncertainty of experimental data; consequently more robust methods of investigation have been developed to overcome this obstacle. One example that is worth mentioning is generalized modelling, [218]. Here, the processes that are taken into account are not restricted to specific functional forms. In this way, a single generalized model can describe a class of systems which share a similar structure. More precisely, this approach is based on a normalization procedure that is used to express the differential equation in terms of natural parameters of the system, more easy to estimate. Then, the Jacobian in a steady

state is computed as a function of these parameters and the dynamical properties of the model are studied in the framework of local bifurcation theory, see [219]. This approach has been utilised to study MAPK cascades [220].

Finally, it is important to mention the general framework of monotone systems as they comprise one of the most important classes of dynamical systems in theoretical biology. The basic definitions and references about the mathematical foundation of monotone systems can be found in [221, 222]. The main idea behind this approach is to study the behaviour of complex networks as the interconnection of multiple monotone systems, see [223, 224]. This type of methodology does not rely on the specific parameters values of a certain phenomenon but it is instead aimed at highlighting general behaviours of a wide variety of biological processes.

Bibliography

[1] *Biologia molecolare della cellula.* Bruce Alberts, Dennis Bray, Julian Lewis, Martin Raff, Keith Roberts, James D. Watson. 3rd Edition, Zanichelli.

[2] *Fondamenti di biochimica.* Donald Voet, Judith G. Voet, Charlotte W. Pratt. Zanichelli.

[3] *Robbins e Cotran - Le basi patologiche delle malattie.* Vinay Kumar, Abul K. Abbas, Nelson Fausto. 7th Edition, Elsevier Masson.

[4] *Tumor cell metabolism: cancer's Achilles' heel.* G. Kroemer, J. Pouyssegur. Cancer Cell 13, pp. 472-482, 2008.

[5] *Otto Warburg's contributions to current concepts of cancer metabolism.* Willem H. Koppenol, Patricia L. Bounds, Chi V. Dang. Nature Reviews, Cancer, Vol. 11, pp. 325-337, 2011.

[6] *Energy metabolism in tumor cells.* Rafael Moreno-Sánchez, Sara Rodríguez-Enríquez, Alvaro Marín-Hernández, Emma Saavedra. FEBS Journal 274, pp. 13931418, 2007.

[7] *Overexpression of GLUT-1 glucose transporter in human breast cancer: an immunohistochemical study.* R. S. Brown, R. L. Wahl. Cancer Vol. 72, n. 10, pp. 2979-2985,1993.

[8] *GLUT1 glucose transporter expression in colorectal carcinoma: a marker for poor prognosis.* R. S. Haber, A. Rathan, K. R. Weiser, A. Pritsker, S. H. Itzkowitz, C. Bodian, G. Slater, A. Weiss, D. E. Burstein. Cancer 83, pp. 34-40, 1998.

[9] *Role for glucose transporter 1 protein in human breast cancer.* M. Grover-McKay, S. A. Walsh, E. A. Seftor, P. A. Thomas, M. J. C. Hendrix. Pathology Oncology Research Vol. 4, n. 2, pp. 115-120, 1998.

[10] *Glutamine and glucose metabolism during thymocyte proliferation: pathways of glutamine and glutamate metabolism.* K. Brand. Biochem. J. 228, pp. 353-361, 1985.

[11] *Aerobic glycolysis during lymphocyte proliferation.* T. Wang, C. Marquardt, J. Foker. Nature Vol. 261, pp. 702-705, 1976.

[12] *Q's next: the diverse functions of glutamine in metabolism, cell biology and cancer.* R. J. DeBerardinis, T. Cheng. Oncogene Vol. 29, pp. 313-324, 2010.

[13] *Cancer metabolism: facts, fantasy, and fiction.* X. L. Zu, M. Guppy. Biochemical and Biophysical Research Communications 313, pp. 459-465, 2004.

[14] *Inhibition of pyruvate kinase M2 by reactive oxygen species contributes to cellular antioxidant responses.* Dimitrios Anastasiou, George Poulogiannis, John M. Asara, Matthew B. Boxer, Jian-kang Jiang, Min Shen, Gary Bellinger, Atsuo T. Sasaki, Jason W. Locasale, Douglas S. Auld, Craig J. Thomas, Matthew G. Vander Heiden, Lewis C. Cantley. Science Vol. 334, pp. 1278-1283, 2011. doi:10.1126/science.1211485.

[15] *Warburg effect and redox balance.* Robert B. Hamanaka, Navdeep S. Chandel. Science Vol. 334, pp. 1219-1220, 2011.

[16] *Antioxidants, oxidative damage and oxygen deprivation stress: a review.* O. Blokhina, E. Virolainen, K. V. Fagerstedt. Annals of Botany 91, pp. 179-194, 2003.

[17] *Oxidative stress, tumor microenvironment, and metabolic reprogramming: a diabolic liaison.* Tania Fiaschi, Paola Chiarugi. International Journal of Cell Biology, 2012. doi:10.1155/2012/762825.

[18] *Novel role of NADPH oxidase in angiogenesis and stem/progenitor cell function.* M. Ushio-Fukai, N. Urao. Antioxidants & Redox Signaling Vol. 11, n. 10, pp. 2517-2533, 2009. doi: 10.1089/ars.2009.2582.

[19] *Oxidative stress promotes myofibroblast differentiation and tumour spreading.* Aurore Toullec, Damien Gerald, Gilles Despouy, Brigitte Bourachot, Melissa Cardon, Sylvain Lefort, Marion Richardson, Guillem Rigaill, Maria-Carla Parrini, Carlo Lucchesi, Dorine Bellanger, Marc-Henri Stern, Thierry Dubois, Xavier Sastre-Garau, Olivier Delattre, Anne Vincent-Salomon, Fatima Mechta-Grigoriou. EMBO Molecular Medicine 2, pp. 211-230, 2010.

[20] *Mitochondrial $O_2^{\bullet}$ and H_2O_2 mediate glucose deprivation-induced cytotoxicity and oxidative stress in human cancer cells.* Iman M. Ahmad, Nukhet Aykin-Burns, Julia E. Sim, Susan A. Walsh, Ryuji Higashikubo, Garry R. Buettner, Sujatha Venkataraman, Michael A. Mackey, Shawn W. Flanagan, Larry W. Oberley, Douglas R. Spitz. The Journal of Biological Chemistry Vol. 280, n. 6, pp. 4254-4263, 2005.

[21] *2-deoxy-D-glucose combined with cisplatin enhances cytotoxicity via metabolic oxidative stress in human head and neck cancer cells.* Andrean L. Simons, Iman M. Ahmad, David M. Mattson, Kenneth J. Dornfeld, Douglas R. Spitz. Cancer Research 67, 2007. doi:10.1158/0008-5472.CAN-06-3717.

[22] *Increased levels of superoxide and hydrogen peroxide mediate the differential susceptibility of cancer cells vs normal cells to glucose deprivation.* Nkhet Aykin-Burns, Iman M. Ahmad, Yueming Zhu, Larry W. Oberley, and Douglas R. Spitz. Biochem. Journal 418, 2009. doi:10.1042/BJ20081258.

[23] *Glucose deprivation-induced oxidative stress in human tumor cells: a fundamental defect in metabolism?*. D. R. Spitz, J. E. Sim, L. A. Ridnour, S. S. Galoforo, Y. J. Lee. Annals New York Academy of Sciences 899, pp. 349-362, 2000.

[24] *Metabolic oxidative stress activates signal transduction and gene expression during glucose deprivation in human tumor cells*. R. V. Blackburn, D. R. Spitz, X. Liu, S. S. Galoforo, J. E. Sim, L. A. Ridnour, J. C. Chen, B. H. Davis, P. M. Corry, Y. J. Lee. Free Radical Biology & Medicine Vol. 26, n. 3-4, pp. 419-430, 1999.

[25] *HIF-1 inhibits mitochondrial biogenesis and cellular respiration in VHL-deficient renal cell carcinoma by repression of c-myc activity*. Huafeng Zhang, Ping Gao, Ryo Fukuda, Ganesh Kumar, Balaji Krishnamachary, Karen I. Zeller, Chi V. Dang, Gregg L. Semenza. Cancer Cell 11, pp. 407-420, 2007.

[26] *Evaluation of myc E-Box phylogenetic footprints in glycolytic genes by chromatin immunoprecipitation assays*. Jung-whan Kim, Karen I. Zeller, Yunyue Wang, Anil G. Jegga, Bruce J. Aronow, Kathryn A. ODonnell, Chi V. Dang. Molecular and Cellular Biology Vol. 24, n. 13, pp. 5923-5936, 2004.

[27] *HIF and c-Myc: sibling rivals for control of cancer cell metabolism and proliferation*. John D. Gordan, Craig B. Thompson, M. Celeste Simon. Cancel Cell 12, 2007. doi: 10.1016/j.ccr.2007.07.006

[28] *Deregulation of glucose transporter 1 and glycolytic gene expression by c-Myc*. Rebecca C. Osthus, Hyunsuk Shim, Sunkyu Kim, Qing Li, Rahul Reddy, Mita Mukherjee, Yi Xu, Diane Wonsey, Linda A. Lee, Chi V. Dang. The Journal of Biological Chemistry Vol. 275, n. 29, pp. 21797-21800, 2000.

[29] *c-Myc transactivation of LDH-A: Implications for tumor metabolism and growth*. H. Shim, C. Dolde, B. C. Lewis, C. Wu, G. Dang, R. A. Jungmannn, R. Dalla-Favera, C. V. Dang. Proc. Natl. Acad. Sci. USA Vol. 94, pp. 66586663, 1997.

[30] *Akt stimulates aerobic glycolysis in cancer cells*. Rebecca L. Elstrom, Daniel E. Bauer Monica Buzzai, Robyn Karnauskas, Marian H. Harris, David R. Plas, Hongming Zhuang, Ryan M. Cinalli, Abass Alavi, Charles M. Rudin, Craig B. Thompson. Cancer Research 64, pp. 3892-3899, 2004.

[31] *The interplay between MYC and HIF in cancer*. Chi V. Dang, Jung-Whan Kim, Ping Gao, Jason Yustein. Nature Review Cancer Vol. 8, pp. 51-56, 2008.

[32] *Dysregulation of glucose transport, glycolysis, TCA cycle and glutaminolysis by oncogenes and tumor suppressors in cancer cells*. Jin-Qiang Chen, Jose Russo. Biochimica et Biophysica Acta 1826, pp. 370-384, 2012.

[33] *SirT3 suppresses hypoxia inducible factor 1α and tumor growth by inhibiting mitochondrial ROS production.* E.L. Bell, B.M. Emerling, S.J.H. Ricoult, L. Guarente. Oncogene 30, pp. 2986-2996, 2011.

[34] *SIRT3 is a mitochondrial localized tumor suppressor required for maintenance of mitochondrial integrity and metabolism during stress.* Hyun-Seok Kim, Krish Patel, Kristi Muldoon-Jacobs, Kheem S. Bisht, Nukhet Aykin-Burns, J. Daniel Pennington, Riet van der Meer, Phuongmai Nguyen, Jason Savage, Kjerstin M. Owens, Athanassios Vassilopoulos, Ozkan Ozden, Seong-Hoon Park, Keshav K. Singh, Sarki A. Abdulkadir, Douglas R. Spitz, Chu-Xia Deng, David Gius. Cancer Cell 17, pp. 41-52, 2010. doi:10.1016/j.ccr.2009.11.023.

[35] *SIRT3 opposes reprogramming of cancer cell metabolism through HIF1α destabilization.* Lydia W.S. Finley, Arkaitz Carracedo, Jaewon Lee, Amanda Souza, Ainara Egia, Jiangwen Zhang, Julie Teruya-Feldstein, Paula I. Moreira, Sandra M. Cardoso, Clary B. Clish, Pier Paolo Pandolfi, Marcia C. Haigis. Cancer Cell 19, pp. 416-428, 2011. doi:10.1016/j.ccr.2011.02.014.

[36] *Hypoxia signalling controls metabolic demand.* M. Christiane Brahimi-Horn, Johanna Chiche, Jacques Pouysségur. Current Opinion in Cell Biology 19, pp. 223-229, 2007.

[37] *Regulation of life span by mitochondrial respiration: the HIF-1 and ROS connection.* Ara B. Hwang, SeungJae Lee. Aging Vol. 3, n. 3, pp. 304-310, 2011.

[38] *Hypoxia inducible factors: central regulators of the tumor phenotype.* John D. Gordan, M. Celeste Simon. Curr. Opin. Genet. Dev. 17, pp. 71-77, 2007.

[39] *Pyruvate kinase M2 is a PHD3-stimulated coactivator for hypoxia-inducible Factor 1.* Weibo Luo, Hongxia Hu, Ryan Chang, Jun Zhong, Matthew Knabel, Robert OMeally, Robert N. Cole, Akhilesh Pandey, Gregg L. Semenza. Cell 145, pp. 732-744, 2011. doi:10.1016/j.cell.2011.03.054.

[40] *p53: new roles in metabolism.* K. Bensaad, K. H. Vousden. Trends in Cell Biology Vol. 17, n. 6, pp. 286-291, 2007.

[41] *Phosphate-activated glutaminase (GLS2), a p53-inducible regulator of glutamine metabolism and reactive oxygen species.* Sawako Suzuki, Tomoaki Tanaka, Masha V. Poyurovsky, Hidekazu Nagano, Takafumi Mayama, Shuichi Ohkubo, Maria Lokshin, Hiroyuki Hosokawa, Toshinori Nakayama, Yutaka Suzuki, Sumio Sugano, Eiichi Sato, Toshitaka Nagao, Koutaro Yokote, Ichiro Tatsuno, and Carol Prives. Pnas Vol. 107, n. 16, pp. 7461-7466, 2010.

[42] *Glutaminase 2, a novel p53 target gene regulating energy metabolism and antioxidant function.* Wenwei Hu, Cen Zhang, Rui Wu, Yvonne Sun, Arnold Levine, and Zhaohui Feng. Pnas Vol. 107, n. 16, pp. 7455-7460, 2010.

[43] *TIGAR, a p53-inducible regulator of glycolysis and apoptosis.* Karim Bensaad, Atsushi Tsuruta, Mary A. Selak, M. Nieves Calvo Vidal, Katsunori Nakano, Ramon Bartrons, Eyal Gottlieb, Karen H. Vousden. Cell 126, pp. 107-120, 2006.

[44] *The tumor suppressor p53 down-regulates glucose transporters GLUT1 and GLUT4 gene expression.* Fabiana Schwartzenberg-Bar-Yoseph, Michal Armoni, Eddy Karnieli. Cancer Research 64, pp. 2627-2633, 2004.

[45] *p53 negatively regulates transcription of the pyruvate dehydrogenase kinase Pdk2.* Tanupriya Contractor, Chris R. Harris. Cancer Research 72, pp. 560-567, 2012.

[46] *p53 regulates mitochondrial respiration.* Satoaki Matoba, Ju-Gyeong Kang, Willmar D. Patino, Andrew Wragg, Manfred Boehm, Oksana Gavrilova, Paula J. Hurley, Fred Bunz, Paul M. Hwang. Science Vol. 312, pp. 1650-1653, 2006.

[47] *p53 regulates biosynthesis through direct inactivation of glucose-6-phosphate dehydrogenase.* Peng Jiang, Wenjing Du, Xingwu Wang, Anthony Mancuso, Xiang Gao, Mian Wu, Xiaolu Yang. Nature Cell Biology Vol. 13, n. 3, pp. 310-316, 2011. doi: 10.1038/ncb2172

[48] *p53 guards the metabolic pathway less travelled.* Eyal Gottlieb. Nature Cell Biology Vol. 13, n. 3, pp. 195-197 ,2011.

[49] *The glucose dependence of Akt-transformed cells can be reversed by pharmacologic activation of fatty acid β-oxidation.* M. Buzzai, D. E. Bauer, R. G. Jones, R. J. DeBerardinis, G. Hatzivassiliou, R. L. Elstrom, C. B. Thompson. Oncogene 24, pp. 4165-4173, 2005.

[50] *The biology of cancer: metabolic reprogramming fuels cell growth and proliferation.* R. J. DeBerardinis, J. J. Lum, G. Hatzivassiliou, C. B. Thompson. Cell Metabolism 7, pp. 11-20, 2008.

[51] *Phosphofructokinase type 1 kinetics, isoform expression, and gene polymorphisms in cancer cells.* R. Moreno-Sánchez, A. Marín-Hernández, J. C. Gallardo-Pérez, H. Quezada, R. Encalada, S. Rodríguez-Enríquez, E. Saavedra. Journal of Cellular Biochemistry 113, pp. 1692-1703, 2012.

[52] *Rat liver phosphofructokinase: kinetic activity under near-physiological conditions.* G. D. Reinhart, H. A. Lardy. Biochemistry 19, pp. 1477-1484, 1980.

[53] *Differential expression of phosphofructokinase-1 isoforms correlates with the glycolytic efficiency of breast cancer cells.* P. Zancan, M. Sola-Penna, C. M. Furtado, D. Da Silva. Molecular Genetics and Metabolism 100, pp. 372378, 2010.

[54] *Cloning of cDNA encoding for a novel isozyme of fructose 6-phosphate, 2-kinase/fructose 2,6-bisphosphatase from human placenta.* A. Sakai, M. Kato, M. Fukasawa, M. Ishiguro, E. Furuya, R. Sakakibara. The Journal of Biochemistry 119, pp. 506-511, 1996.

[55] *Sequence and structure of the human 6-phosphofructo-2-kinase/fructose-2,6-bisphosphatase heart isoform gene (PFKFB2).* D. Heine-Suñer, M. A. Díaz-Guillén, A. J. Lange, S. Rodríguez de Córdoba. European Journal of Biochemistry 254, pp. 103-110, 1998.

[56] *Energy metabolism in tumor cells.* R. Moreno-Sánchez, S. Rodríguez-Enríquez, A. Marín-Hernández, E. Saavedra. Febs 274, pp. 1393-1418, 2007.

[57] *An inducible gene product for 6-phosphofructo-2-kinase with an AU-rich instability element: Role in tumor cell glycolysis and the Warburg effect.* J. Chesney, R. Mitchell, F. Benigni, M. Bacher, L. Spiegel, Y. Al-Abed, J. H. Han, C. Metz, R. Bucala. Proceedings of the National Academy of Sciences Vol. 96, pp. 3047-3052, 1999.

[58] *Cells overexpressing fructose-2,6-bisphosphatase showed enhanced pentose phosphate pathway ux and resistance to oxidative stress.* J. Boada, T. Roig, X. Perez, A. Gamez, R. Bartrons, M. Cascante, J. Bermúdez. Febs Letters 480, pp. 261-264, 2000.

[59] *Inhibition of tumor cell growth by a specific 6-phosphofructo-2-kinase inhibitor, N-bromoacetyllethanolamine phosphate, and its analogues.* T. Hirata, M. Watanabe, S. Miura, K. Ijichi, M. Fukasawa, R. Sakakibara. Bioscience, Biotechnology and Biochemistry 64, pp. 2047-2052, 2000.

[60] *Hypoxia-inducible Factor-1-mediated expression of the 6-phosphofructo-2-kinase/fructose-2,6-bisphosphatase-3 (PFKFB3) gene: Its possible role in the Warburg effect.* A. Minchenko, I. Leshchinsky, I. Opentanova, N. Sang, V. Srinivas, V. Armstead, J. Caro. Journal of Biological Biochemistry Vol. 227, n. 8, pp. 6183-6187, 2002. doi:10.1074/jbc.M110978200.

[61] *Glutamine homeostasis and mitochondrial dynamics.* Jos M. Mats, Juan A. Segura, Jos A. Campos-Sandoval, Carolina Lobo, Lorenzo Alonso, Francisco J. Alonso, Javier Mrquez. The International Journal of Biochemistry & Cell Biology 41, pp. 20512061, 2009.

[62] *Glutamine transporters in mammalian cells and their functions in physiology and cancer.* Yangzom D. Bhutia, Vadivel Ganapathy. Biochimica et Biophysica Acta 1863, pp. 25312539, 2016.

[63] *Metabolic reprogramming in cancer: Unraveling the role of glutamine in tumorigenesis.* Dania Daye, Kathryn E. Wellen. Seminars in Cell & Developmental Biology 23, pp. 362-369, 2012.

[64] *Beyond aerobic glycolysis: Transformed cells can engage in glutamine metabolism that exceeds the requirement for protein and nucleotide synthesis.* R. J. DeBerardinis, A. Mancuso, E. Daikhin, I. Nissim, M. Yudkoff, S. Wehrli, C. B. Thompson. Pnas Vol. 104, n. 49, pp. 19345-19350, 2007.

[65] *Myc regulates a transcriptional program that stimulates mitochondrial glutaminolysis and leads to glutamine addiction.* D. R. Wise, R. J. DeBerardinis, A. Mancuso, N. Sayed, X.-Y. Zhang, H. K. Pfeiffer, I. Nissim, E. Daikhin, M. Yudkoff, S. B. McMahon, C. B. Thompson. Pnas Vol. 105, n. 48, pp. 18782-18787, 2008.

[66] *c-Myc suppression of miR-23 enhances mitochondrial glutaminase and glutamine metabolism.* P. Gao, I. Tchernyshyov, T.-C. Chang., Y.-S. Lee, K. Kita, T. Ochi, K. Zeller, A. M. De Marzo, J. E. Van Eyk, J. T. Mendell, C. V. Dang. Nature Vol. 458, n. 7239, pp. 762-765, 2009.

[67] *Molecular mechanisms of glutamine action.* R. Curi, C. J. Lagranha, S. Q. Doi, D. F. Sellitti, J. Procopio, T. C. Pithon-Curi, M. Corless, P. Newsholme. Journal of Cellular Physiology 204, pp. 392-401, 2005.

[68] *Glutamine sensitivity analysis identifies the xCT antiporter as a common triple-negative breast tumor therapeutic target.* L. A. Timmerman, T. Holton, M. Yuneva, R. J. Louie, M. Padró, A. Daemen, M. Hu, D. A. Chan, S. P. Ethier, L. J. van 't Veer, K. Polyak, F. McCormick, J. W. Gray. Cancer Cell 24, pp. 450-465, 2013.

[69] *ASCT2/SLC1A5 controls glutamine uptake and tumour growth in triple-negative basal-like breast cancer.* M. van Geldermalsen, Q. Wang, R. Nagarajah, A. D. Marshall, A. Thoeng, D. Gao, W. Ritchie, Y. Feng, C. G. Bailey, N. Deng, K. Harvey, J. M. Beith C. I. Selinger, S. A. O'Toole, J. E. J. Rasko, J. Holst. Oncogene 35, pp. 3201-3208, 2016.

[70] *Targeting glutamine transport to suppress melanoma cell growth.* Q. Wang, K. A. Beaumont, N. J. Otte, J. Font, C. G. Bailey, M. van Geldermalsen, D. M. Sharp, J. C. Tiffen, R. M. Ryan, M. Jormakka, N. K. Haass, J. E.J. Rasko, J. Holst. International Journal of Cancer 135, pp. 1060-1071, 2014.

[71] *The SLC1 high-affinity glutamate and neutral amino acid transporter family.* Y. Kanai, B. Clémençon, A. Simonin, M. Leuenberger, M. Lochner, M. Weisstanner, M. A. Hediger. Molecular Aspects of Medicine 34, pp. 108-120, 2013.

[72] *The x_c^- cystine/glutamate antiporter: a potential target for therapy of cancer and other diseases.* M. Lo, Y.-Z. Wang, P. W. Gout. Journal of Cellular Physiology, pp. 593-602, 2008. doi: 10.1002/jcp.21366

[73] *The SLC6 transporters: perspectives on structure, functions, regulation, and models for transporter dysfunction.* G. Rudnick, R. Krämer, R. D. Blakely, D. L. Murphy, F. Verrey. Pflugers Archiv Vol. 466, n. 1, pp. 25-42, 2014.

[74] *The amino acid transporter SLC6A14 in cancer and its potential use in chemotherapy.* Y. D. Bhutia, E. Babu, P. D. Prasad, V. Ganapathy. Asian Journal of Pharmaceutical Sciences 9, pp. 293-303, 2014.

[75] *Interaction of tryptophan derivatives with SLC6A14 (ATB0,+) reveals the potential of the transporter as a drug target for cancer chemotherapy.* S. Karunakaran, N. S. Umapathy, M. Thangaraju, T. Hatanaka, S. Itagaki, D. H. Munn, P. D. Prasad, V. Ganapathy. Biochemistry Journal 414, pp. 343-355, 2008. doi:10.1042/BJ20080622.

[76] *Selective expression of the large neutral amino acid transporter at the bloodbrain barrier.* R. J. Boado, J. Yi Li, M. Nagaya, C. Zhang, W. M. Pardridge. Pnas Vol. 96, n. 21, pp. 12079-12084, 1999.

[77] *L-type amino acid transport and cancer: targeting the mTORC1 pathway to inhibit neoplasia.* Q. Wang, J. Holst. American Journal of Cancer Research Vol. 5, n. 4, pp. 1281-1294, 2015.

[78] *The glutamate/GABA-glutamine cycle: aspects of transport, neurotransmitter homeostasis and ammonia transfer.* L. K. Bak, A. Schousboe, H. S. Waagepetersen. Journal of Neurochemistry 98, pp. 641-653, 2006.

[79] *Transcriptional control of human p53-regulated genes.* T. Riley, E. Sontag, P. Chen, A. Levine. Nature Vol. 9, pp. 402-412 ,2008.

[80] *Primary structure, genomic organization, and functional and electrogenic characteristics of human system N 1, a Na^+- and H^+-coupled glutamine transporter.* Y.-J. Fei, M. Sugawara, T. Nakanishi, W. Huang, H. Wang, P. D. Prasad, F. H. Leibach, V. Ganapathy. The Journal of Biological Chemistry Vol. 275, n. 31, pp. 23707-23717, 2000.

[81] *Structure, function, and tissue expression pattern of human SN2, a subtype of the amino acid transport system N.* T. Nakanishi, M. Sugawara, W. Huang, R. G. Martindale, F. H. Leibach, M. E. Ganapathy, P. D. Prasad, V. Ganapathy. Biochemical and Biophysical Research Communications 281, pp. 1343-1348, 2001.

[82] *Identification of SLC38A7 (SNAT7) protein as a glutamine transporter expressed in neurons.* M. G. A. Hägglund, S. Sreedharan, V. C. O. Nilsson, J. H. A. Shaik, I. M. Almkvist, S. Bäcklin, Ö. Wrange, R. Fredriksson. The Journal of Biological Chemistry Vol. 286, n. 23, pp. 20500-20511, 2011.

[83] *Transport of L-glutamine, L-alanine, L-arginine and L-histidine by the neuron-specific Slc38a8 (SNAT8) in CNS.* M. G. A. Hägglund, S. V. Hellsten, S. Bagchi, G. Philippot, E. Löfqvist, V. C. O. Nilsson, I. Almkvist, E. Karlsson, S. Sreedharan, A. Tafreshiha, R. Fredriksson. Journal of Molecular Biology 427, pp. 1495-1512, 2015.

[84] *Mitochondrial localization and structure-based phosphate activation mechanism of Glutaminase C with implications for cancer metabolism.* A. Cassago, A. P. S. Ferreira, I. M. Ferreira, C. Fornezari, E. R. M. Gomes, K. Su Greene, H. M. Pereira, R. C. Garratt, S. M. G. Dias, A. L. B. Ambrosio. Pnas Vol. 109, n. 4, pp 1092-1097, 2012.

[85] *Molecular basis for the differential use of glucose and glutamine in cell proliferation as revealed by synchronized HeLa cells.* S. L. Colombo, M. Palacios-Callender, N. Frakich, S. Carcamo, I. Kovacs, S. Tudzarova, S. Moncada. Pnas Vol. 108, n. 52, pp. 21069-21074, 2011.

[86] *Reductive glutamine metabolism by IDH1 mediates lipogenesis under hypoxia.* C. M. Metallo, P. A. Gameiro, E. L. Bell, K. R. Mattaini, J. Yang, K. Hiller, C. M. Jewell, Z. R. Johnson, D. J. Irvine, L. Guarente, J. K. Kelleher, M. G. Vander Heiden, O. Iliopoulos, G. Stephanopoulos. Nature Vol. 481, pp. 380-384 ,2012.

[87] *Isotopomer analysis of citric acid cycle and gluconeogenesis in rat liver: reversibility of isocitrate dehydrogenase and involvement of ATP-citrate lyase in gluconeogenesis.* C. Des Rosiers, L. Di Donato, B. Comte, A. Laplante, C. Marcoux, F. David, C. A. Fernandez, H. Brunengraber. The Journal of Biological Chemistry Vol. 270, n. 17, pp. 10027-10036, 1995.

[88] *Glutathione metabolism and its implications for health.* G. Wu,Y.-Z. Fang, S. Yang, J. R. Lupton, N. D. Turner. The Journal of Nutrition 134, pp. 489-492, 2004.

[89] *Targeting mitochondrial glutaminase activity inhibits oncogenic transformation.* J.-B. Wang, J. W. Erickson, R. Fuji, S. Ramachandran, P. Gao, R. Dinavahi, K. F. Wilson, A. L. B. Ambrosio, S. M. G. Dias, C. V. Dang, R. A. Cerione. Cancer Cell Vol. 18, n. 3 , pp. 207-219, 2010.

[90] *Glucose-independent glutamine metabolism via TCA cycling for proliferation and survival in B-cells.*A. Le, A. N. Lane, M. Hamaker, S. Bose, A. Gouw, J. Barbi, T. Tsukamoto, C. J. Rojas, B. S. Slusher, H. Zhang, L. J. Zimmerman, D. C. Liebler, R. J. C. Slebos, P. K. Lorkiewicz, R. M. Higashi, T. W. M. Fan, C. V. Dang. Cell Metabolism Vol. 15, n. 1, pp. 110-121, 2012.

[91] *Targeting mitochondrial glutaminase activity inhibits oncogenic transformation.* J.-B. Wang, J. W. Erickson, R. Fuji, S. Ramachandran, P. Gao, R. Dinavahi, K. F. Wilson, A. L. B. Ambrosio, S. M. G. Dias, C. V. Dang, R. A. Cerione. Cancer Cell Vol. 18, n. 3, pp. 207-219, 2010.

[92] *The hexosamine biosynthetic pathway couples growth factor-induced glutamine uptake to glucose metabolism.* K. E. Wellen, C. Lu, A. Mancuso, J. M. S. Lemons, M. Ryczko, J. W. Dennis, J. D. Rabinowitz, H. A. Coller, C. B. Thompson. Genes & Development 24, pp. 2784-2799, 2010.

[93] *Glucose sensing by MondoA: Mlx complexes: a role for hexokinases and direct regulation of thioredoxin-interacting protein expression.* C. A. Stoltzman, C. W. Peterson, K. T. Breen, D. M. Muoio, A. N. Billin, D. E. Ayer. Pnas Vol. 105, n. 19, pp. 6912-6917, 2008.

[94] *Glutamine-dependent anapleurosis dictates glucose uptake and cell growth by regulating MondoA transcriptional activity.* M. R. Kaadige, R. E. Looper, S. Kamalanaadhan, D. E. Ayer. Pnas Vol. 106, n. 35, pp. 14878-14883, 2009.

[95] *Serine biosynthesis and transport defects.* A. W. El-Hattab. Molecular Genetics and Metabolism 118, pp. 153-159, 2016.

[96] *Serine, glycine and the one-carbon cycle: cancer metabolism in full circle.* J. W. Locasale. Nature Reviews Cancer Vol. 13, n. 8, pp. 572-583, 2013.

[97] *Phosphoglycerate dehydrogenase: potential therapeutic target and putative metabolic oncogene.* C. K. Zogg. Journal of Oncology 2014. http://dx.doi.org/10.1155/2014/524101.

[98] *The importance of serine metabolism in cancer.* Katherine R. Mattaini, Mark R. Sullivan, Matthew G. Vander Heiden. The Journal of Cell Biology, Vol. 214, n. 3, pp. 249-257, 2016. https://doi.org/10.1083/jcb.201604085.

[99] *Serine, but not glycine, supports one-carbon metabolism and proliferation of cancer cells.* Christiaan F. Labuschagne, Niels J.F. van den Broek, Gillian M. Mackay, Karen H. Vousden, Oliver D.K. Maddocks. Cell Reports 7, pp. 1248-1258, 2014.

[100] *Phosphoglycerate dehydrogenase diverts glycolytic flux and contributes to oncogenesis.* J. W. Locasale, A. R. Grassian, T. Melman, C. A. Lyssiotis, K. R. Mattaini, A. J. Bass, G. Heffron, C. M. Metallo, T. Muranen, H. Sharfi, A. T. Sasaki, D. Anastasiou, E. Mullarky, N. I. Vokes, M. Sasaki, R. Beroukhim, G. Stephanopoulos, A. H. Ligon, M. Meyerson, A. L. Richardson, L. Chin, G. Wagner, J. M. Asara, J. S. Brugge, L. C. Cantley, M. G. V. Heiden. Nature Genetics Vol. 43, n. 9, pp. 869-874, 2013.

[101] *Glycine decarboxylase activity drives non-small cell lung cancer tumor-initiating cells and tumorigenesis.* W. C. Zhang, N. g. Shyh-Chang, H. Yang, A. Rai, S. Umashankar, S. Ma, B. S. Soh, L. L. Sun, B. C. Tai, M. E. Nga, K. K. Bhakoo, S. R. Jayapal, M. Nichane, Q. Yu, D. A. Ahmed, C. Tan, W. P. Sing, J. Tam, A. Thirugananam, M. S. Noghabi, Y. H. Pang, H. S. Ang, W. Mitchell, P. Robson, P. Kaldis, R. A. Soo, S. Swarup, E. H. Lim, B. Lim. Cell 148, pp. 259-272, 2012.

[102] *Compartmentalization of mammalian folate-mediated one-carbon metabolism.* A. S. Tibbetts, D. R. Appling. Annual Review of Nutrition 30, pp. 57-81, 2010.

[103] *Functional genomics reveal that the serine synthesis pathway is essential in breast cancer.* R. Possemato, K. M. Marks, Y. D. Shaul, M. E. Pacold, D. Kim, K. Birsoy, S. Sethumadhavan, H.-K. Woo, H. G. Jang, A. K. Jha, W. W. Chen, F. G. Barrett, N. Stransky, Z.-Y. Tsun, G. S. Cowley, J. Barretina, N. Y. Kalaany, P. P. Hsu, K. Ottina, A. M. Chan, B. Yuan, L. A. Garraway, D. E. Root, M. Mino-Kenudson, E. F. Brachtel, E. M. Driggers, D. M. Sabatini. Nature 476, pp. 346-350, 2011.

[104] *Phosphoglycerate dehydrogenase induces glioma cells proliferation and invasion by stabilizing forkhead box M1.* J. Liu, S. Guo, Q. Li, L. Yang, Z. Xia, L. Zhang, Z. Huang, N. Zhang. Journal of Neuro-Oncology 111, pp. 245-255, 2013.

[105] *Serine metabolism supports the methionine cycle and DNA/RNA methylation through De Novo ATP synthesis in cancer cells.* O. D.K. Maddocks, C. F. Labuschagne, P. D. Adams, K. H. Vousden. Molecular Cell 61, pp. 210-221, 2016.

[106] *Alterations in cancer cell metabolism: The Warburg effect and metabolic adaptation.* Yazdan Asgari, Zahra Zabihinpour, Ali Salehzadeh-Yazdi, Falk Schreiber, Ali Masoudi-Nejad. Genomics 105, pp. 275-281, 2015.

[107] *The Warburg effect: evolving interpretations of an established concept.* Xiaozhuo Chen, Yanrong Qian, Shiyong Wu. Free Radical Biology and Medicine 79, pp. 253-263, 2015.

[108] *The Warburg effect: how does it benefit cancer cells?.* Maria V. Liberti, and Jason W. Locasale. Trends in Biochemical Sciences, Vol. 41, n. 3, 2016.

[109] *Understanding the Warburg effect: the metabolic requirements of cell proliferation.* Matthew G. Vander Heiden, Lewis C. Cantley, Craig B. Thompson. Science, Vol. 324, pp. 1029-1033, 2009.

[110] *Why do cancers have high aerobic glycolysis?.* Robert A. Gatenby, Robert J. Gillies. Nature Reviews, Cancer Vol. 4 pp. 891-899, 2004.

[111] *ATP/ADP ratio, the missed connection between mitochondria and the Warburg effect.* Eduardo N. Maldonado, John J. Lemasters. Mitochondrion 19, pp. 78-84, 2014.

[112] *HIF-1α pathway: role, regulation and intervention for cancer therapy.* Georgina N. Masoud, Wei Li. Acta Pharmaceutica Sinica B, Vol. 5, n. 5, pp. 378-389, 2015.

[113] *Regulation of the Warburg effect in early-passage breast cancer cells.* Ian F. Robey, Renu M. Stephen, Kathy S. Brown, Brenda K. Baggett, Robert A. Gatenby, Robert J. Gillies. Neoplasia Vol. 10, n. 8, pp. 745-756, 2008.

[114] *Nonessential amino acid metabolism in breast cancer.* Renee C. Geck, Alex Toker. Advances in Biological Regulation, *In Press.*

[115] *Leptin regulates energy metabolism in MCF-7 breast cancer cells.* Mª del Mar Blanquer-Rossell, Jordi Olivier, Jorge Sastre-Serra, Adamo Valle, Pilar Roca. The International Journal of Biochemistry & Cell Biology 72, pp. 18-26, 2016.

[116] *AMPK activation increases fatty acid oxidation in skeletal muscle by activating PPARα and PGC-1.* W. J. Lee, M. Kim, H.-S. Park, H. S. Kim, M. J. Jeon, K. S. Oh, E. H. Koh, J. C. Won, M.-S. Kim, G. T. Oh, M. Yoon, K.-U. Lee, J.-Y. Park. Biochemical and Biophysical Research Communications 340 pp. 291295, 2006.

[117] *Peripheral metabolic actions of leptin.* D. M. Muoio, G. L. Dohm. Best Practice & Research Clinical Endocrinology and Metabolism Vol. 16, n. 4, pp. 653-666, 2002.

[118] *Leptin is a growth factor in cancer.* P. Somasundar, D. W. McFadden, S. M. Hileman, L. Vona-Davis. Journal of Surgical Research 116, pp. 337-349, 2004.

[119] *Leptin stimulates fatty acid oxidation and peroxisome proliferator-activated receptor α gene expression in mouse C2C12 myoblasts by changing the subcellular localization of the α2 form of AMP-activated protein Kinase.* A. Suzuki, S. Okamoto, S. Lee, K. Saito, T. Shiuchi, Y. Minokoshi. Molecular and Cellular Biology Vol. 27, n. 12, pp. 4317-4327, 2007.

[120] *Leptin stimulates fatty-acid oxidation by activating AMP-activated protein kinase.* Y. Minokoshi, Y.-B. Kim, O. D. Peroni, L. G. D. Fryer, C. Müller, D. Carling, B. B. Kahn. Nature Vol. 415, pp. 339-343 , 2002.

[121] *Is obesity an independent prognosis factor in woman breast cancer?.* B. Majed, T. Moreau, K. Senouci, R. J. Salmon, A. Fourquet, B. Asselain. Breast Cancer Research and Treatment 111, pp. 329-342, 2008.

[122] *Obesity hormone leptin: a new target in breast cancer?.* E. Surmacz. Breast Cancer Research Vol. 9, n. 1 ,2007. doi:10.1186/bcr1638.

[123] *Concomitant activation of the JAK/STAT, PI3K/AKT, and ERK signaling is involved in leptin-mediated promotion of invasion and migration of hepatocellular carcinoma cells.* N. K. Saxena, D. Sharma, X. Ding, S. Lin, F. Marra, D. Merlin, F. A. Anania. Cancer Research Vol. 67, n. 6, pp. 2497-2507, 2007.

[124] *Multifaceted leptin network: the molecular connection between obesity and breast cancer.* N. K. Saxena, D. Sharma. Journal of Mammary Gland Biology and Neoplasia Vol. 18, n. 0, pp. 309-320, 2013.

[125] *Obesity and cancer.* K. Y. Wolin, K. Carson, G. A. Colditz. The Oncologist 15, pp. 556-565, 2010.

[126] *Cooperation and competition in the evolution of ATP-producing pathways.* T. Pfeiffer, S. Schuster, S. Bonhoeffer. Science Vol. 292, n. 5516, pp. 504-507 ,2001.

[127] *Quantitative determinants of aerobic glycolysis identify flux through the enzyme GAPDH as a limiting step.* A. A Shestov, X. Liu, Z. Ser, A. A. Cluntun, Y. P. Hung, L. Huang, D. Kim, A. Le, G. Yellen, J. G. Albeck, J. W. Locasale. eLife 2014. doi: 10.7554/eLife.03342.

[128] *Metabolic flux and the regulation of mammalian cell growth.* J. W. Locasale, L. C. Cantley. Cell Metabolism Vol. 14, n. 4, pp. 443-451, 2011.

[129] *Constant growth rate can be supported by decreasing energy flux and increasing aerobic glycolysis.* N. Slavov, B. A. Budnik, D. Schwab, E. M. Airoldi, A. van Oudenaarden. Cell Reports Vol. 7, n. 3, pp. 705-714, 2014.

[130] *Aerobic glycolysis: meeting the metabolic requirements of cell proliferation.* S. Y. Lunt, M. G. V. Heiden. Annual Review of Cell and Developmental Biology 27, pp. 441-464, 2011.

[131] *ATP citrate lyase inhibition can suppress tumor cell growth.* G. Hatzivassiliou, F. Zhao, D. E. Bauer, C. Andreadis, A. N. Shaw, D. Dhanak, S. R. Hingorani, D. A. Tuveson, C. B. Thompson. Cancer Cell Vol. 8, pp. 311-321, 2005.

[132] *The control of the metabolic switch in cancers by oncogenes and tumor suppressor genes.* A. J. Levine, A. M. Puzio-Kuter. Science 330, pp. 1340-1344 ,2010.

[133] *Organization of enzyme concentration across the metabolic network in cancer cells.* N. S. Madhukar, M. O. Warmoes, J. W. Locasale. PLoS ONE Vol. 10, n. 1, 2015. doi:10.1371/journal.pone.0117131.

[134] *Phosphoenolpyruvate is a metabolic checkpoint of anti-tumor T cell responses.* P.-C. Ho, J. D. Bihuniak, A. N. Macintyre, M. Staron, X. Liu, R. Amezquita, Y.-C. Tsui, G. Cui, G. Micevic, J. C. Perales, S. H. Kleinstein, E. D. Abel, K. L. Insogna, S. Feske, J. W. Locasale, M. W. Bosenberg, J. C. Rathmell, S. M. Kaech. Cell Vol. 162, n. 6, pp. 1217-1228, 2015.

[135] *A reaction-diffusion model of cancer invasion.* R. A. Gatenby, E. T. Gawlinski. Cancer Research 56, pp. 5745-5753, 1996.

[136] *Metabolic competition in the tumor microenvironment is a driver of cancer progression.* C.-H. Chang, J. Qiu, D. OSullivan, M. D. Buck, T. Noguchi, J. D. Curtis, Q. Chen, M. Gindin, M. M. Gubin, G. J.W. van der Windt, E. Tonc, R. D. Schreiber, E. J. Pearce, E. L. Pearce. Cell Vol. 162, n. 6, pp. 1229-1241, 2015.

[137] *Acidity generated by the tumor microenvironment drives local invasion.* V. Estrella, T. Chen, M. Lloyd, J. Wojtkowiak, H. H. Cornnell, A. Ibrahim-Hashim, K. Bailey, Y. Balagurunathan, J. M. Rothberg, B. F. Sloane, J. Johnson, R. A. Gatenby, R. J. Gillies. Cancer Research Vol. 73, n. 5, pp. 1524-1535, 2013.

[138] *ATP-citrate lyase links cellular metabolism to histone acetylation.* K. E. Wellen, G. Hatzivassiliou U. M. Sachdeva, T. V. Bui, J. R. Cross, C. B. Thompson. Science Vol. 324, n. 5930, pp. 1076-1080, 2009.

[139] *Quantitative dynamics of the link between cellular metabolism and histone acetylation.* A. G. Evertts, B. M. Zee, P. A. DiMaggio, M. Gonzales-Cope, H. A. Coller, B. A. Garcia. The Journal of Biological Chemistry Vol. 288, n. 17, pp. 12142-12151, 2013.

[140] *A two-way street: reciprocal regulation of metabolism and signalling.* K. E. Wellen, C. B. Thompson. Nature Reviews Molecular Cell Biology Vol. 13, pp. 270-276, 2012.

[141] *Metabolic regulation of epigenetics.* C. Lu, C. B. Thompson. Cell Metabolism 16, pp. 9-17, 2012.

[142] *Determination of local oxygen consumption rates in tumors.* M. W. Dewhirst, T. W. Secomb, E. T. Ong, R. Hsu, J. F. Gross. Cancer Research 54, pp. 3333-3336, 1994.

[143] *Interstitial pH and pO_2 gradients in solid tumors in vivo: high-resolution measurements reveal a lack of correlation.* G. Helmlinger, F. Yuan, M. Dellian, R. K. Jain. Nature Medicine Vol. 3, n. 2, pp. 177-182, 1997.

[144] *Fluctuation in red cell flux in tumor microvessels can lead to transient hypoxia and reoxygenation in tumor parenchyma.* H. Kimura, R. D. Braun, E. T. Ong, R. Hsu, T. W. Secomb, D.s Papahadjopoulos, K. Hong, M. W. Dewhirst. Cancer Research 56, pp. 5522-5528, 1996.

[145] *Dynamic remodeling of the vascular bed precedes tumor growth: MLS ovarian carcinoma spheroids implanted in nude mice.* A. Gilead, M. Neeman. Neoplasia Vol. 1, n. 3, pp. 226-230, 1999.

[146] *Imatinib (STI571)-mediated changes in glucose metabolism in human leukemia BCR-ABL-positive cells.* S. Gottschalk, N. Anderson, C. Hainz, S. G. Eckhardt, N. J. Serkova. Clinical Cancer Research Vol. 10, pp. 6661-6668, 2004.

[147] *The M2 splice isoform of pyruvate kinase is important for cancer metabolism and tumour growth.* H. R. Christofk, M. G. V. Heiden, M. H. Harris, A. Ramanathan, R. E. Gerszten, R. Wei, M. D. Fleming, S. L. Schreiber, L. C. Cantley. Nature 452, pp. 230-233 ,2008.

[148] *Glucose utilization in vivo by human pulmonary neoplasms.* K. B. Nolop, C. G. Rhodes, L. H. Brudin, R. P. Beaney, T. Krausz, T. Jones, J. M. B. Hughes. Cancer Vol. 60, n. 11, pp. 2682-2689, 1987.

[149] *The reverse Warburg effect: aerobic glycolysis in cancer associated fibroblasts and the tumor stroma.* S. Pavlides, D. Whitaker-Menezes, R. Castello-Cros, N. Flomenberg, A. K. Witkiewicz, P. G. Frank, M. C. Casimiro, C. Wang, P. Fortina, S. Addya, R. G. Pestell, U. E. Martinez-Outschoorn, F. Sotgia, M. P. Lisanti. Cell Cycle Vol. 8, n. 23, pp. 3984-4001, 2009.

[150] *Ketones and lactate "fuel" tumor growth and metastasis: evidence that epithelial cancer cells use oxidative mitochondrial metabolism.* G. Bonuccelli, A. Tsirigos, D. Whitaker-Menezes, S. Pavlides, R. G. Pestell, B. Chiavarina, P. G. Frank, N. Flomenberg, A. Howell, U. E. Martinez-Outschoorn, F. Sotgia, M. P. Lisanti. Cell Cycle Vol. 9, n. 17, pp. 3506-3514, 2010.

[151] *Evidence for a stromal-epithelial "lactate shuttle" in human tumors: MCT4 is a marker of oxidative stress in cancer-associated fibroblasts.* D. Whitaker-Menezes, U. E. Martinez-Outschoorn, Z. Lin, A. Ertel, N. Flomenberg, A. K. Witkiewicz, R. C. Birbe, A. Howell, S. Pavlides, R. Gandara, R. G. Pestell, F. Sotgia, N. J. Philp, M. P. Lisanti. Cell Cycle Vol. 10, n. 11, pp. 1772-1783, 2011.

[152] *Maximum activities of key enzymes of glycolysis, glutaminolysis, pentose phosphate pathway and tricarboxylic acid cycle in normal, neoplastic and suppressed cells.* Mary Board, Susan Humm, Eric A. Newsholme. Biochem. Journal Vol. 265, pp. 503-509, 1990.

[153] *Isozyme patterns of normal, benign, and malignant human breast tissues.* Doris Balinsky, Charles E. Platz, Jeffrey W. Lewis. Cancer Research 43, pp. 5895-5901, 1983.

[154] *Comparison of glycolitic enzyme and isoenzyme activity in breast cancers and dysplaisa.* Katica Bajin Katic. Med Pregl, LXV (5-6): 200-205, 2012.

[155] *Pyruvate kinase: Function, regulation and role in cancer.* William J. Israelsena, Matthew G. Vander Heidena. Seminars in Cell & Developmental Biology 43 (2015), pp. 4351.

[156] *Pyruvate kinase type M2: A key regulator of the metabolic budget system in tumor cells.* Sybille Mazurek. The International Journal of Biochemistry & Cell Biology 43 , pp. 969 980, 2011.

[157] *Interaction of M1 and M2 isozymes pyruvate kinase from human tissues with phosholipids.* Anna Dabrowska, Jadwiga Pietkiewicz, Katarzyna Dabrowska, Elzbieta Czapinska, Regina Danielewicz. Biochimica et Biophysica Acta 1383 , pp. 123129, 1998.

[158] *Pyruvate kinase type M2 and its role in tumour growth and spreading.* Sybille Mazurek, C. Bruce Boschek, Ferdinand Hugo, Erich Eigenbrodt. Seminars in Cancer Biology 15, pp. 300308, 2005.

[159] *Comparative kinetic study of human pyruvate kinases isolated from adult and fetal livers and from hepatoma.* D. Balinsky, E. Cayanis, I. Bersohn. Biochemistry, Vol. 12, n. 5, pp. 863-870 ,1973.

[160] *Mitochondrial phosphoenolpyruvate carboxykinase (PEPCK-M) is a pro-survival, endoplasmic reticulum (ER) stress response gene involved in tumor cell adaptation to nutrient availability.* Andrs Mndez-Lucas, Petra Hyrossov, Laura Novellasdemunt, Francesc Vials, and Jose C. Perales. The Journal of Biological Chemistry, Vol. 289, NO. 32, pp. 2209022102, August 8, 2014.

[161] *PCK2 activation mediates an adaptive response to glucose depletion in lung cancer.* K. Leithner, A. Hrzenjak, M. Trtzmller, T. Moustafa, H.C. Kfeler, C. Wohlkoenig, E. Stacher, J. Lindenmann, A.L. Harris, A. Olschewski, H. Olschewski. Oncogene Vol. 34, pp. 10441050, 2015.

[162] *Kinetic and functional properties of human mitochondrial phosphoenolpyruvate carboxykinase.* Miriam Escs, Pedro Latorre, Jorge Hidalgo, Ramn Hurtado-Guerrero, Jos AlbertoCarrodeguas, Pascual Lpez-Buesa. Biochemistry and Biophysics Reports Vol. 7, pp. 124129, 2016.

[163] *Phosphoenolpyruvate synthesis and release by mitochondria from guinea pig liver.* Alan J. Garber, F. J. Ballard. The Journal of Biological Chemistry, Vol. 244, n. 17, pp. 4696-4703, 1969.

[164] *Phosphoenolpyruvate shuttle - transport of energy from mitochondria to cytosol.* Zdenek Drahota, Hana Rauchov, Marie Mikov, Phool Kaul, Arnost Bass. FEBS Letters, Vol. 157, n. 2, pp. 347-349, 1983.

[165] *The mitochondrial isoform of phosphoenolpyruvate carboxykinase (PEPCK-M) and glucose homeostasis: Has it been overlooked?.* Romana Stark, Richard G. Kibbey. Biochimica et Biophysica Acta 1840, pp. 1313-1330, 2014.

[166] *The role of mitochondrial transport in energy metabolism.* Salvatore Passarellaa, Anna Atlante, Daniela Valenti, Lidia de Bari. Mitochondrion Vol.2, pp. 319-343, 2003.

[167] *Kinetic study of the tricarboxylate carrier in rat liver mitochondria.* Ferdinando Palmieri, Italo Stipani, Ernesto Quagliariello. Eur. Journal Biochem. 26, pp. 587-594, 1972.

[168] *Kinetic characterization of lactate dehydrogenase in normal and malignant human breast tissues.* Abdolhassan Talaiezadeh, Ali Shahriari, Mohammad Reza Tabandeh, Payam Fathizadeh, Siavash Mansouri. Talaiezadeh et al. Cancer Cell International, 15:19, 2015.

[169] *SIRT3 deacetylates and increases pyruvate dehydrogenase activity in cancer cells.* Ozkan Ozden, Seong-Hoon Park, Brett A. Wagner, Ha Yong Song, Yueming Zhu, Athanassios Vassilopoulos, Barbara Jung, Garry R. Buettner, David Gius. Free Radical Biology and Medicine Vol. 76, pp. 163172, 2014.

[170] *The pyruvate dehydrogenase complex in cancer: implications for the transformed state and cancer chemotherapy.* Paul M. Bingham and Zuzana Zachar. Dehydrogenases, 2012.

[171] *PDK1-dependent metabolic reprogramming dictates metastatic potential in breast cancer.* Fanny Dupuy, Sbastien Tabaris, Sylvia Andrzejewski, Julie St. Pierre, Russell G. Jones, Peter M. Siegel. Cell Metabolism, pp. 22, 577589, 2015.

[172] *Kinetic characterization of the pyruvate and oxoglutarate dehydrogenase complexes from human heart.* Yuri V. Kiselevsky, Svetlana A. Ostrovtsova, Slavomir A. Strumilo. Acta Biochimica Polonica, Vol. 37, n. 1, 1990.

[173] *Pyruvate carboxylase is up-regulated in breast cancer and essential to support growth and invasion of MDA-MB-231 cells.* Phatchariya Phannasil, Chanitra Thuwajit, Malee Warnnissorn, John C. Wallace, Michael J. MacDonald, Sarawut Jitrapakdee. PLoS ONE 10(6): e0129848. doi:10.1371/journal.pone.0129848, 2015.

[174] *Breast cancer-derived lung metastases show increased pyruvate carboxylase-dependent anaplerosis.* Stefan Christen, Doriane Lorendeau, Roberta Schmieder, Thomas Georg

Philipp Grünewald, Katrien De Bock, Sarah-Maria Fendt. Cell Reports 17, pp. 837848, 2016.

[175] *Sheep kidney pyruvate carboxylase. Studies on its activation by acetyl coenzyme A and characteristics of its acetyl coenzyme A independent reaction.* Leonie K. Ashman, D. Bruce Keech, John C. Wallace, Jan Nielsen. The Journal of Biological Chemistry, Vol. 247, n. 18, pp. 58185824, 1972.

[176] *Pyruvate carboxylase from chicken liver. Steady state kinetic studies indicate a two-site ping-pong mechanism.* Roland E. Barden, Chien-Hung Fung, Merton F. Utter, Michael C. Scrutton. The Journal of Biological Chemistry, Vol. 247, n. 4, pp. 1323-1333, 1972.

[177] *Loss of the respiratory enzyme citrate synthase directly links the Warburg effect to tumor malignancy.* Chin-Chih Lin, Tsung-Lin Cheng, Wen-Hui Tsai, Hui-Ju Tsai, Keng-Hsun Hu, Hao-Chun Chang, Chin-Wei Yeh, Ying-Chou Chen, Ching-Chun Liao, Wen-Tsan Chang. Scientific Reports, 2 : 785, doi:10.1038/srep00785, 2012.

[178] *Citrate synthase expression affects tumor phenotype and drug resistance in human ovarian carcinoma.* Lilan Chen, Ting Liu, Jinhua Zhou, Yunfei Wang, Xinran Wang, Wen Di, Shu Zhang. PLoS ONE 9(12): e115708, doi:10.1371/journal.pone.0115708, 2014.

[179] *The kinetic properties of citrate synthase from rat liver mitochondria.* D. Shepherd, P. B. Garland. Biochem. Journal. Vol. 114, pp. 597-610.

[180] *Kinetic studies of citrate synthase from rat kidney and rat brain.* Yoichi Matsuoka, Paul A. Srere. The Journal of Biological Chemistry, Vol. 248, n. 23, pp. 8022-8030, 1973.

[181] *Cancer-associated isocitrate dehydrogenase mutations inactivate NADPH-dependent reductive carboxylation.* Roberta Leonardi, Chitra Subramanian, Suzanne Jackowski, Charles O. Rock. Journal of Biological Chemistry, Vol. 287, pp. 14615-14620, 2012.

[182] *Isocitrate dehydrogenase 1 and 2 mutations in cancer: alterations at a crossroads of cellular metabolism.* Zachary J. Reitman, Hai Yan. Journal of the National Cancer Institute, Vol. 102, n. 13, pp. 932-941 ,2010.

[183] *Screen for IDH1, IDH2, IDH3, D2HGDH and L2HGDH mutations in glioblastoma.* Daniel Krell, Mawuelikem Assoku, Malcolm Galloway, Paul Mulholland, Ian Tomlinson, Chiara Bardella. PLoS ONE, Vol. 6, n. 5, 2011.

[184] *The role of mitochondrial NADPH-dependent isocitrate dehydrogenase in cancer cells.* Katarína Smolková, Petr Jezek. International Journal of Cell Biology, Vol. 2012.

[185] *Regulation of mitochondrial α-ketoglutarate metabolism by product inhibition at α-ketoglutarate dehydrogenase.* Colleen M. Smith, Jadwiga Bryla, John R. Williamson. The Journal of Biological Chemistry, Vol. 249, n.5, pp.1497-1505, 1974.

[186] *Purification and properties of diphosphopyridine nucleotide-linked isocitrate dehydrogenase of mammalian liver.* G. W. E. Plaut, T. Aogaichi. the Journal of Biological Chemistry, Vol. 243, n. 21, pp. 5572-5583, 1968.

[187] *Regulation of NAD^+-linked isocitrate dehydrogenase and 2-oxoglutarate dehydrogenase by Ca^{2+} ions within toluene-permeabilized rat heart mitochondria. Interactions with regulation by adenine nucleotides and $NADH/NAD^+$ ratios.* Guy A. Rutter, Richard M. Denton. Biochem. Journal, Vol. 252, pp. 181-189, 1988.

[188] *Inhibition of mitochondrial 2-oxoglutarate dehydrogenase impairs viability of cancer cells in a cell-specific metabolism dependent manner.* V. I. Bunik, G. Mkrtchyan, A. Grabarska, H. Oppermann, D. Daloso, W. L. Araujo, M. Juszczak, W. Rzeski, L. Bettendorff, A. R. Fernie, J. Meixensberger, A. Stepulak, F. Gaunitz. Oncotarget Vol. 7, n. 18, pp. 26400-26421, 2016.

[189] *SDH mutations in cancer.* C. Bardella, P. J. Pollard, I. Tomlinson. Biochimica et Biophysica Acta 1807, pp. 1432-1443, 2011.

[190] *Glucose metabolism and cancer.* R. J. Shaw. Current Opinion in Cell Biology 18, pp. 598-608, 2006.

[191] *Kinetic studies of the regulation of mitochondrial malate dehydrogenase by citrate.* Josep L. Gelpí, Alberto Dordal, Joan Montserrat, Adela Mazo, Antonio Corts. Biochem. Journal, Vol. 283, pp. 289-297, 1992.

[192] *Rat liver cytosolic malate dehydrogenase: purification, kinetic properties, role in control of free cytosolic NADH concentration. Analysis of control of ethanol metabolism using computer simulation.* Kathryn E. Crow, Terence J. Braggins, Richard D. Batt, Michael J. Hardman. The Journal of Biochemical Chemistry, Vol. 257, n. 23, pp. 14217-14225, 1982.

[193] *Substrate inhibition of the mitochondrial and cytoplasmic malate dehydrogenase.* Larry H. Bernstein, Matthew B. Grisham, Kenneth D. Cole, Johannes Everse. The Journal of Biological Chemistry, Vol. 253, n.24, pp. 8697-8701, 1978.

[194] *Characterization of cytosolic malic enzyme in human tumor cells.* Gerhard Loeber, Mark B. Dworkin, Anthony Infante, Horst Ahorn. FEBS Letters 344, pp. 181-186, 1994.

[195] *Knockdown of malic enzyme 2 suppresses lung tumor growth, induces differentitation and impacts PI3K/AKT signaling.* Jian-Guo Ren, Pankaj Seth, Clary B. Clish, Pawel K. Lorkiewicz, Richard M. Higashi, Andrew N. Lane, Teresa W. M. Fan, Vikas P. Sukhatme. Scientific Reports, 4:5414, doi:10.1038/srep05414.

[196] *Molecular Mechanism for the Regulation of Human Mitochondrial $NAD(P)^+$-Dependent Malic Enzyme by ATP and Fumarate.* Zhiru Yang, Charles W. Lanks, and Liang Tong. Structure, Vol. 10, pp. 951960, July, 2002.

[197] *Purification, kinetic behavior, and regulation of NAD(P)$^+$ malic enzyme of tumor mitochondria.* Randall W. Moreadith, Alberto L. Lehninger. The Journal of Biological Chemistry, Vol. 259, n. 10, pp. 6222-6227, 1984.

[198] *Purification and characterization of the cytosolic NADP$^+$-dependent malic enzyme from human breast cancer cell line.* Gu-Gang Chang, Jehng-Kang Wang, Ter-Mei Huang, Hwei-Jen Lee, Wei-Yuan Chou, Ching-Liang Meng. Eur. Journal Biochem. Vol. 202, pp. 681-688, 1991.

[199] *Malic enzyme in human liver: intracellular distribution, purification and properties od cytosolic isozyme.* M. Zelewski, J. Swierczynski. European Journal of Biochemistry 201, pp. 339-345, 1991.

[200] *The mitochondrial malic enzymes: submitochondrial localization and purification and properties of the NAD(P)$^+$-dependent enzyme from adrenal cortex.* The Journal of Biological Chemistry Vol. 250, n. 15, pp. 5877-5884, 1975.

[201] *Differential glutamate metabolism in proliferating and quiescent mammary epithelial cells.* Jonathan L. Coloff, J. Patrick Murphy, Craig R. Braun, Steven P. Gygi, Laura M. Selfors, Joan S. Brugge. Cell Metabolism 23, pp. 867880, 2016.

[202] *Nonlinear kinetics of glutamate dehydrogenase. Studies with substrates-glutamate and nicotinamide-adenine dinucleotide.* J. S. Barton, J. R. Fisher. Biochemistry Vol. 10, n. 4, pp. 577-585, 1971.

[203] *Determination of phosphate-activated glutaminase activity and its kinetics in mouse tissues using metabolic mapping (quantitative enzyme histochemistry).* D. Botman, W. Tigchelaar, C. J. F. Van Noorden. Journal of Histochemistry & Cytochemistry Vol. 62, n. 11, pp. 813-826, 2014.

[204] *Co-expression of glutaminase K and L isoenzymes in human tumour cells.* C. Pérez-Gómez, J. A. Campos-Sandoval, F. J. Alonso, J. A. Segura, E. Manzanares, P. Ruiz-Sánchez, M. E. González, J. Máequez, J. M. Matés. Biochemical Journal 386, pp. 535-542, 2005.

[205] *A novel glutaminase isoform in mammalian tissues.* V. de la Rosa, J. A. Campos-Sandoval, M. Martín-Rufían, C. Cardona, J. M. Matés, J. A. Segura, F. J. Alonso, J. Márquez. Neurochemistry International 55, pp. 76-84, 2009.

[206] *Kinetics and localization of brain phosphate activated glutaminase.* E. Kvamme, I. Aa. Torgner, B. Roberg. Journal of Neuroscience Research 66, pp. 951-958, 2001.

[207] *Effect of oxaloacetate and phosphorylation on ATP-citrate lyase activity.* S. N. Pentyala, W. B. Benjamin. Biochemistry Vol. 34, n. 35, 1995.

[208] *Purification and kinetic studies of the citrate cleavage enzyme.* K. M. Plowman, W. W. Cleland. The Journal of Biological Chemistry Vol. 242, n. 18, pp. 4239-4247, 1967.

[209] *The glyceraldehyde 3-phosphate dehydrogenases of liver and muscle: cooperative interactions and conditions for functional reversibility.* C. M. Smith, S. F. Velick. The Journal of Biological Chemistry Vol. 247, n. 1, pp. 273-284, 1972.

[210] *Theoretical studies on the regulation of oxidative phosphorylation in intact tissues.* B. Korzeniewski, Biochimica et Biophysica Acta 1504, pp. 31-45, 2001.

[211] *Kinetic studies of glutamic oxaloacetic transaminase isozymes.* C. P. Henson, W. W. Cleland. Biochemistry Vol. 3, n. 3, pp. 338-345 ,1964.

[212] *A mathematical model of the mitochondrial NADH shuttles and anaplerosis in the pancreatic β-cell.* P. O. Westermark, J. Hellgren Kotaleski, A. Björklund, V. Grill, A. Lansner. American Journal of Physiology-Endocrinology and Metabolism 292, pp. E373-E393, 2007.

[213] *The reversible Hill equation: how to incorporate cooperative enzymes into metabolic models.* J.-H. S. Hofmeyr, A. Cornish-Bowden. Computer Applications in the Biosciences Vol. 13, n. 4, pp. 377385, 1997.

[214] *Derivation of a reversible Hill equation with modifiers affecting catalytic properties.* P. O. Westermark, J. Hellgren-Kotaleski, A. Lansner. Transactions on Biology and Biomedicine Vol. 1, pp. 91-98, 2004.

[215] *MCbiclust: a novel algorithm to discover large-scale functionally related gene sets from massive transcriptomics data collections.* Robert B. Bentham, Kevin Bryson, Gyorgy Szabadkai. Preprint September, 2016. doi: http://dx.doi.org/10.1101/075374.

[216] *Metabolic control analysis: a survey of its theoretical and experimental development.* D. A. Fell. Biochemistry Journal 286, pp. 313-330, 1992.

[217] *Metabolic control analysis: a tool for designing strategies to manipulate metabolic pathways.* R. Moreno-Sánchez, E. Saavedra, S. Rodríguez-Enríquez, V. Olín-Sandoval. Journal of Biomedicine and Biotechnology 2008. doi:10.1155/2008/597913.

[218] *Generalized models as a universal approach to the analysis of nonlinear dynamical systems.* T. Gross, U. Feudel. Physical Review E 73, pp. 016205-016214, 2006.

[219] *Analytical search for bifurcation surfaces in parameter space.* T. Gross, U. Feudel. Physica D 195, pp. 292-302, 2004.

[220] *Bifurcations and chaos in the MAPK signaling cascade.* M. Zumsande, T. Gross. Journal of Theoretical Biology 265, pp. 481-491, 2010.

[221] *Monotone control systems.* D. Angeli, E. D. Sontag. IEEE Transactions on Automatic Control Vol. 48, n. 10, pp. 1684-1698, 2003.

[222] *Multi-stability in monotone input/output systems.* D. Angeli, E. D. Sontag. Systems & Control Letters 51, pp. 185-202, 2004.

[223] *Intracellular regulatory networks are close to monotone systems.* A. Maayan, R. Iyengar, E. D. Sontag. IET Systems Biology 2, pp. 103-112, 2008.

[224] *Nonmonotone systems decomposable into monotone systems with negative feedback.* G. A. Enciso, H. L. Smith, E. D. Sontag. Journal of Differential Equations 224, pp. 205-227, 2006.

[225] *Applications of genome-scale metabolic models in biotechnology and systems medicine.* C. Zhang, Q. Hua. Frontiers in Physiology 6, 2016. doi: 10.3389/fphys.2015.00413.

[226] *The growing scope of applications of genome-scale metabolic reconstructions: the case of E. Coli.* A. M. Feist, B. Ø. Palsson. Nature Biotechnology Vol. 26, n. 6, pp. 659-667, 2008.

[227] *What is flux balance analysis?.* J. D. Orth, I. Thiele, B. Ø. Palsson. Nature Biotechnology Vol. 28, n. 3, pp. 245-248, 2010.